The effect of experimental conditions on the performance of a small-scale dissolution-permeation model in drug development

Master's Thesis

University of Jyväskylä
Faculty of Mathematics and Science
Department of Chemistry

06.06.2022

Sara Hiidenhovi

Abstract

Most of the newly-developed drugs are poorly-soluble and the amount of drug substance available for drug development is very limited. Therefore, there is a need to find new solubility-enhancing formulations and small-scale methods and models to study them. Drug development has utilized animal models to study drug substances' *in vivo* behavior, by ranking the formulations according to the dissolved drug substance amounts with *in vivo* conditions. These rankings can be compared to *in vitro* results, which are obtained from small-scale dissolution-permeation model's measurements.

The aim of this study was to investigate what effect experimental conditions have on a small-scale dissolution-permeation model in drug development and if the studied *in vitro* model could efficiently simulate rat's gastrointestinal *in vivo* conditions. Studied experimental conditions were dose effect and used medium's effect. Experiments were performed with four different solubility enhancing suspension formulations. The aim was to find if used small-scale model was able to produce same ranking between suspension formulations as was previously obtained with rat studies. It was also investigated if correlation could be obtained between *in vitro* and *in vivo* results.

The results indicated differences between experimental conditions. Especially used medium caused variation between results. From the results was seen that dose itself did not have a major effect, but used medium also enhanced dose's impact. Results showed that measurements made with phosphate buffer pH 3.0 were able to produce constant and accurate results even with lower dose. With FeSSIF, higher dose was preferable, and the medium composition and thus its performance in dissolution-permeation studies needs more research.

The same ranking between four suspension formulations were obtained with both media and both doses. Rankings were same as *in vivo* tests have been obtained. In the studies were also obtained relatively high correlations between *in vitro* and *in vivo* results. Due to correct suspension formulation rankings and good correlation between *in vitro* and *in vivo* results, it could be concluded that studied dissolution-permeation model could simulate rat's gastrointestinal conditions. Therefore it could be used in the future, with this drug substance, for small-scale dissolution-permeation studies.

Tiivistelmä

Useimmat uudet lääkeaineet ovat heikosti liukenevia ja lääkeaineen määrä lääkekehityksessä on hyvin rajallinen. Sen vuoksi on tarve löytää uusia liukoisuutta parantavia formulaatioita ja pienen mittakaavan metodeja ja malleja niiden tutkimiseen. Lääkekehitys on hyödyntänyt eläinkokeita lääkeaineiden *in vivo* -käyttäytymisen tutkimiseen järjestelemällä eri formulaatioita paremmuusjärjestykseen perustuen niiden *in vivo* -olosuhteissa liuottamaan lääkeaineen määrään. Näitä järjestyksiä voidaan verrata *in vitro* -tuloksiin, jotka saadaan pienen mittakavaan dissoluutio-permeaatiomallin mittauksista.

Tutkimuksen tavoitteena oli tutkia kokeellisten olosuhteiden vaikutusta pienen mittakavaan dissoluutio-permeaatiomallin toimivuuteen lääkekehityksessä. Lisäksi haluttiin tutkia kykeneekö tutkittava *in vitro* -malli tehokkaasti mallintamaan rotan *in vivo* suolisto-olosuhteita. Tutkittavat kokeelliset olosuhteet olivat käytettävän annoksen ja väliaineen vaikutukset. Tutkimukset suoritettiin neljällä eri liukoisuutta parantavalla formulaatiosuspensiolla. Tavoitteena oli selvittää tuottaako käytetty pienen mittakaavan malli saman järjestyksen formulaatiosuspensioiden välillä kuin aiemmissa rotilla suoritetuissa mittauksissa oltiin havaittu. Lisäksi tutkittiin *in vitro* ja *in vivo* -tulosten välistä korrelaatiota.

Tuloksista nähtiin eroja kokeellisten olosuhteiden välillä. Erityisesti käytetyn väliaineen huomattiin aiheuttavan muuntelua tulosten välillä. Tuloksista havaittiin, että annoksella ei ollut yksinään suurta vaikutusta, mutta käytetty väliaine lisäsi myös annoksen vaikutusta. Voitiin todeta, että fosfaattipuskuri pH 3.0 väliaineessa tehdyt mittaukset tuottivat tasaisempia ja täsmällisempiä tuloksia jopa alemmalla annoksella. Sen sijaan FeSSIF väliaineessa korkeampi annos oli suositeltavampi. Tulosten perusteella FeSSIF väliaineen koostumusta ja siten sen vaikutusta dissoluutio-permeaatiomalliin tulisi tutkia vielä lisää.

Neljän eri suspensioformulaatioiden välillä saatiin sama järjestys molemmilla väliaineilla ja annosmäärillä. Nämä olivat samat kuin aiemmissa *in vivo* -testeissä havaitut järjestykset. Tutkimuksissa saatiin myös suhteellisen korkeita korrelaatioita *in vitro* ja *in vivo* -tulosten välillä. Täten tutkittu dissoluutio-permeaatiomalli soveltuu mallintamaan rotan suolisto-olosuhteita ja sitä voidaan tulevaisuudessa käyttää tämän lääkeaineen pienen mittakaavan dissoluutio-permeaatiotutkimuksissa.

Acknowledgements

This Master's Thesis was made with collaboration of University of Jyväskylä and Orion Oyj. Experimental part of the master's thesis was made in Turku, at Orion Oyj's department of chemical analytics, during the autumn and winter of 2021. Master's Thesis' project was done in Pharmaceuticals Sciences organization, in the Biopharmaceutics and Chemical analytics team. Master's Thesis was completed during the spring of 2022. The Master's Thesis was supervised by Jarmo Louhelainen from University of Jyväskylä, and Terhi Oja and Sari Pappinen from Orion Oyj. The subject for this Master's Thesis was proposed by the Orion oyj. The material and references for literature review were mainly searched from the publications of pharmaceutical industry through Pubmed® database.

I wish to express my gratitude to my supervisor Jarmo Louhelainen for his guidance, valuable opinions and especially for the encouragement throughout the project. I would also like to thank Orion Oyj for this great possibility and interesting topic. I'm extremely grateful to Terhi Oja and Krista Ojala for believing in me from the start and offering me this opportunity. I would like to express my deepest gratitude to my supervisor Terhi Oja for always helping me whenever needed, for her patience and, above all, for her kindness and support. I would like to extend my sincere thanks also to my supervisor Sari Pappinen for her inspiring guidance, invaluable advices and support throughout this project. Many thanks also to the entire Turku's chemical analytics team for their help and encouragement. Thank you especially for research associates Jaana Meri and Anu Sylander for the HPLC analysis, orientations and most of all how warmly they welcomed me as part of the team.

Last but not least, my deepest and dearest gratitude to my family. Thank you for my brothers for all the support and help, and most of all, the joy you bring to my life. And to my dear mom and dad: I can never thank you enough for your help, guidance and constant encouragement throughout my studies. Thank you for always being there for me and for believing in me, even when I did not. Your love and endless support is what I treasure most in the world.

Turku, June 2022

Sara Hiidenhovi

Table of Contents

Abbreviations and definitions

API	Active pharmaceutical ingredient
ASB	Acceptor sink buffer
ASD	Amorphous solid dispersion
AUC	Area under the curve
BA	Bioavailability
BCS	Biopharmaceutical classification system
BE	Bioequivalance
C_{max}	Maximum concentration
CMC	Critical micelle concentration
DR	Drug dissolution rate
FaSSIF	Fasted state simulated intestinal fluid
FaSSGF	Fasted state simulated gastric fluid
FeSSIF	Fed state simulated intestinal fluid
GI	Gastrointestinal
HIF	Human intestinal fluid
HPLC	High-performance liquid chromatography
HPMC	Hypromellose
IDR	Intrinsic dissolution rate
IR	Immediate release
IVIVC	*In vitro-in vivo* correlation
MC	Methyl cellulose
MR	Modified-release
PAMPA	Parallel artificial membrane permeability assay
pH_{max}	pH of maximum solubility in the pH-solubility profile
pK_a	Acid dissociation constant
PTFE	Polytetrafluoroethylene
PVDF	Polyvinylidene fluoride
R^2	Correlation coefficient
rSIF	Rat simulated intestinal fluid
SIF	Simulated intestinal fluid
SGF	Simulated gastric fluid
T_{max}	Maximum peak time

TPGS	D-α-tocopheryl polyethylene glycol succinate
Tween80	Polysorbate 80 NF EP
USFDA	United States Food and Drug Administration
USP	United States Pharmacopeia
UPLC	Ultra-performance liquid chromatography
UV	Ultraviolet
WHO	World Health Organization

LITERATURE REVIEW

1 Introduction

Oral route is the most preferred for the administration of new drugs. It is commonly used due to its high patient compliance, low costs, safety and efficiency, as well as its minimal discomfort to the patient. Its limiting factors are permeability, absorption, dissolution, solubility, stability, and biological activity.[1] During early drug development, one of the first questions is whether or not the drug substance can be effectively administered for its intended effect.[2] To achieve drug's bioavailability (BA) after oral administration, oral drug absorption is crucial. It is controlled by, for example, dissolution rate and intestinal permeability. Without becoming a dissolved substance, the drug cannot permeate through intestinal membrane, and complete efficacy cannot be achieved. Thus the determination of the dissolution and permeability properties of a drug provides crucial information about its absorption.[3]

To predict drug substances' behavior, the Biopharmaceutical Classification System (BCS) has been developed. It classifies drug substances in four categories based on their aqueous solubility and intestinal permeability.[4] The BCS is used as a framework to select drug candidates for development.[3] Low-solubility candidates are becoming more common these days and most of the newly-developed molecules for the pharmaceutical industry are poorly-soluble drugs from the BCS classes II and IV.[5,6] Therefore, there is a need to find new formulation techniques that help to improve formulations of drug substances with low solubility.[6] To enhance a drug substance's dissolution and permeability behavior, different formulations have used, for example, co-crystal formation, particle size reduction, and amorphization. These delivery options are found to be enhancing the physicochemical and pharmacokinetic behaviors of poorly aqueous-soluble drugs.[7]

Efficient formulation and drug development needs accurate predictions of oral drug formulations' *in vivo* performance. Drug development has utilized animal models to study drug substances' physicochemical behavior, but these studies can be time-consuming, expensive, and raise ethical questions. The increasing demand for dissolution- and permeability-enhancing formulations has led to a great need to develop new rapid and accurate *in vitro* methods.[1,6,8] Reliable *in vitro* models have been developed to determine, for example, the permeation of drug compounds in preclinical and clinical phases.[1] Biorelevant *in vitro* tools to predict the *in vivo*

performance of oral dosage form drugs may result in candidate compounds not being improperly removed in the early development or, conversely, helping to cut out formulations which are non-functional at early stages of drug development. Biorelevant *in vitro* tools could also decrease the need for animal and human testing between clinical trial formulations and therefore also decrease risk of failure in the late stage bioequivalance (BE) tests.[8]

However, the amount of active pharmaceutical ingredient (API) is very limited in the early drug development phases. Typically, there are only a few milligrams of API to use in early drug development.[9] Therefore, there is a great need for small-scale dissolution-permeation models which are able to accurately model drug substances' *in vivo* behavior. Miniaturized experimental tests have been developed that can allow high throughput measurements of permeability and dissolution rate using only a small amount of API. The most common approaches and equipment have been, for example, miniaturized dissolution vessels, microtiter plate-based methods, imaging-based methods, and small-scale automated dissolution equipment with concentration determination made by using ultraviolet (UV) fiber optic probes.[9]

The literature review of this Master's Thesis concentrated first on gastrointestinal (GI) tract and biorelevant media to mimic GI fluid. In the literature review was also discussed about drug substances' classification, and different factors affecting drug dissolution and permeability were presented. Later on was discussed about different ways to enhance the solubility of drug substance, and different methods previously used to model drug substance's *in vivo* behavior were presented.

The aim of this study was to investigate the effect that experimental conditions have on the performance of a small-scale dissolution-permeation model. The effect of dose and used medium was studied. It was investigated whether the miniaturized *in vitro* model, MicroFLUX (Pion Inc., Billerica, MA, USA) apparatus could efficiently simulate rats' GI tract by observing the correlation between measured data and previously obtained *in vivo* data. MicroFLUX model is a relatively fast and cost-effective small-scale method to study dissolution and permeation of API and thus a potential model to predict *in vivo* behavior of oral drug formulations. In this study, four different suspension formulations were used, and in addition to correlation studies, the aim was to find if the used *in vitro* model was able to produce the same ranking between suspension formulations, as was previously obtained with *in vivo* measurements. Ranking between suspension formulations represented the formulation ability to dissolve API. If good correlation and correct ranking are obtained, the studied *in vitro* model could be used to model

in vivo conditions and thus would be able to predict which suspension formulation has the best dissolution-permeation ability in *in vivo* conditions.

2 Gastrointestinal tract

2.1 Biological background: stomach and small intestine

The human GI tract begins at the mouth, and includes the esophagus, stomach, small intestine, large intestine, and rectum, and ends at the anus (Figure 1). The entire tract is lined with mucous membrane and, through it, drugs can be transferred into the systematic circulation. The mucous membrane, also known as mucosa, is highly perfused by a capillary network that enables drug absorption.[3] This literature review focuses on the stomach and small intestine, as the experimental part's measurements were performed under these conditions.

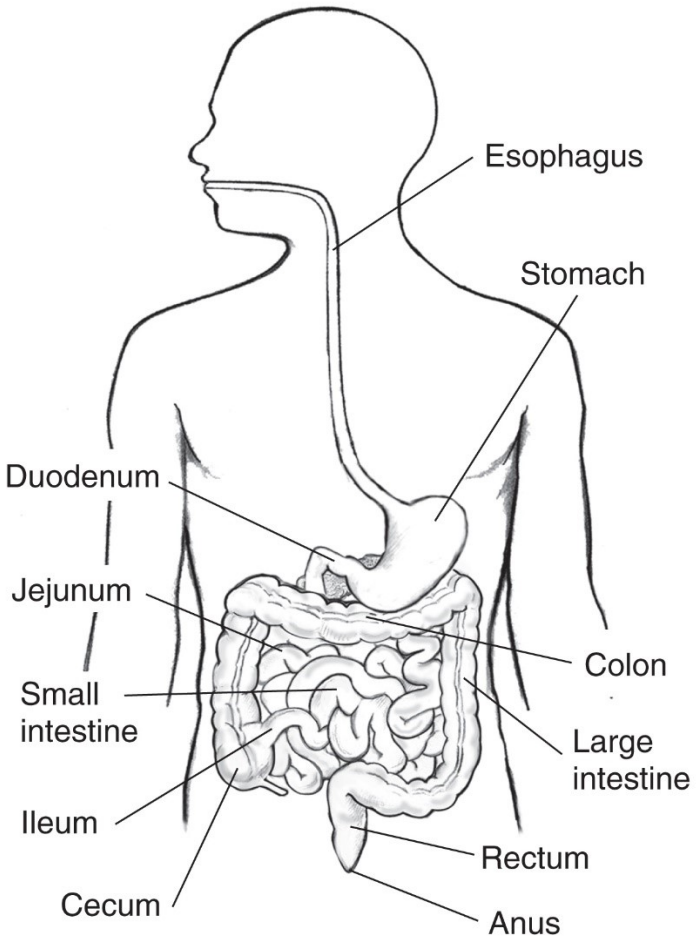

Figure 1. Illustration of human GI tract. Reprinted from National Institute of Diabetes and Digestive and Kidney Diseases, National Institutes of Health 2022 with permission.[10]

The stomach is a muscular organ located in the left upper part of the abdominal cavity. The main functions of stomach are storage and mechanical breakdown of ingested food, dispensing digested food into the intestine, and secretion of different enzymes and acids.[11–13] The stomach is divided into four regions: cardia, fundus, body, and pylorus.[11,12] All portions of the stomach are lined with simple columnar epithelium. On top of the epithelium is mucus which covers the interior surface of the stomach. In the fundus and body of the stomach, the mucosa has shallow depressions, called gastric pits, which communicate with gastric glands. Gastric glands contain two types of secretory cells: parietal and chief cells. Together, these cells secrete gastric juice and maintain the acidity of the stomach conditions. Parietal cells secrete glycoprotein intrinsic factor, which helps to absorb vitamin B_{12} across the intestinal lining. These cells are also crucial for secreting HCl. Carbonic acid is formed in parietal cells and the dissociation of it releases bicarbonate and hydrogen ions. Hydrogen ions are transported into the lumen of gastric glands. Chloride ions from interstitial fluid are exchanged for bicarbonate ions. This secretion of parietal cells can keep the pH of stomach at 1.5-2.0. Chief cells secrete pepsinogen which is converted to pepsin by the acid in the gastric lumen.[12]

The small intestine is the longest organ of the GI tract. It is a tube which can be about 6 m long. It is divided into three major divisions: the duodenum, the jejunum, and the ileum. The structural wall features of the small intestine increase its absorptive surface area. It has, for example, microvillis that are projections on the surface of epithelial cells.[11] The small intestine is extensively folded and villi cover it, making the surface area 15-30 times greater. This large surface absorbs, for example, the fluid, drugs, electrolytes, and nutrients. Intestinal cells are polarized, with an apixal membrane that faces lumen, and a basolateral membrane that faces the extracellular space and communicates with the bloodstream. The water movement across the intestinal epithelium is done passively via osmotic or hydraulic pressure gradients. The intestinal epithelium functions as a semipermeable membrane. It allows solvent molecules to pass freely but it prevents the passage of solute.[13] The small intestine's main priorities are to digest and absorb. Even though digesting starts before small intestine, most of the digestion and absorption take place in there. Ninety percent of nutrient absorption takes place there. Chemical digestion is finished there and digestion products are absorbed from the small intestine into the circulatory system, where they are transferred to body cells.[11,12] The small intestine's mucosa is able to produce only a few of the enzymes that are needed in digestion. The pancreas provides digestive enzymes to the small intestine, as well as buffers to neutralize chyme. The small intestine also gets bile fluid secreted from the liver. Bile fluid is a solution that is stored in the

gallbladder for discharge later into the small intestine.[12] It facilitates the digestion and intestinal absorption of fatty acids, cholesterol and other lipids.[11]

2.2 Gastrointestinal fluid

GI fluid forms a complex and heterogeneous system. In the GI fluid, changes occur in pH and the presence and concentrations of different components vary. Components are either endogenously excreted or obtained from digestion. GI fluid contains, for example, bile salts, electrolytes, lipids, lipid digestion products, enzymes, and proteins. The GI fluid's composition also varies depending upon the individual and the anatomical location of the tract. It will also continuously change depending on the fasted and fed states.[14]

Approximately 10 L of secretions and ingested liquid enter the intestine every day. Only 100 mL of water are excreted and the absorptive efficiency is thus 99%.[13] Intestinal juice helps to buffer acids, moistens chyme, and keeps the digestive enzymes and digested products in solution. Most of the fluid is formed when water flows by osmosis out of the mucosa into the concentrated chyme. The rest of the intestinal fluid is formed by secretion from the intestinal glands.[12]

The entry of chyme into the duodenum activates the secretion of pancreatic juice. The watery pancreatic secretion works as buffer solution with a pH of 7.5-8.8. Secretion also contains bicarbonate and phosphate buffers that help to increase the pH of the chyme. Intestinal absorptive effectiveness is enhanced by the movable mucosa.[12]

Bile fluid is produced and secreted in the liver. It is secreted through the hepatic duct into the gallbladder (Figure 2). When food is eaten, the liver is stimulated by secretin and cholecystokinin to form bile fluid. Bile fluid is then secreted into the duodenum. Bile salts' circulation is linked to the enterohepatic circulation. This circulation includes the biliary tract, liver, gallbladder, and portal venous system. The bile duct enters the duodenum at the duodenal papilla, which unites with the pancreatic duct just before entering the duodenum. Bile fluid contains water, bile salts, phospholipids, electrolytes, and cholesterol. Bile salts include the Na^+ and K^+ salts of the bile acids, such as cholic acid, which are conjugated to glycine and taurine.[15]

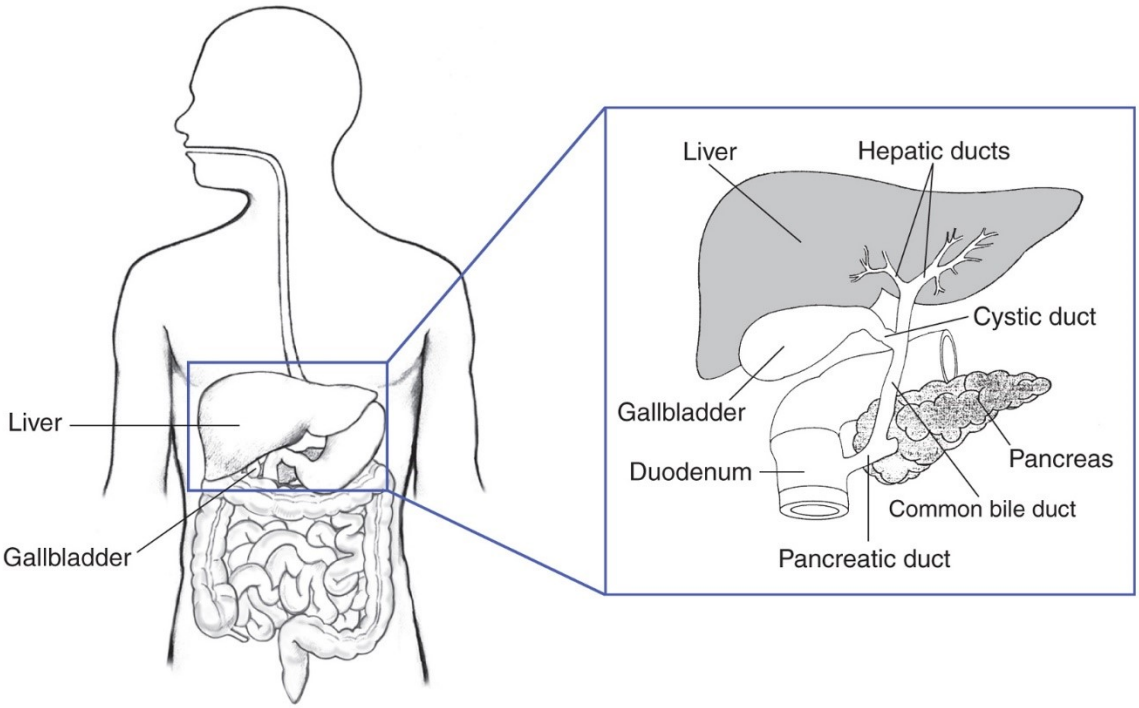

Figure 2. Illustration of the biliary system, with the liver, gallbladder, duodenum, pancreatic duct, common bile duct, pancreas, cystic duct, and hepatic ducts labeled. Reprinted from National Institute of Diabetes and Digestive and Kidney Diseases, National Institutes of Health 2022 with permission.[16]

2.3 Rat's gastrointestinal tract

Rodents, including rats and mice, are predominantly used in the pre-clinical testing of drugs and *in vivo* investigations of oral drugs. This is due to their small size and low cost. For BA studies, rats are more useful because of their larger size and higher capacity for blood samples.[17] However, anatomical, physiological, and biochemical differences in the GI tract of rodents and humans can cause differences in drug absorption.[15]

Bile fluid, pH, and pancreatic juice can change dissolution rates, solubility, membrane transport, and transit times of drug molecules. Small animals, such as mice, rats, and rabbits, are better suited for the drug absorption and BA value studies from powder and solution formulations. Rodents' stomach are divided into two parts: glandular and non-glandular (Figure 3). The non-glandular part is thin walled and transparent, while the glandular stomach's wall is thicker. The non-glandular portion is used in the digestion and storage of food, and in the glandular portion are located simple tubular gastric glands, such as mucus-secreting neck

cells, HCl-secreting parietal cells, and pepsinogen-secreting chief cells. The human stomach is of a mostly gastric and glandular type, lined with gastric, cardiac, and pyloric mucosa. These gastric and pyloric mucosa contain parietal and chief cells, and cardiac cells secrete mostly mucus.[15]

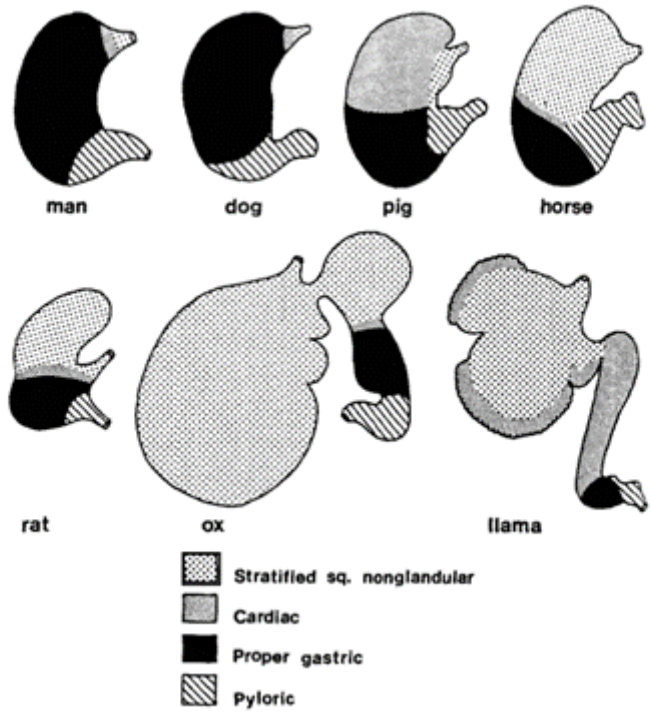

Figure 3. Variations in the type and distribution of gastric mucosa of humans and commonly-used laboratory animals. Reprinted from Kararli 2006 with permission.[15] Copyright 2022 John Wiley and Sons.

The stability, solubility, and absorption of drugs is affected by the pH of the GI tract. For example, drugs may precipitate due to unsuitable pH. Some drugs have been developed with coatings that will dissolve only when the pH of the environment is over a threshold level. The rat's stomach pH value is typically 3.2 in the fed state and 3.9 in the fasted state. It is thus opposite to the human stomach's pH. In humans, the buffering effects of food cause that the fasted gastric pH is lower than the fed gastric pH. The pH of the human stomach in fed state can, however, change depending on the meal composition, with high protein meals increasing the buffering effect. With rodents, fed or fasting states have no effect on intestinal pH. The small intestinal pH is higher than the gastric pH, due to buffering with bicarbonate ions and secretion of pancreatic juice. Rat's average intestinal pH is 6.6 and it is lower than human's, which intestinal pH is typically about 7-8.5. The low intestinal pH in rats has effects for the *in vivo* testing with oral drugs. Drugs which dissolve at a basic pH might precipitate at the lower

pH of the rat. This can have implications and may prevent drug absorption. Lower pH also effects pH-responsive drug carriers. For example, polymers that are pH-responsive and dissolve at a basic pH are insoluble at a lower pH. To investigate these types of carriers, it may be crucial to study targeted drug release at the distal intestinal tract.[17]

Another valid factor in the dissolution of drug in the GI tract is the fluid content. The contents of the GI tract are usually semi-solid. In rats, in the fed state, there are more solid contents in the GI tract than in the fasted state. In the fed state, the water content is also higher. The water concentration decreases along the GI tract. Among rodents, the rat is a better option to simulate for the dissolution of drug delivery systems, due to its intestine's larger water content. In humans, the water content in the large intestine is about 2.6 g/kg body mass, assuming a 70-kg body weight. For rats, the same value is 7.14 g/kg body mass assuming a 175 g body weight. The human small intestine contains water 3.8 g/kg, whereas the value for rat's intestine is 11.1 g/kg body weight. After considering the total body mass, rat has more water per kg body weight in the GI tract than do humans.[17]

In rats, the biliart and pancreatic ductal systems are interdependent. Pancreatic ducts flow directly into the common bile duct. Unlike humans, rats do not have gallbladder to store the bile fluid (Figure 4). The bile fluid is secreted at a continuous rate in dilute form and large volumes. The typical bile fluid flow for human is about 2.2-22.2 mL d^{-1} kg^{-1} and for rats it is 48-92 mL d^{-1} kg^{-1}.[15] Because rats do not have a gallbladder, their GI tract is exposed to constant bile fluid flow which causes higher bile fluid concentrations than in other species which are used in preclinical tests. Rats' bile salt concentrations are typically in the range of 12-51 mM.[18]

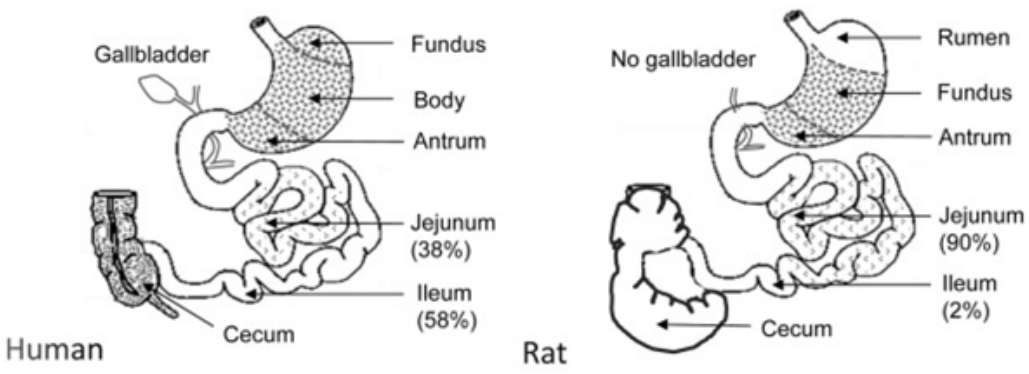

Figure 4. Schematic drawing and comparison of a human's and a rat's GI tract anatomy. Reprinted from Kodama. et al. 2013 with permission.[19] Copyright 2013 Kodama et al.

2.4 Biorelevant dissolution media

In an aqueous solution, the drug solubility is regulated by the solution's composition. For example, the solution pH affects the solubility of ionizable drugs.[14] In order to imitate a complex and variable composition of GI fluids on drug solubility and absorption, biorelevant media is used as a general implement in drug development and quality control.[14,20] It reduces the size and number of studies in human and animals that are needed to identify a drug product in both the fed and fasted states, and therefore to pre-screen formulations *in vitro*. It is important to choose suitable media for *in vitro* tests to correctly predict, for example, the food effect in pharmacokinetic studies.[21] To be able to do studies about BA of oral drug formulations, it is important to do dissolution tests under conditions with parameters resembling the human GI tract's physiology. Biorelevant media have been created to mimic stomach and small intestine conditions in fed and fasted states, and therefore enable investigations of the APIs of, for example, their physiological dissolution and solubility behavior *in vitro* to predict *in vivo* behavior.[21,22] The latest knowledge of GI tract physiology is used to update biorelevant media. This has caused the development of a multiple of media versions that mimic conditions in different parts of the GI tract.[20]

Biorelevant media includes fasted state simulated gastric fluid medium (FaSSGF), three versions of fasted state simulated intestinal fluid medium (FaSSIF V1, FaSSIF V2 and FaSSIF V3), and fed state simulated intestinal fluid medium (FeSSIF). With these media it is possible to test, for example, both the drug solubility and drug stability under the GI conditions, as well as permeability. Knowledge of biorevelant media gives a better understanding of the rate and extent of drug absorption. It has been found that, by using biorelevant media, it is possible to obtain reproducible and reliable results.[20]

The simulated gastric fluid (SGF) of the United States Pharmacopeia (USP) is a traditional medium to simulate gastric conditions in fasted state.[21] SGF contains HCl and sodium chloride and has a pH of 1.2. It simulates many qualities of gastric juice. Average gastric pH is usually in the range 1.5-1.9, which means that poorly-soluble weak bases may overestimate the *in vivo* dissolution rate in SGF. However, for neutral compounds and weak acids, this difference in pH does not make a difference in the dissolution.[21]

FaSSGF simulates fasted-state gastric conditions in the stomach.[20] FaSSGF was developed by Vertzoni et al. and it contains not only SGF composition but also pepsin and low amounts of

bile salt. FaSSGF has provided a better estimation of intragastric solubility during BA studies in the fasted states. It gives a better assessment for drug solubility and dissolution rate in the fasted stomach and thus it is useful for *in vitro* analyzes.[21]

In order to imitate a complex composition of GI fluids, simulated intestinal fluids (SIF) have also been developed. SIF simulates physiologically-relevant physicochemical conditions such as pH and osmolality.[14] SIF is a frequently used medium to mimic small intestinal conditions. It was first introduced as a standard test solution in the USP. The pH of the medium has since changed. It was previously 7.5 which was the assumed pH of small intestine. Since then, it has been found that a pH gradient occurs within the small intestine: the pH change is less acidic at distal locations, and the previously assumed pH of 7.5 is located only in the terminal ileum. Drug absorption during small intestine transit is most efficient when drug release happens at proximal small intestine sites. In the duodenum and the proximal jejunum exists the most relevant pH values. Thus, the pH of the SIF was later revised to be pH 6.8, which represents the pH that is typically measured in the mid-jejunum.[21]

The fasted or fed state of drug dosage influence the drug dissolution conditions in the proximal part of the small intestine. The meal causes changes in the hydrodynamics and the intralumenal volume. The chyme's pH is lower than the intestinal fluid's pH in the fasted state after a meal. On the other hand, osmolality and buffer capacity increase in the fed state. The bile fluid output also influences the BA of the drug, while the interactions with the drug and the digested meal's composition may also have effects. These variations demand the dissolution media to simulate and represent different states of the small intestine as closely as possible.[21]

FaSSIF represents fasted-state intestinal conditions. It was developed to specifically demonstrate fasting conditions in the proximal small intestine. This medium consists of bile salts and phospholipids, which help the wetting of solids as well as the solubilization of lipophilic drugs into mixed micelles. Because of this, the dissolution of lipophilic and poorly-soluble drugs can be observed better than with simple aqueous solutions. FaSSIF composition contains sodium taurocholate as a representative bile salt. Taurine conjugate does not tend to precipitate or change the micellar size within the range of pH 4-7, which is typical to the proximal small intestine due to its very low acid dissociation constant (pK_a). The fasted state's buffer capacity is lower than in the fed state.[21]

Updated versions of FaSSIF, FaSSIF-V2 and FaSSIF-V3, have been developed. In these media, the composition was updated to better reflect the composition of the fluids in the human small intestine as well as to obtain better stability of the media during dissolution tests. The third version of FaSSIF-V3 has a composition that is more complex than in V1 and V2. Versions differ in terms of physicochemical properties such as pH, surface tension, and osmolality. However, it is unknown which of the versions is most reliable for producing results closely reflecting the behavior of the API.[22]

FeSSIF simulates fed-state intestinal conditions.[20] The luminal composition in the stomach is dependent on the composition of the ingested meal in the fed state. Different compositions can cause a variation in pH values in the range of 3-6 or even in neutral pH values. Fed state medium has to address these changes in pH range, gastric acid secretion and digestion, as well as pepsin concentration. The ideal fed state medium has to mimic similar nutritional and physicochemical properties of initial gastric conditions and especially those in the upper part of the small intestine after a meal. FeSSIF contains acetate buffer, which allows it to achieve higher buffer capacity, higher osmolality, and maintain lower pH values. FeSSIF also contains taurocholate and lecithin in higher concentrations than does FaSSIF, and which imitates the biliart response to meal intake.[21] Media can be made from instant powders: FaSSIF/FeSSIF/FaSSGF-powder (Biorelevant.com Ltd., London, UK).[20] Table 1 shows the composition of the different biorelevant media which were prepared according to the standard operating procedures provided by Biorelevant.com Ltd. FaSSIF V3 is presented as described by Fuchs et al.[20,23]

Table 1. The compositions of the different biorelevant media[20,24]

	FaSSGF	FaSSIF V1	FaSSIF V2	FaSSIF V3	FeSSIF
Cholesterol (mM)	-	-	-	0.20	-
Lecithin (mM)	0.02	0.75	0.20	0.04	3.75
Lysolecithin (mM)	-	-	-	0.32	-
Sodium glycocholate (mM)	-	-	-	1.40	-
Sodium oleat (mM)	-	-	-	0.32	-
Sodium taurocholate (mM)	0.08	3.00	3.00	1.40	15.00
Acetic acid (mM)	-	-	-	-	144.00
Hydrochloric acid	qs pH 1.6	-	-	-	-
Maleic acid (mM)	-	-	19.12	10.26	-
Potassium dihydrogen phosphate (mM)	-	28.65	-	-	-
Sodium chloride (mM)	34.20	105.85	68.62	93.30	203.18
Sodium hydroxide (mM)	-	10.50	34.80	16.56	101.00

Another option for biorelevant media is human intestinal fluid (HIF). It is used for direct solubility measurements. To achieve HIF, aspiration by oral intubation, determination of the catheter's anatomical location, and sample collection are required. HIF is stated to be the most relevant system for solubility studies and it has been referred to as the gold standard. HIF gives accurate *in vivo* absorption predictions. Its restrictions are difficult sampling, inherent variability, and small fluid volumes.[14] HIF represents large intra- and inter-individual variations, because the sampling has occurred in various portions of the GI tract at different prandial states. Food intake stimulates hormonal and neural signaling from the GI tract in response to presence of nutrients and gastric distension, and this affects the HIF composition of fed state. The HIF composition of the fasting state differs in terms of intestinal bile fluid and pancreatic secretions during the human interstitial motility cycle. Even though HIF is considered to be the gold standard, it is not practical for routine solubility investigations. It is time- and resource-consuming and involves sampling from human subjects, which may raise ethical questions.[25]

Phosphate-based buffers have been widely used as a dissolution medium. The presence of phosphates in human GI fluids is meaningless and thus phosphate-containing medium is not the best option to reflect *in vivo* conditions. Instead of that, the GI lumen has been shown to be buffered by bicarbonate. As previously stated, various anatomical components form the GI tract and have different functions, like secretion of digestive enzymes. The pancreatic secretions contain digestive enzymes and sodium bicarbonate solution. The acidic content of stomach is

controlled and neutralized by bicarbonate ions. However, bicarbonate buffer faces challenges when dissolution tests are carried out. In a bicarbonate buffer system, CO_2 has a tendency to exit the aqueous solution, which means that the system needs to be continuously purged with CO_2. Another problem which can affect the dissolution process, is that the purging of CO_2 can form bubbles in the medium.[26]

Rodents are commonly used to assess the oral exposure of drug candidates. Rat simulated intestinal fluid (rSIF) is used to describe drug solubility in rats. A rSIF was developed to simulate intestinal conditions *in vivo*. It mimics phospholipid and bile salt concentrations, pH, buffer capacity, osmolarity, and surface tension. The homostatic condition was expected for rats due to their constant bile fluid flow. This simulated rat medium does not distinguish fasted or fed states. Rat intestinal pH is about 6.0, which rSIF mimics. Its composition consists of similar compounds which can also be found in FeSSIF (Table 2). However these media's compositions still differ from each other quite significantly and therefore it should be considered carefully which medium should be used for which measurement. The surface tension in rSIF is balanced with phospholipid and bile salt concentrations. Cholic acid and chenodeoxycholic acid sodium are used to obtain targeted surface tension. Factors that limit absorption in a rat due to the absence of a gallbladder, may differ compared to human absorption. Rats are likely to be better solubilizers of lipophilic compounds.[18]

Table 2. The compositions of rSIF and FeSSIF media[18,20,24]

	rSIF	FeSSIF
Sodium taurocholate (mM)	5.00	15.00
NaCl (mM)	18.70	203.18
Lecithin (mM)	5.16	3.75
Maleic Acid (mM)	29.86	-
Sodium oleate (mM)	0.26	-
Sodium cholate hydrate (mM)	12.50	-
Sodium chenodeoxycholic acid (mM)	7.50	-
Glyceryl Monooleate (mM)	1.67	-
Acetic acid (mM)	-	144.00
Sodium hydroxide (mM)	-	101.00

3 Factors affecting dissolution and permeation of drug substances

3.1 Drug substance and biopharmaceutical classification

A drug substance is described to be any substance, or mixture of substances, meant to be utilized in the production of a pharmaceutical product. When it is used to manufacture a drug, it becomes an active ingredient of the drug product.[27]

Amidon et al. devised the Biopharmaceutical classification system in 1995.[28,29] The BCS is a predictive tool for estimating the effects of formulation on the human drug oral BA. The BCS is used with *in vitro* dissolution tests to support to forecast *in vivo* product performance. The factors which are rate-limiting and determine the extent of oral drug absorption can be recognized by understanding the solubility of a compound in biorelevant medium and its permeability through biological membranes. With human pharmaceuticals, drugs can be classified into four BCS categories, as shown in Table 3.[30] Drug substances are classified based on their solubility and permeability to biomembranes.[2]

Table 3. The Biopharmaceutical classification system[29,30]

Class	Solubility	Permeability
I	High	High
II	Low	High
III	High	Low
IV	Low	Low

The classification of biopharmaceuticals is used to correlate *in vitro* drug dissolution and *in vivo* BA. As previously stated, the classification is based on drug dissolution and GI permeability, which are parameters that control drug absorption rate and extent. Biopharmaceutic drug classes are four types. Class I consists of high solubility-high permeability drugs, which means that the drug is well absorbed and the limiting factor to drug absorption is drug dissolution or gastric emptying. With this class of compounds, the dissolution profile needs to be well defined and reproducible to ensure BA. Class II contains low solubility-high permeability drugs, which means that drug dissolution *in vivo* is controlling the drug absorption. Absorption is often slower than with the Class I drugs. With Class II drugs, the dissolution profile must be the most clearly defined and reproducible. Class III contains high solubility-low permeability drugs, for which the factor limiting absorption is permeability. The

dissolution profile needs to be well defined but the simplification in dissolution specification is applicable for immediate release (IR) dosage forms. Class IV drugs are low solubility-low permeability drugs, which have significant problems for oral delivery and thus they have very poor oral BA. For almost all drugs given orally, drug dissolution is necessary for drug absorption and clinical response. The ability to predict oral drug absorption has been limited, because of the complexity of the GI tract's processes as well as drugs' complex pharmacokinetics.[29,30]

The BCS has also been used in the regulation of BE of oral drug products. The BCS can be used as a guiding tool to suggest a strategy to enhance the efficiency of drug development. It is able to give proper selection of dosage form and BE tests, which can be used to recommend, for example, a class of IR solid dosage forms. As previously stated, the concept behind BCS and orally-administered drugs' *in vivo* performance depends on permeability and solubility. The solubility of the API will not be a dominant parameter if the absorption of the drug is limited by the rate of permeation. In these cases, the *in vitro* dissolution studies can be utilized to present BE or BA of the drug product with *in vitro-in vivo* correlation (IVIVC). However, if absorption is limited by the dissolution-rate, it means that the drug in the GI fluid is able to pass freely through the biomembranes at a higher rate than it is released from the dosage form or it dissolves.[2]

3.2 Dissolution and solubility

The primary step in the oral absorption process is drug dissolution in the physiological environment. Dissolution is a process by which a solid substance, for example a drug product, goes into the solution, and a mass transfer of molecules occurs from the solid surface into the liquid phase. Dissolution ability can also described to be the amount of solids that dissolve into a solution per unit time under standard conditions such as temperature, solvent composition, pH, and constant solid surface area.[2]

Only dissolved drug is able to permeate the mucosa in the GI tract. The solubility and dissolution rate of the drug (*DR*) are essential for drugs' *in vivo* behavior. The first theories of the dissolution process were presented by Noyes and Whitney[31] and later extended by Nernst and Brunner[32] into Fick's law of diffusion.[21] The DR can be presented with the following

equation (1) based on Nernst-Brunner and Levich's modifications of the Noyes-Whitney model:[33,34]

$$DR = \frac{dX_d}{dt} = \frac{A\ x\ D}{\delta}\ x\ \left[\frac{C_s - X_d}{V}\right] \qquad (1)$$

where D is the diffusion coefficient of the drug, A is the effective surface area of the drug, δ is the effective diffusion boundary thickness adjacent to the dissolving surface, C_s is the saturation solubility of the drug under luminal conditions, X_d is the amount of drug already in solution, and V is the volume of the dissolution medium.[21]

The IR drug product is considered to be rapidly dissolving by the United States Food and Drug Administration (USFDA) BCS guidelines when no less than 85% of the labeled amount of the API dissolves within 30 minutes by using USP apparatus 1 at 100 rpm in a volume of 900 mL or less in either 0.1 N HCl, pH 4.5 buffer, or pH 6.8 buffer medium.[4]

Some of the parameters on drug dissolution are caused by a drug's physicochemical properties, but they are also affected by the GI tract's conditions and by the composition of the dosage form. Also, the composition of the GI content may affect drug solubility. For example, lipophilic drugs, bile salt concentration, and fat level are significant factors. For ionizable drugs, pH and buffer capacity are the most relevant.[21] Food can also affect dissolution and permeability. Bile salt-mediated micellar formulation is capable of affecting the dissolution rate. Micelle formulation can affect the type and magnitude of food-effect that can be predicted by *in vitro* dissolution tests. Micelle formation also influence the solubilization of solubility-limited drugs.[35]

When choosing the right dissolution conditions for a drug formulation, it is important to know the solubility of the API.[21] Dissolution rate and solubility are not the same. The rate of dissolution is a dynamic process and is more closely related to drug absorption and BA than to the rate of solubility. Nevertheless, the rate of dissolution of the API is related to its solubility in the dissolution medium.[2]

Solubility is a property of substance and it might be the absorption-limiting factor for drug molecules.[18] Solubility is the amount of substance that has passed into solution when equilibrium is reached between undissolved substance and solution at a given pressure and

temperature. When the maximum dose is soluble in 250 ml or less of an aqueous medium within a certain pH range, the API is considered to be highly soluble. The volume of 250 mL is the typical volume of water that is consumed during the oral administration of dosage form and thus is the minimum fluid volume that is expected to be in the stomach at the time of drug administration. In the USFDA guidelines, the pH solubility profile of the API is determined at 37 ± 1ºC in aqueous medium with pH in the range of 1.0-7.5.[4]

3.3 Absorption

Oral drug absorption is described to be the movement of the drug from the GI tract into the bloodstream.[3] Most of the absorption in the GI tract happens in the small intestine region. As previously described, the human small intestine is divided into three areas: the duodenum, jejunum, and ileum. Nutrient and drug absorption occurs mainly in the jejunum. It has the largest surface and is the site of the most active carrier-mediated transport.[1] Drug absorption is affected by dissolution, solubility, and permeability.[3] Food has a major role in these drug properties, as well as to drug's chemical stability, and thus affects on the absorption of the orally taken drug. It can also influence physiological factors such as increased luminal fluid volume, increased pH, and transport across the GI tract.[35]

The rate of dissolution and solubility are the primary factors to control the oral absorption of the drug in the solid dosage form from the GI tract. The solubility and dissolution rate determine how fast a drug is able to reach maximum concentration (C_{max}) in the GI fluid. Intestinal permeability determines the rate at which a dissolved drug goes through the intestinal wall into the portal blood circulation. Thus the determination of the dissolution, solubility, and permeability can offer valuable information about absorption. After oral administration, GI transit and environments such as surface area and membrane, GI fluids' content, pH, and enzymes interact with drug molecules and affect drug absorption.[3]

Because most of drugs are orally administered, it is important to consider during drug development, how much of a drug will be bioavailable after oral administration and how fast it occurs. For a drug to be orally bioavailable, it is required that the drug molecule is reasonably stable to enzymatic and chemical degradation, able to pass through the intestinal epithelial

barrier to the portal circulation, and able to go across the liver and then enter the systemic circulation. Oral BA (*F*) is represented by equation (2):[3]

$$F = f_a \cdot f_g \cdot f_h \qquad (2)$$

where f_a is the fraction of drug absorbed, f_g is the fraction that escapes metabolism in the GI tract, and f_h is the fraction that escapes the first-pass hepatic metabolism. Each value ranges from 0, which is completely metabolized or unabsorbed, to 1 which is fully unmetabolized or absorbed. Thus oral drug absorption is a valuable factor to control a drug's BA.[3]

3.4 Permeability

As previously described, the extent and rate of drug absorption from the GI tract are very complex phenomena and dependent on many different factors. These are physicochemical factors and factors related to the dosage form. However, the fundamental key parameters that control a drug's absorption are its permeability through the GI membrane, and its solubility and dissolution.[5] Only dissolved drug is able to permeate and thus also be absorbed.[36]

Drug permeability can be determined by different methods; for example, by doing pharmacokinetic studies in human subjects including mass balance studies, using stable isotopes or radiolabeled drug substances to determine the drug absorption. One option is also to do absolute BA studies, in which oral BA is determined against the intravenous BA as reference. Another option is to do *in vivo* or *in situ* intestinal perfusion in a suitable animal model or *in vitro* studies using excised intestinal tissues. These methods and models are best for the passively transported drugs.[4]

The classification of permeability is based on the absorption of an API in humans and on measurements of the rate of mass transferred across human intestinal membrane. In the USFDA BCS guidelines, when the absorption in humans is 90% or more, the API is considered to be highly permeable. According the World Health Organization (WHO) guidance, when absorption value is 85% or more, the drug substance is considered to be highly permeable.[4]

Permeability consists of the drug's diffusion coefficient through the membrane, partition coefficient of the drug in the membrane, and the membrane's thickness.[37] Intestinal

permeability is the flow of substance across the organ.[5] Permeability (*P*) can be represented with following equation (3):[37]

$$P = \frac{\propto D}{h} \qquad (3)$$

where α is the partition coefficient of the drug into the membrane, D is the diffusion coefficient of the drug in the membrane, and h is the thickness of the barrier.[37]

The motion of ions, nutrients, and other endogenous substances across different bio-membranes is a dynamic molecular process. Selective permeability is an important property of biological membranes. It is determined by the physicochemical features of the channel-forming membrane proteins and the lipid bilayer together with the molecular structure and the physicochemical properties of the drug molecules. Transports through biological membranes with a various composition happen via direct and indirect energy-demanding carrier-mediated mechanisms that can even function against a concentration gradient. Along a concentration gradient can occur passive membrane diffusion, facilitated membrane diffusion, and paracellular diffusion. Biological membranes compose a lipid bilayer, which consists of hundreds of different types of lipid molecules. These lipid molecules have a polar head group and a non-polar tail which allow them to have amphiphilic molecular properties. These membrane lipid molecules differ in terms of size, polarity, and chemical structure, which guarantee them a wide range of physical properties and functions.[38]

The movement of drugs through biomembranes is intrinsic for pharmacokinetic and pharmacodynamic processes. This transport is divided into transcellular and paracellular processes. Transcellular transport is either passive diffusion or carrier-mediated and it occurs through the intestinal cell, across both the apical and basolateral membranes, whereas paracellular transport happens between the epithelial cells (Figure 5).[38]

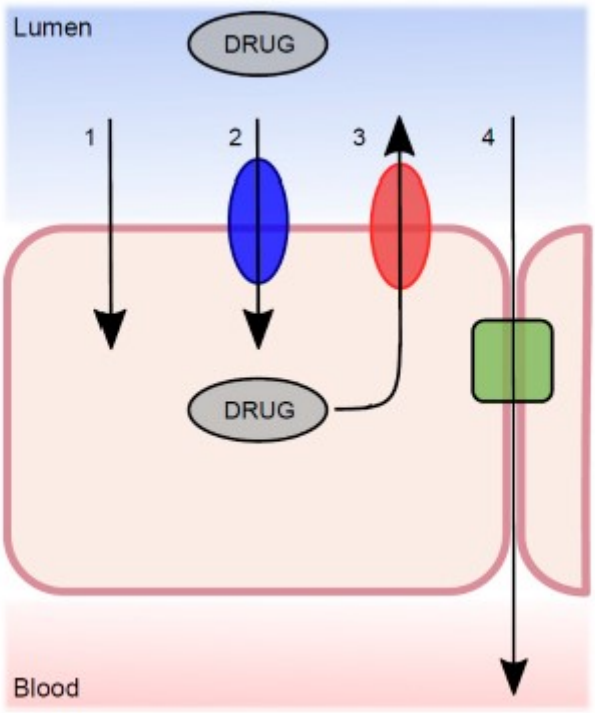

Figure 5. The transport mechanism from the lumen through the intestinal epithelium. (1) Passive transcellular diffusion; (2) absorptive carrier-mediated transport; (3) efflux carrier-mediated transport; and (4) passive paracellular diffusion. Reprinted from Dahlgren and Lennernäs 2019 with permission.[38] Copyright 2019 Dahlgren and Lennernäs.

3.5 Supersaturation and precipitation

Supersaturation can occur in the small intestine. It occurs when drug concentrations exceed the equilibrium solubility in the intestinal environment. It is a thermodynamically metastable state and can cause precipitation. Supersaturated drug concentrations can be generated by the addition of ions that are able to participate in the precipitation process, pH changes, solvent shifts, or the dissolution of unstable high-energy forms.[39] Compared to an equilibrium condition, also known as saturation, the chemical potential of a supersaturated system is increased. A supersaturated system is thermodynamically unstable and thus it has a tendency to try to return to the equilibrium state. Drug precipitation causes that equilibrium state has the lowest chemical potential. However, the increased intraluminal drug concentration can enhance flux across the intestinal wall, if a supersaturated state in GI lumen stays in a metastable state, which is sufficient for absorption.[40]

For poorly-soluble drugs in the BCS classes II and IV, absorption can be limited by the maximum available intraluminal drug concentration. Thus, numerous approaches in drug formulation development have been focused on to enhance the dissolution rate and drug solubility improvement in the GI tract. However, drugs may be in solution at a higher concentration than their saturation solubility in a state of supersaturation which is not caused by their solubility in GI fluids. The degree of supersaturation is determined by the supersaturation ratio (*S*) by the following equation (4):[40]

$$S = \frac{C}{C_{eq}} \qquad (4)$$

where C is the concentration of a supersaturated system and C_{eq} is the equilibrium solubility (saturation).[40]

Supersaturation can be used as a strategy to enhance the intestinal absorption of poorly-soluble drugs. To utilize this strategy, two steps need to be considered: first generation and then maintenance of the metastable supersaturated state. This concept is also known as a spring and parachute approach. The spring is the form where a thermodynamically unstable, supersaturated solution is generated starting from a higher energy form of the drug. Many formulation options can induce the generation of supersaturated solutions; for example, delivery of drugs in solution and delivery of high-energy solid forms. When supersaturation is achieved, drug molecules have a tendency to precipitate. Therefore, if the aim is to profit from the supersaturated state, it is necessary to maintain the increased concentration as long as it is sufficient for absorption. This is made possible by using pharmaceutical excipients or other components that are able to interfere with crystal growth which cause a temporary inhibition of precipitation. These are called the parachutes or precipitation inhibitors.[40]

After drug administration, self-emulsifying systems, such as lipid-based drug delivery systems, exhibit complex aqueous digestion and dispersion in the GI tract. This can result in drug supersaturation, which then effects the absorption by enhancing it, or the high drug concentrations may cause precipitation and variable oral BA. Lipid-based formulations are commonly used with poorly-soluble drug candidates. Their biopharmaceutical performance is usually enhanced with crystalline formulations.[41]

3.6 Pharmacokinetics

Pharmacology studies the action, effects, and interaction of drugs on living systems. Pharmacology is divided into pharmacodynamics and pharmacokinetics (Figure 6). The essential aspect of pharmacokinetics is the factors that can influence BA. Pharmacokinetics is able to produce valuable insights into the biologic behavior of adjunctive and interventional medications. Pharmacokinetics are essential studies of the distribution, absorption, metabolism, and excretion of drugs; in other words, how the body affects the drug.[42]

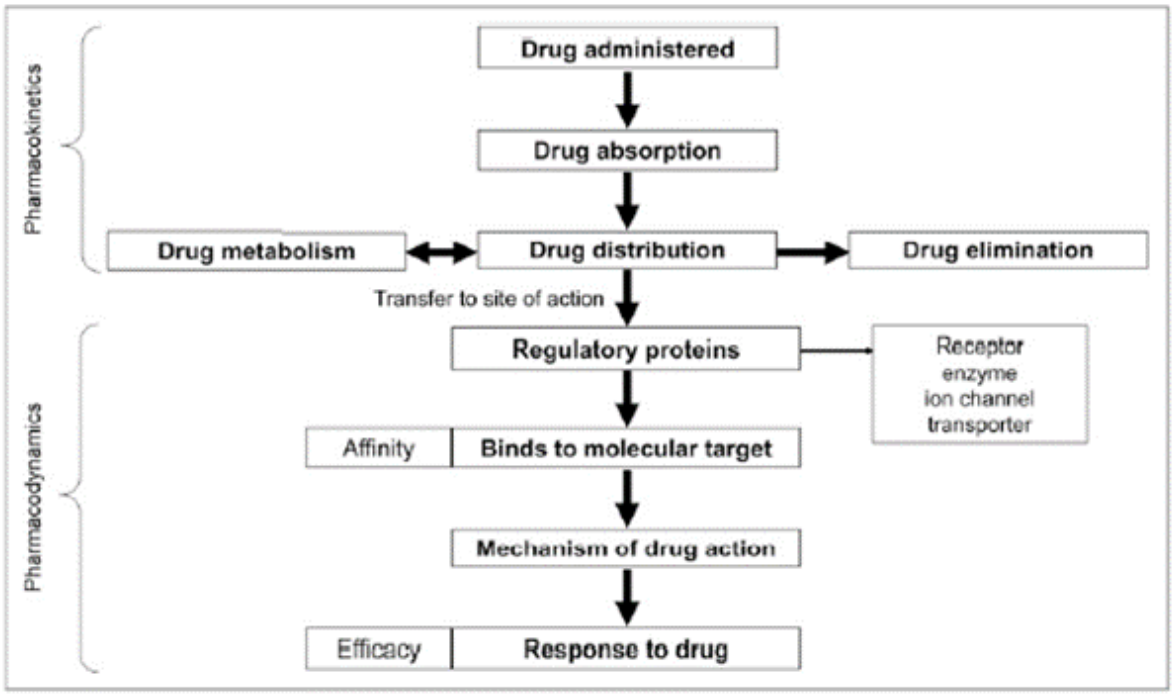

Figure 6. Schematic of relationship between pharmacokinetics and pharmacodynamics. Reprinted from Currie 2018 with permission.[42] Copyright 2018 the Society of Nuclear Medicine and Molecular Imaging.

Pharmacokinetics studies the biotransformation, absorption, distribution, and elimination of drugs in humans and animals. Absorption and distribution express the transit of the drug molecules from the dosage form to the blood circulation and the transit from blood to tissues. Biotransformation and the flow of molecules from the blood to the outside of the body by urine and bile fluid, might cause drug elimination. Measuring concentrations of drugs in blood or other fluids at different times after the administration, gives information about drug absorption, the passage of the drug molecules, and drug elimination. Pharmacokinetics' studies may be used in conjunction with studies made with laboratory animals and may give useful references

for drug research and development. For example, drug molecules can be more effective *in vivo* rather than *in vitro* because of their favorable kinetics.[43]

Typical pharmacokinetic parameters are C_{max}, maximum peak time (T_{max}), and area under the curve (AUC). C_{max} and T_{max} are dependent on the experimental procedure because the concentrations decrease after the dose. T_{max} corresponds to the time of infusion if the drug is infused at a constant rate. AUC can be used in different ways, depending on the context. It can be used as an index of the drug exposure of the body or as an index of the drug exposure of chosen tissues.[43] AUC from the time of administration to infinity can be used to calculate the total drug burden or total drug dose by the following equation (5):[42]

$$AUC_{0-\infty} = FD/Vk \qquad (5)$$

where F is the fraction of drug absorbed, D is dose, V is volume of distribution and k is elimination rate constant.[42]

4 Improving solubility of poorly-soluble drugs

4.1 Formulations

High-throughput screening and combinatorial chemistry have led to increasing the poorly-soluble drug candidates in drug discovery.[44] Aqueous solubility critically affects a drug's dissolution rate. This effect makes the BA of orally-administered drugs low.[7] To complete drug development, a suitable formulation strategy is key for the pharmaceutical development of poorly-soluble drugs. Efficient approaches could be crystal modification, micronization, amorphization, or pH modification. Oral drug absorption is also dependent on different drug properties such as particle size and the solubility of different drug forms. Thus, the choice of dosage form and optimization of the formulation have great value. It is important to understand the physicochemical and biopharmaceutical properties of drugs and their potential limitations.[7,45]

Understanding the physicochemical and biopharmaceutical properties of drugs helps when developing pharmaceutical products. As previously stated, BCS is useful tool in formulation

developments. Taking into consideration the different solubility and permeation characteristics of four BCS classes enables accurate formulation designs. BCS Class I drugs are highly soluble and highly permeable. For this class, there is no rate-limiting step for oral absorption and, to ensure rapid dissolution in the GI tract, conventional tablet or capsule formulations are used. BCS Class II drugs have low solubility and high permeability. They are commonly rate-limited by their dissolution, so the main priority is to increase dissolution rate. To enhance dissolution rate, the saturation solubility and the effective surface area need to be increased by, for example, crystal modification and amorphization. BCS Class III drugs have high solubility and low permeability. This class rate-limiting factor is membrane permeability in the GI tract. To enhance the permeability, it is necessary to increase the lipophilicity of a drug by changing its chemical structure. If a drug is hydrophilic, permeation is enhanced by adding to the chemical structure, for example, fatty acids, bile salts, surfactants, or polysaccharides. BCS Class IV drugs have low solubility and low permeability. For these drugs, the rate-limiting steps for absorption are both solubility and permeability. Formulation approaches similar to BCS Class II drugs could also be applied to BCS Class IV drugs.[7]

The poor aqueous solubility, and thus poor oral BA, has been the challenge in drug research and development. The limited dissolution rate, which is caused by low solubility, usually results in the low BA of orally-administered drugs. This may lead to dose escalation, until the blood-drug concentration reaches the therapeutic drug concentration range. However, this can cause topical toxicity in the GI tract. Various approaches have been developed to enhance the solubility, dissolution rate, and oral BA. Formulation strategy is the key tool for pharmaceutical development. Basic approaches for poorly water-soluble compounds are crystal modification, amorphization, and particle size changes.[7]

4.1.1 Salt formation and crystal modification

Salt formation is usually used for an ionizable drugs to enhance solubility and dissolution rate. Salts can be created via proton transfer from an acid to a base. When the difference of pK_a between an acid and a base, is greater than three, it can form a stable ionic bond. The counter ion containing salt is able to change the pH of the dissolution surface of a salt particle in the diffusion layer. This leads in an increased dissolution rate of the salts compared to free forms. The change of pH greatly influences the aqueous solubility of an ionizable drug. The solubility of a weak basic drug enhances exponentially with lowering pH at the pH range between pK_a

and pH of maximum solubility in the pH-solubility profile (pH_{max}). The dissolution rate and solubility of salts are impacted by the counter ion containing the salt. The suitable salt form has to be developed from the perspectives of both physicochemical and biopharmaceutical properties for poorly water-soluble drugs.[7] Using salt selection is a challenging method to translate from *in vitro* solubility to *in vivo* BA. Usually, salt forms with the highest solubility are chosen. These forms have the best solid-state properties for further drug development.[45] A particular salt usually has a different dissolution rate than the parent compound has. Salt formation limitations include reactivity with atmospheric water and CO_2, which leads to precipitation and epigastric distress due to high alkalinity.[46]

Co-crystal has been noticed to improve the rate of dissolution of poorly aqueous-soluble drugs. Co-crystal is a crystalline material which consists at least two separate components. Pharmaceutical co-crystal is usually composed in a stoichiometric ratio with an API and non-toxic guest molecule, which is also called as co-crystal former. Compared to salt formation, proton transfer between API and co-crystal former does not happen. The API and co-crystal former can not form a stable co-crystal without hydrogen bonding. To separate salts and co-crystals, ΔpK_a is a reliable indicator. The molecular complexes can be identified as co-crystals when the ΔpK_a is less than zero. When the ΔpK_a is between 0 and 3, the complexes can be even salts or co-crystals, or can have sheared protons. Co-crystals could be a candidate for enhancing the rate of dissolution of poorly-soluble drugs; for example, for the options that are not ionized at physiological pH.[7]

Particle size and the drug's ability to be wetted by luminal fluids are responsible for how much of the surface area of a drug is available for dissolution. Particle size is dependent on crystallization. Pharmaceutical co-crystals are formed by at least two or more separable molecules that are arranged to create a new crystal form. This crystal form's properties are usually better to those of each of the distinct entities. These co-crystals are typically formed between an ionic or molecular drug and a co-crystal former. The former needs to be solid under surrounding conditions. Pharmaceutical co-crystal is formed by slow evaporation from a drug solution containing co-crystal formers, or sublimation or grinding of two or more solid co-crystal formers in a ball mill.[47]

4.1.2 Amorphization

Amorphization is a process that changes a crystalline material into an amorphous state. An amorphous state is typically described as the disorganized arrangement of drug molecules in the solid state. Amorphous solids have random molecules that are short-ranged whereas crystalline solids have long-ranged ordered molecules. In the amorphization process, amorphous solids' lack of long-range structures leads to loose arrangement of molecules. This results in weaker intermolecular attraction forces and thus amorphous-state drug molecules have higher energy compared to crystalline solids. Amorphous-state drugs require less energy to go into solution state. In this state, the solvent molecules surround the drug's molecules and no energy is required to break the crystal lattice,. Therefore, amorphous drugs' solubility is usually higher than that of corresponding crystalline drugs.[7,46,48] Higher solubility increases the dissolution rate of a drug and therefore amorphization has been used to enhance poorly-soluble drug formulations and to improve intestinal absorption and oral BA.[48]

However, amorphous formulations are often chemically and physically less stable than the corresponding crystalline formulation, and stability is the main limitation of drugs in an amorphous state. Amorphous formulations have a tendency to transform from amorphous form to crystalline form, due to the high energy state of drug particles. This can lead to a reduction of oral BA, and thus amorphous formulations should not be formulated on their own.[7,48] Amorphous solid dispersion (ASD) technology was invented for the amorphous-stabilizing strategies.[48] By solid dispersion techniques, it is possible to obtain stable amorphous formulations. ASD is a distribution of active ingredients in amorphous and molecular forms that are surrounded by inert carriers, which are mostly polymers. These carriers disperse the amorphous drugs and thus prevent their recrystallization.[7,48]

The ASD formulations are usually manufactured by spray drying, lyophilization, melt extrusion, or with the use of supercritical fluids with polymeric surfactants. ASD formulations have been found to show 1.5-82-fold and 1.6-113.5-fold improvements in C_{max} and AUC when compared to crystalline formulations that contain bulk API. However, the ASD formulation technique also has its own limitations, such as the need for large amounts of carriers, the tendency to recrystallize during storage, and the possibility of thermal composition during formulation preparation. Thus, the ASD formulation technology can be unsuitable if an amorphous drug already has very low stability.[7]

4.1.3 Changes in particle size

For poorly-soluble drugs, one critical factor influencing the oral absorption is the drug's dissolution rate, which is highly effected by the drug's particle size. However, particle size is a feature that can be controlled. Thus, the search for the most suitable particle size is valuable in drug development, particularly with the compounds for which oral absorption is limited by dissolution rate. Particle size is included in the calculation for the dissolution constant (k_{diss}) in the Noyes-Whitney equation (6):[45]

$$k_{diss} = \frac{3 \times D_{eff} \times S}{r_p^2 \times \rho} \qquad (6)$$

where k_{diss} is the dissolution constant, D_{eff} is the effective diffusion coefficient, ρ is the drug density, r_p is the particle size, and S is the solubility.[45]

As seen in the Noyes-Whitney equation (6) the smaller particle size affects the dissolution, making it more rapid. It is caused by the increase in the drug particle's surface area.[45] The solubility is also related to particle size, because when a particle becomes smaller, the surface area to volume ratio increases (Figure 7). This larger surface area leads to better interaction with the solvent, which increases the solubility. Decreasing the diffusion layer thickness by cutting down the particle size, preferably to <5 μm, would result in accelerated dissolution. Summarized, increasing the surface area and decreasing the diffusion layer thickness leads to an improved dissolution rate.[7,46,47,49]

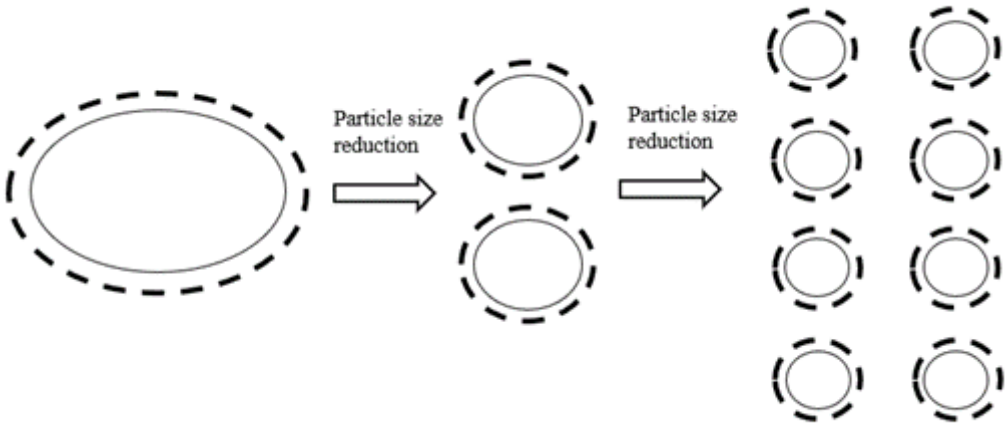

Figure 7. Particle size reduction increases surface area of drug particles. Adapted from Dizaj et al. 2015 with permission.[49]

A reduction in particle size can be accomplished by micronization, jet mill, rotor stator colloidal mill, and ball mill. These lead to an increase in surface area with enhanced dissolution. Micronization improves dissolution rate through larger surface area but does not increase equilibrium solubility. Micronization's weakness is that it can sometimes increase agglomeration of the drug particles. This can lead to a decrease of the surface area that is available for the dissolution. In these circumstances, surfactants can be used as wetting agents to increase the effective surface area.[7,46,47]

With conventional milling, the smallest particle size that can be reached for solid powders is about 2-3 μm. However, mechanical forces, like milling, can lead to limitations such as thermal and physical stress on drug product that can cause degradation. It can also limit the opportunity to control valuable properties of the end product, such as size, shape, morphology, and surface features. Also, the thermal stress, which can happen, for example, during spray drying, can have a negative effect when processing thermosensitive and unstable active compounds. Amorphous regions are thermodynamically unstable and are sensitive to recrystallization in hot and humid condition.[7,46,47]

For poorly aqueous-soluble drugs, particle size reduction to the nano-meter range <1 μm is an appealing approach. As previously mentioned, particle size reduction could achieve enhanced dissolution rate for drugs by increasing surface area and decreasing the diffusion layer thickness. When the particle size is reduced to under 1 μm, it increases the saturation solubility. The nanocrystal formulations are usually caused by wet-milling particles with beads, high-pressure homogenization, or controlled precipitation. Also commonly used are hydrophilic polymers or surfactants to stabilize nanocrystal suspensions. Nanocrystal technologies have been demonstrated to enhance the oral BA of pharmaceuticals and neutraceuticals. Nanocrystal formulations have also shown 1.7-60-fold and 2-30-fold improvement in C_{max} and AUC when compared to crystalline formulations with the particle range in micrometer size.[7]

Nanosuspension technology is a promising option for efficient delivery of poorly aqueous-soluble drugs. Nanosuspension is a sub-micron colloidal dispersion of drugs, which are stabilized by surfactants for either oral or topical use, or pulmonary or parenteral administration. In nanosuspensions, the average particle size is typically from 200 to 600 nm. Nanosuspensions are commonly prepared by media milling, high pressure homogenization in non-aqueous media, high pressure homogenization in water, and with the combination of high pressure homogenization and precipitation.[46] Nanosuspension technology is applied to poorly-soluble

drugs that are incapable of dissolving in both oils and water. A pharmaceutical nanosuspension is a two-phase system. It consists of nano-sized drug particles stabilized by surfactants.[47]

4.2 Excipients and surfactants

Due to a rising amount of APIs with lowered aqueous solubility, the use of solubilizing excipients use has increased. Excipients can enable formulations, enhance patient acceptability, or provide more safe and efficient drugs. They were previously known as pharmacologically inactive materials. Excipients can be inorganic or organic in composition. They may also be synthetic or semi-synthetic, or derived from natural sources or biological. They usually have functional groups that are able to interact with other materials. Solubilizing excipients include cosolvents, phospholipids, surfactants, and polymers. They are able to propagate, initiate, or participate in physical and chemical functions with an active substance. Chemical interactions can cause degradation of the active ingredient, which can reduce the amount available for therapeutic effect. Physical interactions usually affect the rate of dissolution, ease of administration, or uniformity of dose.[50,51]

The amount of excipients added to the dosage is usually higher than API. Excipients can be used in various ways within a formulation and can be binders or diluents, or can disintegrate in a solid dosage form. They have been included in drug formulation to help with administration, manufacturing, and absorption. Excipients are also added to formulations to enhance powder flow or compression. They are commonly used to improve drug stability, disintegration, and dissolution. Excipients are also used to improve oral BA by influencing drug solubility and permeability. The challenge of drug development is to find the best combination of excipients that will be sufficient with adequate BA, stability, and manufacturability. For example, adding more excipients to improve BA will affect the stability of the dosage form. If an excipient is used to stabilize unstable materials, this interaction usually leads to loss of quality.[50,51]

Surfactants are one form of excipients that are required to stabilize dispersed systems or can be used to enhance the solubility of poorly-soluble drugs.[46] They are amphiphilic molecules and composed of a hydrophobic and hydrophilic parts. Surfactant molecules contain two different units: a head and an extended group. The head group usually consists of a polar, ionic, or nonionic part, and the extended group is an apolar, organic residue.[52,53] These types of molecules' amphiphilic structure enables that they can interact with biological membranes. This

property increases permeability across skin or mucosa.[54] The common and widely used method to improve the performance of poorly water-soluble drugs is to use surfactants. Surfactants are used to reduce surface tension and thus enhance the dissolution of poorly water-soluble lipophilic drugs during *in vitro* tests.[55] They are also able to enhance wetting of solids and increase the rate of disintegration of solid into finer particles. The use of surfactants leads to stabilize microemulsions and suspensions into which drug are dissolved.[47] Surfactants have been united into solid dispersion to help processing and also to improve solubilization by micellization, which will be discussed more in detail in the next chapter. Adding surfactants into solid dispersions also results a decreasing in the glass transition temperatures of the composite materials and may lower the thermal processing temperatures.[55] To summarize their various properties, surfactants are used in solubilization, stabilization, wetting, and dissolution.[56]

4.3 Micelles

Due to surfactants' amphiphilic structure, they show self-assembling properties. When the surface is saturated, surfactants start to self-assemble in aqueous environments into supramolecular aggregates; their simplest form is as micelle. Micelles are formed when the concentration of surfactants exceeds their critical micelle concentration (CMC). CMC is typically in the range of 0.05-0.10% for most surfactants. Above a CMC, surfactants are able to form thermodynamically stable micelles. This micelle formation can entrap the drugs within the micelles. This process is also called micellization and usually it results in improvement of the solubility of poorly-soluble drugs.[47,57]

Micelles have well-defined structures and assembly behaviors. They are supramolecular aggregates, with hydrophobic tails that form the central core, and hydrophilic heads that are in contact with the aqueous environment forming outer shell (Figure 8).[57] Micelle formation occurs when an attractive force leads to the organization of molecules while the repulsive force prevents micelles' unlimited growth. The amphiphilic copolymers self-associate, when they are placed in a solvent that is selective for the hydrophobic or hydrophilic polymer.[58]

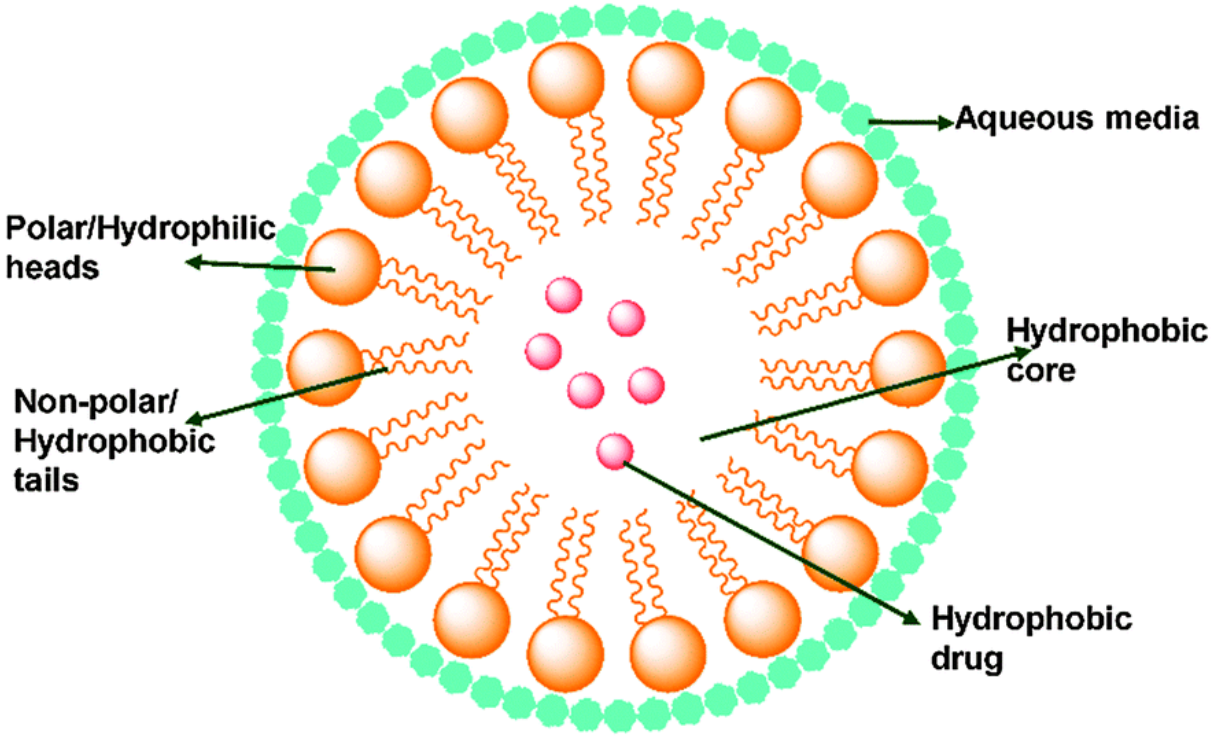

Figure 8. A hydrophobic, drug-loaded, polymeric micelle's structure. Reprinted from Seeta Rama Raju et al. 2015 with permission from the Royal Society of Chemistry.[59]

Micelles' size is commonly <50 nm. Their structure protects insoluble hydrophobic drugs and mimics biological transport systems in terms of function and structure. Micelles' advantages are their small size and the feasibility of their large-scale manufacture. Small micelles can enhance the *in vivo* performance of encapsulated drugs, which leads to high accumulation at the target site due to improved permeability and retention effect. This targeted drug delivery produces minimum drug degradation and loss, and prevents harmful side effects as well as increasing drug BA.[60] In addition to their small size, micelles' advantages are also shell-core structure, prolonged circulation time, and improved drug accumulation at a tumor site. Micelles are relatively easy to manufacture and have simple drug formulation. To determine micelles' size and morphology, transmission electron microscopy and dynamic light scattering are commonly used.[57]

Micelles can be polymeric or surfactant. Polymeric micelles are usually more stable than surfactant micelles. Polymeric micelles are able to solubilize a substantial quantity of hydrophobic molecules in their core. They possess prolonged circulation times *in vivo* due to their structural size and hydrophilic shell. Polymeric micelles have a typical micelle core and shell structure.[58]

Mixed micelles also have a core-shell structure which enables the poorly-soluble drug to incorporate and thus improves the BA and stop the inactivation in a biological medium. Mixed micelles are typically 5-200 nm and are able to accumulate in pathological areas with damaged vasculature. They can improve the epithelial transport of hydrophobic compounds across transcellular routes.[61] Mixed micelles can also improve drug-loading effectiveness and micelle stability when compared to micelles with the individual components. Phospholipid-surfactant mixtures can self-assemble to mixed micelles, depending of the composition. Phospholipid mixed micelles consist monolayers in which phospholipids are nontoxic and biocompatible.[58]

Molecular micelles are commonly consisted of bile salts and phospholipids. When these types of molecules interact with the intestinal fluid, they are able to solubilize and become included into the intestinal colloidal structures. These structures are able to import solubilized drugs closer to the absorption site.[61]

The limitations of micelles are their low stability in changing environments and, being below the CMC, their potential to disassociate. The surfactant composition is not enough to achieve the self-assembly of micelles, when a micelle solution is diluted to a very low concentration. This may lead micelles to distribute at the aqueous-organic solvent interface which may lead to their decomposition. To estimate the stability of micelles at low concentrations, it is critical to know CMC. The CMC is the main chemical-physical parameter which needs to be determined for pure surfactants to characterize the self-assembled aggregation and surface activity. These CMC values can be determined by tensiometry or fluoresxenxe spectroscopy.[53,54,57]

5 Different methods to study dissolution-permeation using *in vitro* procedures

5.1 *In vitro* methods to predict *in vivo* behavior

The development of dissolution media has led to the ability to make highly advanced assumptions of how a drug dissolves *in vivo*. Drug dissolution testing is part of a more complex experiment to simulate GI physiology. This type of testing has limitations which are dependent on the development phase and the delivery system under investigation. The principle of drug supersaturation, to increase the fraction of absorbed drugs, is the base for many modern delivery

systems of poorly-soluble drugs. Supersaturating systems consists of solid dispersions, salts, co-crystals, and nanoparticles. Other important trends in modern dissolution testing are real-time measurements and miniaturization. Sample aging or potential errors may happen with offline analytics. The amount of a drug, especially API, is usually very limited in early development, so parallel experiments can usually only be run on a small scale.[62]

It is crucial for efficient drug development to be able to predict the *in vivo* dissolution, absorption, and precipitation of oral drug formulations, and thus, reliable *in vitro* tests are needed.[8] A pharmacopoeia is a legally-binding collection of quality specifications and standards for drugs used in a region or country. A quality specification is a set of suitable experiments that will certify the purity and identity of the product within the pharmacopoeia's *in vitro* studies. It will also confirm the strength and amount of the API and if necessary, also the performance characteristics. A pharmacopoeia also includes pharmaceutical starting materials, intermediates, excipients, and finished pharmaceutical products. One of the main roles of a modern pharmacopoeia is to supply quality specifications for APIs.[63] Pharmacopoeia set-ups are generally used to test dissolution of drug products *in vitro*. The disintegration test is used to determine whether capsules or tablets decompose in a certain time at 37 ºC. Experimental conditions for this test are proposed by the pharmacopeia and the most suitable disintegration apparatus is used. Disintegration is a state in which any residue of the unit remaining on the screen of the apparatus, expect capsule shell or fragments, is a soft mass having no palpable core. The used medium is either water or USP SGF.[8]

The basket (apparatus 1) and paddle (apparatus 2) are the first *in vitro* dissolution testers introduced in the pharmacopeia. During these experiments it is necessary to consider the dosage form types, media volumes, stirring, and previous use in development. These can be used for all oral dosage forms. The used media volumes are commonly between 500 mL to 1000 mL. These volumes are useful to produce sink conditions for dissolution.[8] Sink condition is the ability of the medium. To achieve sink conditions, it demands at least three times the volume of medium, which is required to form a saturated drug solution.[64] However, these volumes may not always be relevant to *in vivo* situation, depending on whether or not the drug is given with meals. For example, the dosage form is usually ingested in the fasted state with just a glass of water, thus the gastric volume is usually only 250 mL and the volume used in a dissolution test will be too high to reflect the real condition in the stomach. It is found to be inconsistent to verify a relationship between *in vivo* hydrodynamics and stirring. The hydrodynamic effects are product-specific in the *in vitro* tests, and in the GI tract. One issue with stirring is also the coning

effect that can be shown at the bottom of the vessels. However, certain stirring set-ups have been found to be suitable for different drug products. For example, a paddle speed of 30 rpm is found to be the best option for IVIVC for Paracetamol tablets.[8]

A pharmacopeia's type 3 apparatus is the reciprocating cylinder apparatus. The apparatus is disintegration tested, by placing the dosage form in an open cylinder which has a sieve at the bottom. The cylinder is placed in the vessel in a water bath and then moved up and down across the medium. While using apparatus 3, it is necessary to consider a dosage form type, media volumes, hydrodynamics, and earlier use in drug development. The cylinder which moves back and forth is typically used for a diversity of oral dosage forms. It is difficult to create sink conditions because the used volume per vessel is relatively low. Therefore, it is not as suitable as the paddle or basket methods to IR dosage forms. The used media volumes are typically 250 mL per vessel. The hydrodynamic pattern is created by the movement of the cylinder. The hydrodynamic movement is corresponding stirring rated of paddle apparatus.[8]

A pharmacopeia's apparatus 4 is the flow-through cell. It consists of a reservoir containing the dissolution medium, a water bath, and a pump which causes medium to go upwards through the cell. The cell is constructed vertically and contains a filter system that is able to prevent that undissolved particles do not escape from the top of the cell. At the bottom of the cell typically locate small glass beads. To study solid dosage forms which are orally-administered, large and small cells are used. Apparatus 4 is typically used for testing the dissolution characteristics of modified-release (MR) dosage forms due to its ability to expose a single dosage form to different conditions throughout the GI tract.[8]

5.2 Flux

Molecular transport or mass transport of molecules in a solution through a barrier, for example a membrane, is typically measured by fluxes. The flux (*J*) of a solute can be described to be the mass or number of molecules moved through a given cross-sectional area during a certain period of time and it can be calculated using the following equation (7):[37,65]

$$J(t) = \frac{dm}{Adt} \qquad (7)$$

where *m* is the amount of drug crossing a unit area *A* perpendicular to its flow per unit time *t*.[65]

The movement of molecules in solution or molecular transport through different barriers and membranes can be a consequence of diffusion or migration (Figure 9). Migration is defined to be the motion of molecules caused by an external force. External forces can be gravity or hydrodynamic flow. Diffusion is, on the contrary, a process which consists of random thermal motion of molecules in a solution. Thus, diffusion can only cause a net transport of molecules within a concentration gradient.[37]

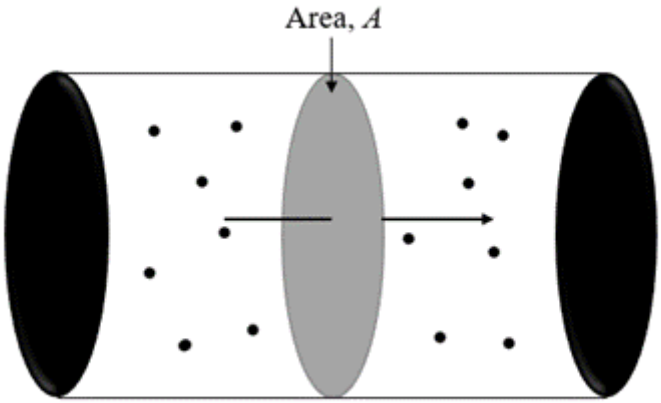

Figure 9. The flux movement of molecules across a membrane's area. Adapted from Brodin et al. 2002 with permission.[37]

Diffusional flux (*J*) can also be described by Fick's law with the following equation (8):[37]

$$J(x,t) = -D\frac{\partial C(x,t)}{\partial (x)} \qquad (8)$$

where *D* is a diffusion coefficient, *C* is the concentration gradient, *t* is time and *x* is position (length).[37]

Flux studies are commonly used in biopharmaceutical studies to research transport of drug candidates through a membrane tissue, such as small intestinal cell culture models. A common set-up for these types of experiments will consists a donor compartment where is a defined concentration of compound in a suitable volume. It also contains some sort of barrier or membrane with a defined thickness and cross-sectional area, and an acceptor compartment where initial concentration is defined (Figure 10).[37]

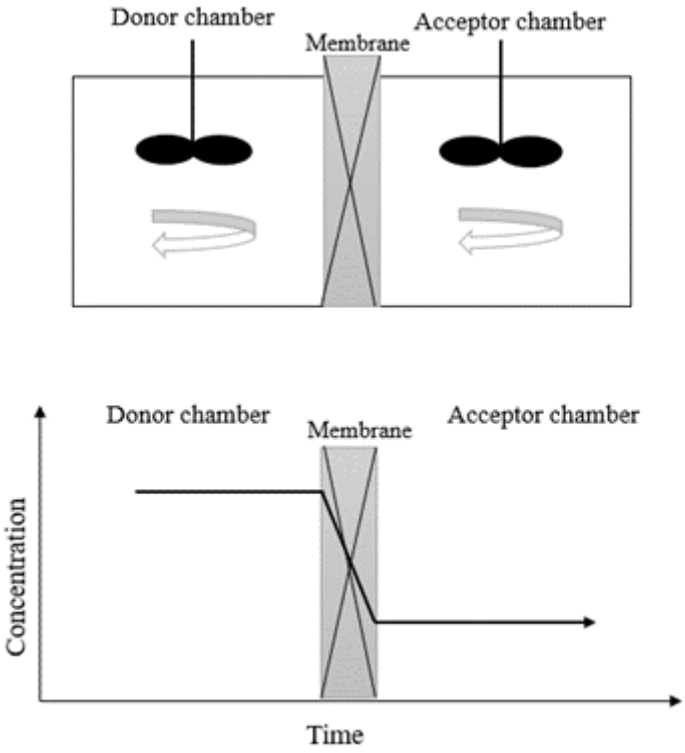

Figure 10. Typical two-compartment system for flux measurements and its concentration gradient. Adapted from Brodin et al. 2002 with permission.[37]

Efficient stirring in both compartments is essential to ensure that there is no concentration gradient within different compartments and thus the whole concentration drop happens through the barrier. Fluxes are measured by taking samples from the acceptor chamber at wanted timepoints after a test compound is added to the donor compartment. In the simple situation, the flux through the membrane transfer an insignificant amount of solute test compound, and the concentration gradient across the membrane is essentially constant. Then a simpler version of Fick's law can be used, as shown in following equation (9):[37]

$$J = P(C_{donor} - C_{acceptor}) \qquad (9)$$

where P is the permeability coefficient and C_{donor} and $C_{acceptor}$ are the concentrations of the drug substance in the donor and acceptor compartments.[37]

5.3 Small-scale methods

The amount of API that is available to do formulation development during early drug development is very limited. Thus, there's a need for the development of small-scale experimental tests that are able to perform high throughput measurements of dissolution rate and solubility using only a small amount of API. The main equipment and approaches include imaging based methods, miniaturized dissolution vessels, and small-scale automated dissolution instruments with *in situ* API concentration determination made by using UV fiber optic probes.[9]

Small-scale experiments avoid the use of large volumes of compendial dissolution testing. These experiments can be made with mini-paddle apparatus. One common mini-paddle vessel (Erweka GmbH, Heusenstamm, Germany) is a miniaturized version of a USP set-up. Only half the medium volume is used in the mini-paddle vessel. The dissolution test is reliable at this scale, but the choice of stirring speed is crucial and needs to be selected carefully. To screen numerous samples using minimal quantities, 96-well plates can be used. It only needs 2-5 mg of drug to compress minidiscs. Concentrations are analyzed offline by ultra-performance liquid chromatography (UPLC). The methods above are performed offline and the determination of equilibrium solubility and dissolution behavior are based on offline UV analytics and filtration or high-performance liquid chromatography (HPLC) analytics.[62]

UV fiber optics is used in real-time, miniaturized, drug dissolution testing. This technique uses sensitive array detectors and high-quality UV-grade optic filters. Drug dissolution can also be monitored from dissolution vessels by UV fiber optics. A UV fiber optic system can be used as an additional method for offline HPLC analysis but UV inline spectroscopy is also relevant for miniaturized dissolution tests. In multicomponent system, there is typically an overlay of UV spectra and interference occurs from particles. This light scattering observed from undissolved particles is wavelength dependent and can cause a baseline offset in the UV range. In the UV fiber optics it is necessary to analyze multiwave spectra and to use chemometrics.[62] When used *in situ*, UV fiber optic probes are able to monitor drug concentration over time during the dissolution by UV absorbance spectroscopy. They are especially suitable to study the early stages of dissolution due to its ability to collect absorbance spectra very frequently. UV fiber optic based equipment that is commonly used includes MicroDiss Profiler, SiriusT3, and inForm instruments (Pion Inc., Billerica, MA, USA).[9]

The MicroDiss system uses UV fiber optics to determine drug dissolution and solubility. It can also be used to research drug supersaturation and precipitation profiles. It is possible to run eight experiments in parallel at the same time. The other way of using this system is with a two chamber system MicroFLUX. This system measures drug concentrations in real-time in both the donor and acceptor compartments. MicroFLUX is based on a membrane to separate the compartments.[62]

SiriusT3 and inForm instruments are fully automated. They include autotitration and sample autoloader modules. SiriusT3 and MicroDiss Profiler have the same sample amount range from 5-10 mg. InForm sample amount is up to 100 mg. All of these equipment uses dissolution medium in the range of 3-80 mL. The dissolution medium's volume and used amount of API highlight the small-scale when compared to traditional determination of, for example, intrinsic dissolution rate (IDR) which is carried in six-vessel USP-specified dissolution baths that use 900 mL of dissolution media and 150-700 mg of API.[9]

For poorly-soluble drugs, a single compartment apparatus for dissolution tests has been used. However single-chamber tests are not the most sufficient tests to predict the *in vivo* behavior of supersaturating drug delivery systems. PermeaLoop™ is a novel prototype dissolution and permeation model which can model quite accurately the *in vivo* situation.[66,67] It was first custom-built by Sironi et al.[67] Permealoop consits of four main parts which are donor and acceptor compartments, a peristaltic pump, and a permeation cell (Figure 11). Permealoop is used by adding the studied drug formulation into the aqueous donor medium. After the addition, formed donor dispersion is pumped into the permeation cell. Donor dispersion consists dissolved fractions of drugs which can go through a biomimetic barrier, for example biomembrane, into the acceptor compartment. The acceptor compartment's medium is pumped into the acceptor side of the permeation cell. The liquid which is transferring across the permeation cell is able to transfer back into the respective reservoir to recirculate. It can also be pumped out of the system in the case of the acceptor chamber. These permeation cells are sculpted in a spiral shape which guarantees proper hydrodynamics and thus the mixing in the cell.[66]

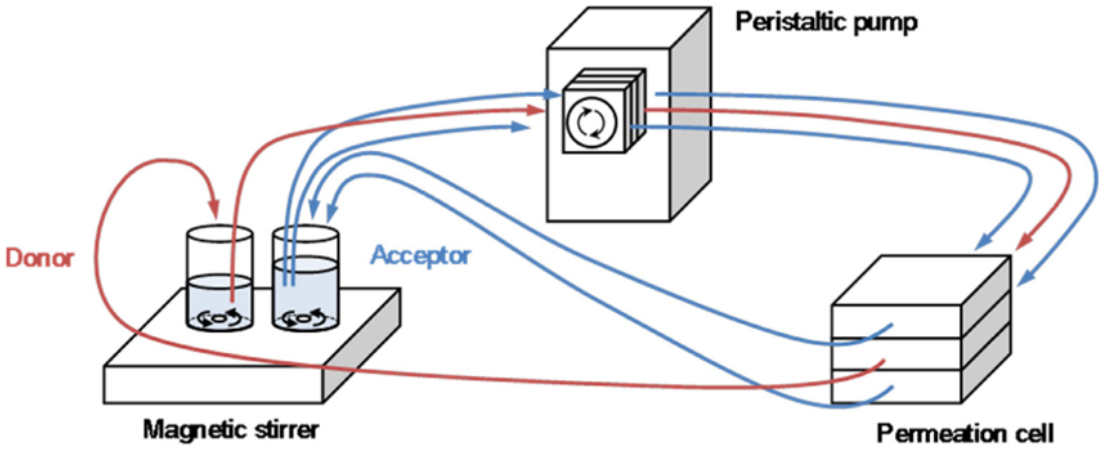

Figure 11. Schematic illustration of the PermeaLoop™ set-up. Reprinted from Sironi et al. 2018 with permission.[67] Copyright 2018 Elsevier.

In recent years, different *in vitro* tools have been developed to improve IVIVC. This has been done by simultaneous testing of absorption and dissolution or dissolution and permeability. The parallel artificial membrane permeability assay (PAMPA) (Pion Inc., Billerica, MA, USA) has been able to show the predictivity of passive permeability. It has also been a reproducible and cost-effective way to study formulations instead of animal testing. This led later on to the development of a scaled-up version of a PAMPA-like set-up, which led to the development of the previously mentioned MicroFLUX as well as MacroFLUX and BioFLUX (Pion Inc., Billerica, MA, USA).[65]

MicroFLUX is intended to be used with small volumes of 16-20 mL. It is a side-by-side diffusion cell apparatus.[65] As previously described in connection of MicroDISS, MicroFLUX measures real-time concentrations by fiber optic UV probes on donor and acceptor chambers which are separated by an artificial membrane (Figure 12). It has the potential to improve IVIVC by simultaneous measurements of dissolution and permeability, and thus reduce animal testing.[68]

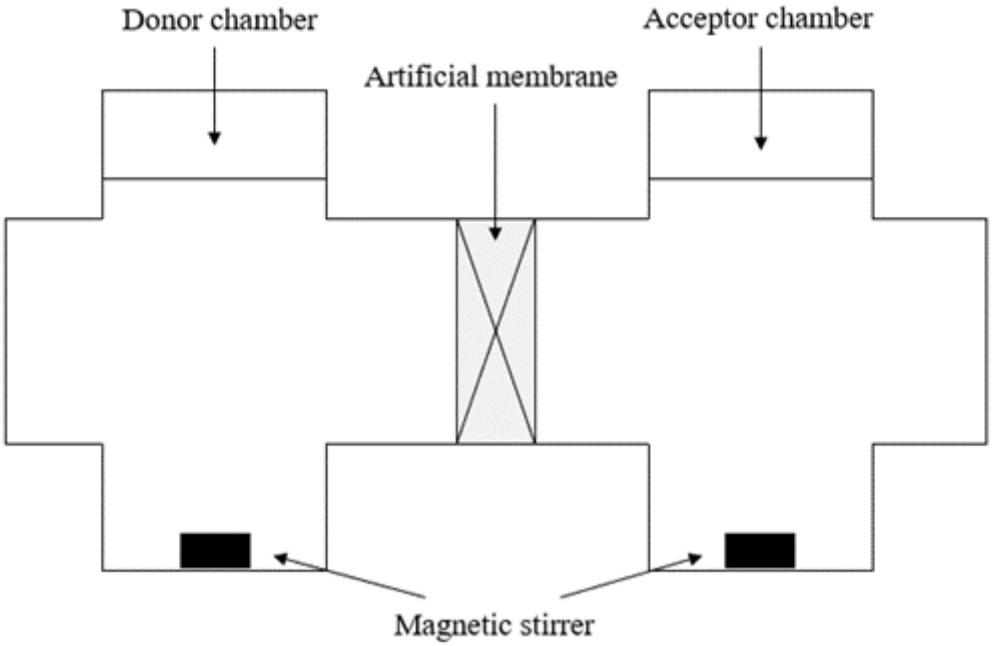

Figure 12. Schematic figure of the MicroFLUX apparatus. Adapted from Borbás et al. 2018 with permission.[68]

MacroFLUX is used with larger volumes than MicroFLUX. The volumes used with MacroFLUX are usually 850-1000 mL.[65] MacroFLUX apparatus subsumes an absorption compartment into USP I or II dissolution apparatus. Therefore it is able to perform simultaneous measurement of dissolution and absorption rates and thus could improve IVIVC. The acceptor chamber is integrated with overhead stirrer, fiber optic UV probe, and permeation membrane. The acceptor chamber is inserted in the vessel of USP I or II apparatus. PAMPA membrane or a filter-supported artificial membrane can be used to separate the acceptor chamber from the donor chamber. Fiber optic UV probes are positioned in the donor and acceptor chambers and produce a real-time concentration profile. From these profiles can be calculated flux results. These *in vitro* flux results could be compared to *in vivo* BE data.[69]

Similarly to MacroFLUX apparatus, BioFLUX apparatus subsumes an absorption chamber into a USP II dissolution apparatus. However, BioFLUX changes the used volume in the dissolution vessel from 900 mL to 200-250 mL, which is more biorelevant. BioFLUX is very similar to MacroFLUX apparatus, as BioFLUX also has the acceptor chamber which is integrated with an overhead stirrer, a fiber optic UV probe, and a permeable membrane (Figure 13). These parts are inserted into the vessel of a USP II apparatus. PAMPA membrane is usually used as an

integrated membrane and it separates the donor chamber from the acceptor chamber. Fiber optic UV probes are positioned in the donor and acceptor chambers and provide real-time concentration monitoring.[65]

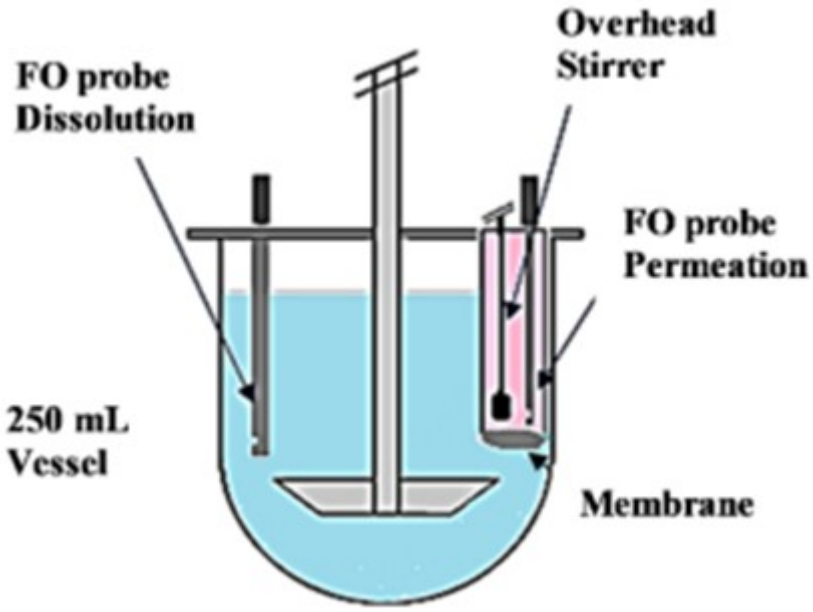

Figure 13. Schematic figure of the dissolution-flux device, BioFLUX. FO = Fiber optic. Reprinted from Borbás et al. 2019 with permission.[65]

EXPERIMENTAL PART

6 Aim of the study

The aim of this study was to investigate what effect experimental conditions have on the performance of a small-scale, dissolution-permeation model. The objective was also to investigate how solubility-enhancing suspension formulations performed *in vitro.* The aim was also to study how these *in vitro* results correlated with previously obtained *in vivo* results, and thus, whether the MicroFLUX dissolution-permeation method could efficiently simulate the conditions of rat's GI tract. The objective was also to investigate, which parameters and result presentation ways would be the most effective and accurate, and could produce the best correlation between *in vitro* and *in vivo* results. For example, the aim was to investigate whether flux or permeated amount -results were better for *in vitro* and *in vivo* comparisons. The objective was also to study whether MicroFLUX method was more efficient way to do dissolution-permeation measurements than donor side sampling tests.

7 Materials and methods

7.1 Materials

Methanol was manufactured by J.T. Baker (VWR, Helsinki, Finland). Dimethyl Sulfoxide (DMSO), acetonitrile, and formic acid were from Merck (Espoo, Finland). Reagents used in measurements are presented in Table 4 with concentration, purity values and manufacturer info.

Table 4. Reagents used in HPLC measurements

Reagent	Concentration	Purity	Manufacturer
Methanol (MeOH)	100 %	HPLC grade	J.T. Baker
Dimethyl Sulfoxide (DMSO)	100 %	> 99.9 %	Merck
Acetonitrile (ACN)	100 %	≥ 99.9 %	Merck
Formic acid (HCOOH)	0.1 %	99.4 %	Merck

Soluplus® was purchased from BASF SE (Ludwigshafen, Germany). Polysorbate 80 NF EP (Tween80), D-Tocopheryl polyethylene glycol 1000 succinate (TPGS) and

Hypromellose (HPMC) were received from Orion Oyj and their more accurate composition was not public information. Methyl Cellulose (MC) was purchased from Fujifilm Wako Pure Chemical Corporation (Osaka, Japan).

Phosphate buffer pH 3.0 was purchased from Oy FF-Chemicals Ab (Haukipudas, Finland). Biorelevant SIF -powder was received from Biorelevant.com Ltd. (London, UK). Acetate buffer pH 5.0 solution was obtained from Reagena Oy Ltd. (Toivala, Finland). Acceptor Sink Buffer (ASB) was purchased from Pion Inc. (Billerica, MA, USA).

Above mentioned materials' accurate purities were not available.

7.2 API and pre-treatments

The API (COMP A) used in this study was obtained from Orion Oyj (Espoo, Finland). COMP A development had been discontinued, but it was chosen for research due to its poorly solubility and the availability of *in vivo* results. Compound's chromatographic purity was 99.3%. COMP A's solubilities in 37 ºC after 48 h, in different media are presented in Table 5. COMP A was manufactured on October 2020 and it was used in the measurements with every API preparation.

Table 5. COMP A's solubility values in 37 ºC with different media after 48 h

	0.1 M HCl, pH 1.0	Phosphate buffer, pH 3.0	Phosphate buffer, pH 7.4	FeSSIF, pH 5.0
Solubility (µg/mL)	0.2	0.1	0.2	2.9

The API underwent three different pre-treatments before it was used in different suspension formulations. The API was also used without pre-treatment in its conventional form. In the nanoform, API was milled to form nanoparticles. Milling was performed at the same time as nanosuspension was formed. One of the pre-treatment forms was a co-crystal mass purchased from TeraCrystal (Cluj Napoca, Romania). The COMP A was also pre-treated to get it into ASD form. The pre-treatment was done by preparing an amorphous solid dispersion mass by forming a batch of API's ASD solution, and freeze-drying it 24 hours. Next the product was

vacuum dried for a further 24 hours. The finished ASD mass was collected and used for the preparation of ASD suspension formulation.

7.3 Vehicles and media

Three different types of vehicles were used in the preparation of suspension formulations: Soluplus, Tween80/MC, and TPGS/HPMC. Soluplus was used as polymeric solubilizer for ASD and co-crystal suspension formulations. Tween80/MC was used as solubilizer for conventional suspension and TPGS/HPMC was used for nanosuspension.

Two different media were used on donor sides. They were phosphate buffer in pH 3.0 and FeSSIF. FeSSIF medium was prepared by dissolving SIF -powder into pH 5.0 acetate buffer solution. Phosphate buffer pH 3.0 simulated stomach conditions and FeSSIF simulated the fed state conditions of the small intestine. According to SIF -powder's manufacturer, the prepared FeSSIF medium was recommended to be used within 48 hours. For all measurements, ASB was used as a medium on the acceptor side. ASB created sink conditions to the acceptor side. Media were incubated to 37 °C before transferring them to MicroFLUX's chambers.

7.4 Preparation of suspension formulations

The target concentration for all of the suspension formulations was 10 ± 1.0 mg/mL. The amount of prepared suspension varied between 4 mL to 5 mL, depending on the amount of API available and the needed amount of suspension formulation on the measurements. Conventional suspension and nanosuspension remained usable for several months. The co-crystal and ASD suspensions remained usable for only two hours after they were prepared due to the risk of instability. All the necessary analyses for these two suspension formulations, for example HPLC analyses, had to be carried out within two hours.

The conventional suspension formulation was prepared by measuring the API into the mortar and it was ground into finer particles. Vehicle solution (Tween80/MC) was added to the API and the suspension was formed by grinding the API into the vehicle solution.

The nanosuspension was prepared by adding TPGS/HPMC vehicle to API. The vehicle and API were added to the grinding chamber of a nanomill pulverisette 7 (FRITSCH, Idar-Oberstein, Germany). Pure Milli-q water and nanoballs were added to the grinding chamber and the chamber was transferred to the nanomill for the milling. The washing vehicle for the nanoballs was prepared with TPGS and HPMC. After the milling, the suspension was transferred to the volumetric flask, and nanoballs were washed by washing vehicle. The suspension obtained from washing was transferred to the volumetric flask.

For the ASD suspension, Soluplus vehicle was used. The suspension was made by measuring previously prepared ASD mass into the mortar. ASD mass was carefully pressed and ground in the mortar to a smooth mass. Soluplus vehicle was added on top of the mass and the ASD suspensions was formed by grinding the mass into the vehicle. The ASD mass was very electric and needed careful handling.

For the co-crystal suspension, Soluplus vehicle was used. Co-crystal API was measured into the mortar and Soluplus vehicle was added into the API. Vehicle and API were ground into co-crystal suspension.

7.5 Dissolution-permeation studies

7.5.1 MicroFLUX apparatus

The dissolution-permeation studies were made by using a MicroFLUX apparatus (Figure 14). The apparatus consisted four chamber complexes. One complex consisted an acceptor chamber which was separated from a donor chamber with a biomimetic gastrointestinal tract lipophilic polyvinylidene fluoride (PVDF) membrane (Pion Inc., Billerica, MA, USA) (Figure 15). Due to four chamber complexes, four replicate measurements could be performed at the same time. The GIT-0 dodecane lipid solution from Pion Inc. (Billerica, MA, USA) was added to the PVDF membrane to form a lipophilic membrane. Before chambers attachment, 28 µL of this membrane lipid solution was added.

MicroFLUX measurements needed two media: donor side and acceptor side. On the donor side, phosphate buffer pH 3.0 and FeSSIF were used. ASB was used on the acceptor side in all of

the measurements. After lipid solution was added to membrane and chambers were connected, 20 mL of phosphate buffer or FeSSIF medium was immediately added on the donor side, and 20 mL of ASB was added on the acceptor side. Media were quickly added, within a few minutes, because the biomimetic lipophilic membrane was not allowed to dry.

After additions of media, chambers were transferred to the MicroFLUX Profiler platform, which was heated by water bath to about 40.5 °C, allowing it to maintain the temperature of the chambers at body temperature of 37 °C. The chambers hydrodynamics were controlled by magnetic stirring and temperature control.

Chambers were monitored with fiber optic UV probes which were positioned in each of the chambers and it was ensured that there were no air bubbles in the probe heads. These probes allowed real-time dissolution and absorption concentration monitoring in donor and acceptor chambers. Concentration was monitored by connecting the fiber optic UV probes to the Rainbow Dynamic Dissolution Monitor® instrument (Pion Inc., Billerica, MA, USA). Pathlength probe heads of 5 mm were used at the end of the UV fiber optic probes. UV-spectra was monitored at the area of 200-720 nm. Results were collected from the UV-spectra's range of 310-360 nm. A second derivative was not used for calculating the results, because of the spectral disorder of low concentration levels. Baseline correction for obtained spectra was made at 580 nm. Collected spectra was analyzed and MicroFLUX apparatus' parameters were controlled by using AuPRO™ software, version 5.5.3.5413 (Pion Inc., Billerica, MA, USA). The software calculated the concentration-time data set using spectra obtained from the chambers and previously measured bluestandard curves with correlation coefficients (R^2) of 0.999.

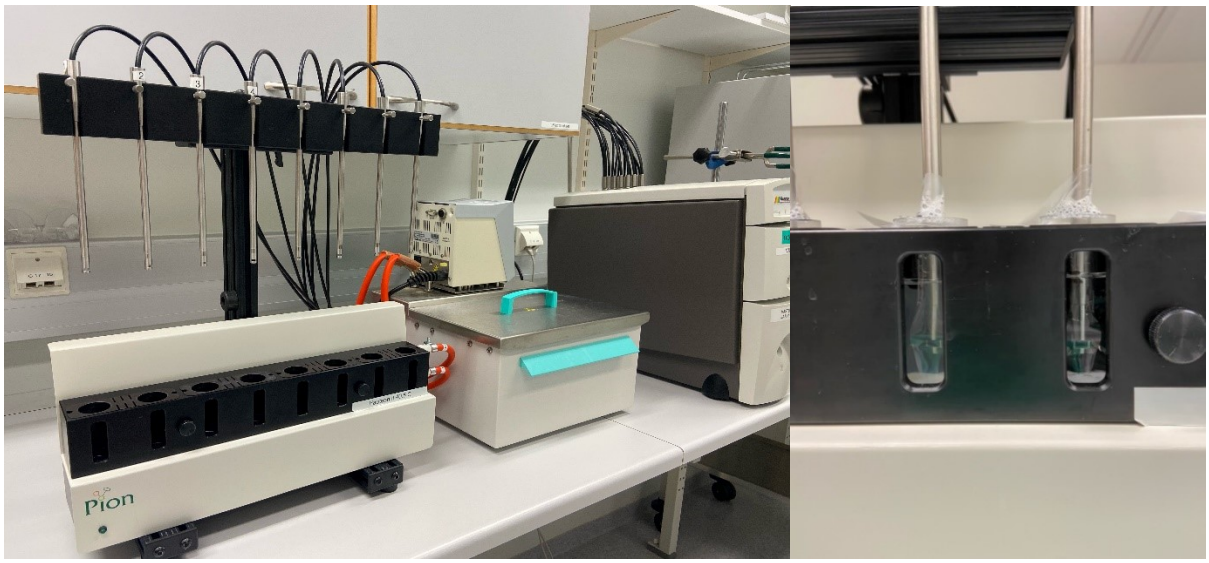

Figure 14. MicroFLUX apparatus and fiber optic probes in the chambers.

Figure 15. MicroFLUX apparatus' chamber complex.

7.5.2 Dissolution-permeation measurements

The measurement's optimization was started with AuPRO software. Before measurements were made, the baseline was checked and previously made bluestandards were added to measurement. MicroFLUX measurements were made with two doses on the donor side (40 µg/mL and 200 µg/mL). Concentrations of suspension formulations were about 10 mg/mL. In order to maintain the right volume throughout the measurements, and right dose effect in the beginning of the measurement, the same amount of buffer solution was removed from each of

the donor chambers as suspension formulations were added. Magnetic stirring and the measurement were started at the same time. Stirring speed in the chambers was 150 rpm. Immediately after starting the measurement and the stirring, the studied suspension formulations were added to each donor chamber. One measurement lasted for five hours.

MicroFLUX's dissolution-permeation studies were performed with four different suspension formulations. The measurements were made at both doses for each suspension formulation and the analyses were performed with donor chamber media, pH 3.0 buffer, and FeSSIF. Even though each MicroFLUX measurement set consisted of four replicate measurements, with some measurements, only two to three replicates were able to be measured due to leaking of the chambers or the observed spectral disorders. The fiber-optic probes collected spectra from both chambers. The collected spectra was analyzed and formed a concentration-time data set. The obtained data was exported to Excel for result analysis, calculations, and graphical presentations. From the data sets, concentration-time profiles were composed for each of the chambers.

7.5.3 Acceptor chamber's measurements

Dissolution-permeation measurements' results and concentration-time profiles were used for different purposes. The concentration in the acceptor chambers was monitored to see the effect of different suspension formulations on what amount of the API can permeate through the artificial lipid membrane and also to predict the amount of API which was dissolved on the donor side. Concentration results in the acceptor chambers were corrected to start from 0 µg/mL in order to compare the results from different chambers with each other.

From the obtained concentration-time profiles in the acceptor chambers, flux (J) was calculated. Time intervals for flux calculations were selected based on the linearity ranges of the acceptor chamber's concentration-time profiles. Linear range was studied from the acceptor chamber's concentration-time profiles. The linear range for each of the suspensions was searched from a 15-minute timepoint onwards. After this timepoint, it could be assumed that the conditions were stabilized and lag time was over, and therefore results were reliable. Linearity was reviewed from the beginning of the measurement before the concentration line began to curve. The linear range in the beginning was the area where the correct flux value could be obtained. A suitable linear range was searched with correlation coefficient being at least 0.99. Linear range was later

used to calculate flux values for each of the suspensions. The time intervals for linear range had to be selected differently for each of the suspensions due to their kinetics and observed noises at low concentrations.

Flux can be seen as a reverse way to measure an amount of dissolved API in the donor chamber. Due to this, flux could be presented as a slope of the acceptor chamber's concentration-time profiles' linear ranges. The slope, and therefore the flux represents the amount of dissolved API in the donor side's medium. The rate is dependent on the concentration of dissolved API, so if the concentration is low on the donor side, the slope and thus flux value are also low. Flux (*J*) was calculated by using the following equation (10):

$$J = \frac{\Delta P}{A \cdot \Delta t} \qquad (10)$$

where ΔP is the linear range's change in amount of permeated drug (µg), A is the area of the membrane (cm^2) and Δt is the timerange (min) of the linear range.

The correlation of flux values to *in vivo* results were searched for by examining the linear range in selected timepoints for each suspension. Correlation was also searched for with flux values, which were obtained from the linear range which had timepoints uniform to every suspension. These uniform timepoints needed to be in the range of every suspension's selected timepoint range. Flux values were compared to *in vivo* data to find the correlations between *in vivo* and *in vitro* results. To observe the obtained correlation data, a logarithmic scale was used.

Concentration-time profiles were used to calculate the amount permeated (*P*) by using the following equation (11):

$$P = C_A \cdot V_C \qquad (11)$$

where C_A is concentration (µg/mL) of acceptor chamber and V_C is the volume (mL) of chamber.

The amount permeated represents the dissolution-permeation model's ability to permeate API through the lipophilic membrane. It can be used also to observe suspension formulations' dissolution abilities by ranking these formulations according to their observed permeated amounts. This is due to the fact that only dissolved API is able to permeate.

The correlation of amount permeated to *in vivo* results, was searched by examining the correlation at different timepoints. Chosen timepoints were 40, 60, 120, 180, 240, 280 and 300 minutes. The aim was to observe the correlation throughout the whole measurement. To observe the obtained correlation data, a logarithmic scale was used.

7.6 HPLC measurements

7.6.1 High-performance liquid chromatography system

HPLC apparatus used in the analyzes was Agilent 1100 (Waldbronn, Germany) equipped with a column Kinetex 2.6 µm C18 100 Å, 50 x 3 mm (Phenomenex, Torrence, CA, USA). Column temperature was 50 °C and flow rate 0.8 mL/min. During the analyses, 0.1% formic acid and acetonitrile were used as eluents (Table 4). The inject volume was 5 µL, 15 µL or 30 µL depending on the sample. Wavelength was 246 nm. Methanol was used as a sample solvent and washing solution. The HPLC apparatus was controlled and obtained data was processed with a Waters' Empower software (Lempo), version 2.0 (Milford, MA, USA). The software calculated concentrations using previously measured standard curves with correlation coefficients of 0.998. Processed data was exported to Excel for result analysis and graphical presentations.

7.6.2 Concentration and dissolved fractions of suspension formulations

Concentration and dissolved fraction analyses were made with HPLC apparatus. Analyses were carried out on fresh ASD, co-crystal and conventional suspension formulations which were prepared on the same day as HPLC analyses were performed. Only the nanosuspension formulation was analyzed by HPLC a few days later after the preparation. The HPLC apparatus gave reliable results if the obtained absorption peak was under 1.5 AU.

The samples for analysis of concentration were prepared by pipetting 100 µL of suspension formulation into a 10 mL volumetric flask and dissolving it to methanol. The dissolved sample was transferred to an HPLC vial for the HPLC analysis. Three replicate samples were prepared.

For the dissolved fraction analysis, 500 µL of suspension formulation was pipetted into two Eppendorf tubes. Samples were centrifuged for 10 minutes, at the temperature of 27 °C and at 10 000 rcf. After centrifugation, sample solutions were filtered into new Eppendorf tubes via 0.45 µm polytetrafluoroethylene (PTFE) filter (Millex, Merck, Espoo Finland). Filtered sample solutions were divided into three Eppendorf tubes. Then 100 µL of filtered sample solution was pipetted into an HPLC vial and 900 µL of methanol was added. Three replicate samples were prepared and dissolved fraction analyses were performed by HPLC apparatus.

7.7 Sampling analyses from donor side

During dissolution-permeation studies, sampling analyses were carried out on two donor side chambers (Ch1 and Ch3). Sampling was carried out on dissolution-permeation measurements with the dose of 40 µg/mL. Since sampling was carried out with normal MicroFLUX measurement, the initial preparations for the measurement were identical to the previously described MicroFLUX measurement. Sampling measurements were made to phosphate buffer pH 3.0 and FeSSIF media. The sample of each timepoint was filtered with a filter of 0.45 µm and with four timepoints, previously filtered samples were filtered again with a filter of 0.02 µm (Whatman Anotop 10, Cytiva, Marlborough, MA, USA). With two replicates of each step, each timepoint resulted in a total of two to four samples. Sampling samples were measured using the HPLC device. The inject volume for HPLC measurements was 15 µL for samples with 0.45 µm filtration, and 30 µL for 0.02 µm filtered samples.

Sampling was performed at seven different timepoints. Timepoints were 30, 60, 90, 120, 180, 240, and 300 minutes. Prior to the start of the MicroFLUX measurement, 80 µL of a buffer under measurement was taken to an Eppendorf tube and 80 µL of MeOH was added onto it to create a blank sample. At each timepoint, 600 µL of the media was pipetted from the two previously selected donor chambers into two Eppendorf tubes. The pipetted sample solution was filtered with a syringe and a 0.45 µm filter. From the filtered sample solution, 50 µL of solution was pipetted into new Eppendorf tubes and 50 µL of MeOH was added. After mixing the obtained sample, it was pipetted into the inner tube vial for HPLC analysis. The remaining sample after 0.45 µm filtration was filtered again through the 0.02 µm filter with a syringe into new Eppendorf tubes with timepoints of 30, 90, 180, and 300 minutes. From the filtered sample solution, 40 µL was pipetted into an inner tube vial and 40 µL of MeOH was added. The 0.02 µm filtered samples were analyzed by HPLC apparatus.

The obtained data was processed and later on exported to Excel for result analysis, calculations, and graphical presentations.

7.8 Donor side dose effect test

The aim was to monitor the change in concentration rate in terms of time as a result of different doses, and find the concentration were the rate changed between different doses. The results ensured the correct doses for the dissolution-permeation measurements. The linearity test was performed with MicroFLUX apparatus, and used 10 mg/mL ASD suspension formulation was made from an old batch of ASD mass (prepared 24.8.2020).

A dose effect test was performed according to normal MicroFLUX measurement, but four different doses were measured in each of the four double-chambers. Selected concentrations in the donor chambers were 10 µg/mL, 25 µg/mL, 50 µg/mL and 100 µg/mL. Each level of concentration was measured by one donor-acceptor chamber complex, so there were no replicate samples. The samples taken were processed and transferred to HPLC for the concentration analysis. The obtained data was exported to Excel for result analysis and graphical presentations.

7.9 Accuracy test

The accuracy test was performed to test that all of the MicroFLUX's 5 mm probe heads worked properly and were suitable for measurements. The accuracy test was also made to confirm that the obtained MicroFLUX results were valid and bluestandard was still usable for all of the measurements. Test was performed with Pion's MicroDISS apparatus with 5 mm pathlength probes. The software used was AuPRO, and bluestandards were used.

Stock solution of 200 µg/mL was prepared from the Orion's COMP A which was dissolved in MeOH. The accuracy test was made in two media, with ASB and phosphate buffer pH 3.0 in combination with methanol in a ratio of 50:50. Sample solutions of different concentrations were prepared from the stock solution. The doses measured in the phosphate buffer/MeOH measurements were 5 µg/mL, 10 µg/mL, 20 µg/mL and 40 µg/mL. Concentrations were

selected according to the assumed concentration levels of the donor sides of dissolution-permeation studies. Media were incubated to 37 °C.

Measurements were performed with MicroDISS tubes. Each measurement set included eight MicroDISS measurements and thus eight replicates. Each concentration sample set was divided into its own MicroDISS tubes. The sample volume in microDISS tubes was approximately 2.5 mL. Measurements were started by checking the baseline and measuring a blank sample that was pure medium. Each medium with different concentration samples was measured one by one. The probes were carefully rinsed with pure water and methanol between each concentration. Each measurement measured five sample points every 30 seconds, allowing one measurements to last 2.5 minutes. The obtained data was exported to Excel for result analysis and graphical presentations.

Accuracy tests were made to eight MicroDISS fiber optic probes in two different media, phosphate buffer pH 3.0, and ASB. Concentration measurements were made every 30 seconds at five timepoints: 0 min, 0.5 min, 1 min, 1.5 min and 2 min. The concentration result used in the review was selected to be the fifth timepoint, at the two-minute time mark. This timepoint was selected because the measurement conditions could be assumed to be stabilized by this timepoint.

Measured doses were blank sample, 5 µg/mL, 10 µg/mL, 20 µg/mL and 40 µg/mL. The target concentration for 5 µg/mL dose was 5 ± 0.5 µg/mL. For 10 µg/mL dose the target concentration was 10 ± 1.0 µg/mL. The target concentration for 20 µg/mL dose was 20 ± 2.0 µg/mL. For 40 µg/mL dose, the target concentration was 40 ± 4.0 µg/mL.

8 Results and discussion

8.1 *In vivo* results

The *in vivo* measurements and data had been made during 2019-2020. It had been performed with rats in the fed state. Rats had been given similar to studied formulations with a dose of 100 mg/kg. Studies had been made to study the *in vivo* performance of four different suspension formulations which were also used in *in vitro* studies. These effects had been calculated and presented with the parameters of mean of the C_{max} and mean of the AUC_{0-24}. (Table 6). AUC_{0-24} had been observed in a timeperiod of 24 hours. From the data can be seen the ranking between suspension formulations. Conventional suspension had the lowest ranking, then was the nanosuspension. ASD and co-crystal suspensions had the highest ranking, depending on the used parameter.

Table 6. C_{max} and AUC_{0-24} values from *in vivo* data

Suspension	Mean C_{max} (ng/mL)	Mean AUC_{0-24} (h*µg/mL)
Conventional	438.7	6.6
Nano	1350.0	27.5
ASD	4543.3	41.0
Co-crystal	3613.3	46.1

8.2 In vitro results

8.2.1 Donor side dose effect

Results showed the change between a dose of 100 µg/mL and 50 µg/mL (Figure 16). Up to a dose of 50 µg/mL, a visual change in concentration rate can be observed. No further change in acceptor chamber concentration can be observed between 50 µg/mL and 100 µg/mL doses. The concentration levels over time remain almost the same even though the dose of 100 µg/mL was twice as high as 50 µg/mL. Results show that the acceptor side concentration might no longer be in the dynamic range when the donor side dose was 100 µg/mL or more.

Prepared ASD suspension's concentration was 10.1 mg/mL, and dissolved fraction was 7.4 mg/mL. These results were in line with the concentrations and dissolved fraction of the

other ASD suspension prepared, so the suspension could be considered suitable for the test and to give the correct results.

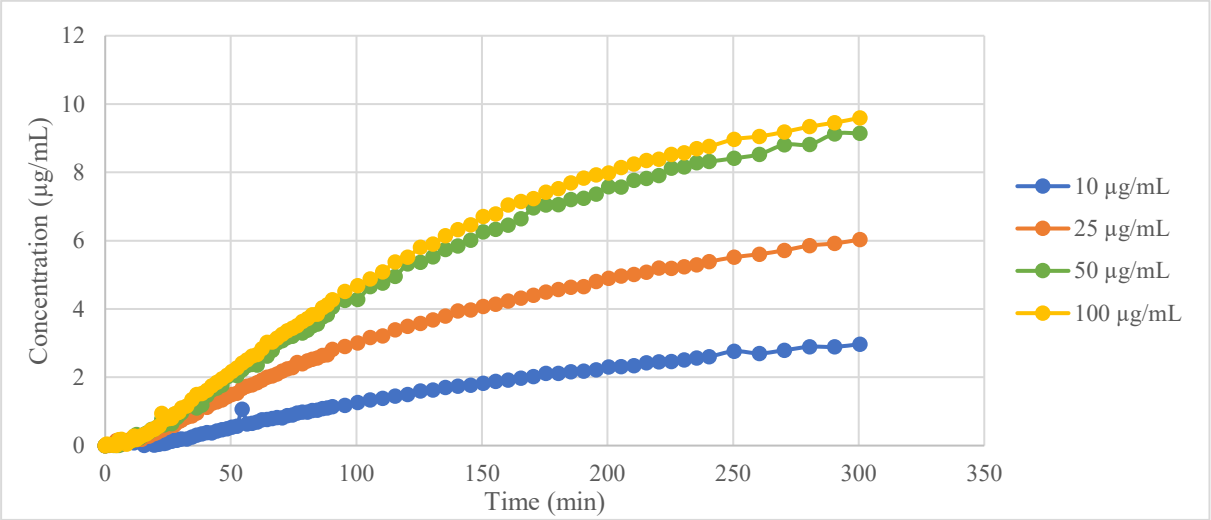

Figure 16. MicroFLUX's dose effect test, results taken from acceptor chambers. ASD suspension's concentrations (µg/mL) over time (min) with different doses shown on the right in medium of phosphate buffer pH 3.0.

Thus it can be concluded that the change in the concentration of the sample between 50 µg/mL and 100 µg/mL has almost no effect on the change in acceptor chamber concentrations and therefore on the flux effect. Therefore the concentration level of 200 µg/mL might not be the most efficient to obtain results and it may be possible to obtain similar results or even better results with lower doses. The linear change in flux value and thus more dynamic area was seen before the concentration level of 50 µg/mL. Therefore the other studied dose for suspension formulations in the donor chambers was selected between 25 µg/mL and 50 µg/mL and was chosen to be 40 µg/mL. This change enabled saving the amount of suspension formulations and therefore the API needed with MicroFLUX measurements.

8.2.2 Acceptor chamber's concentration-time profiles

Two doses showed a small differences between obtained concentration levels. ASD and co-crystal suspensions' concentration levels had the most notable differences between the dose of 200 µg/mL and 40 µg/mL (Figure 17 and Figure 18) in both media. However, with a dose of 200 µg/mL, levels of the acceptor chamber concentrations were not as high as expected. Suspensions had been administered to 200 µg/mL doses at a concentration five times higher

than to 40 µg/mL doses but the difference in the acceptor chamber's concentrations between these two doses were not five times higher. Conventional and nanosuspensions' concentration levels did not change as much between different doses, especially in phosphate buffer. It can be assumed that this was due to a very low concentration of 40 µg/mL doses, in which case, relative to this, the dose increase did not have a significant effect. Conventional and nanosuspensions may have reached their dissolution limits. In FeSSIF, the nanosuspension's concentration level increased a little bit but the change was quite small; from 2.5 µg/mL to 3.4 µg/mL. Nanosuspension was the only suspension with a concentration level a little bit higher, with a dose of 40 µg/mL compared to results with a dose of 200 µg/mL. It was not in line with the results from other suspensions, but the difference between these two doses' concentration levels was quite minimal and might be due to a random change which occurred in measurement. Replicate measurements would be needed to follow the trend with nanosuspension and to examine whether the dose really does effect the obtained concentration level.

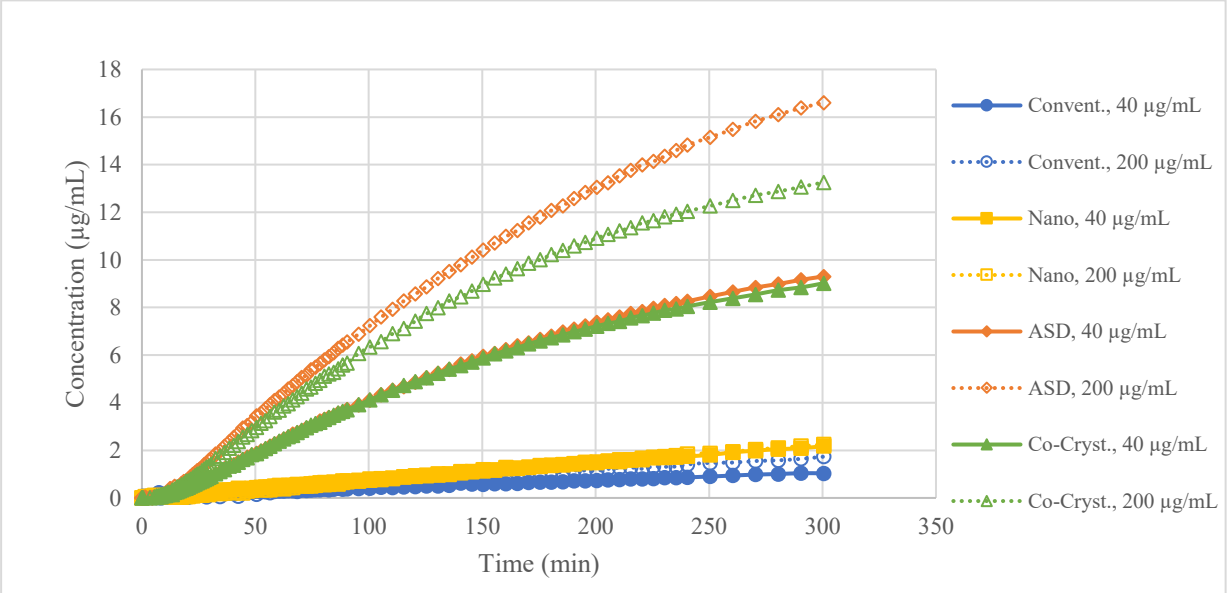

Figure 17. Different suspension formulations' acceptor chambers' concentrations (µg/mL) over time (min) with doses of 40 µg/mL and 200 µg/mL and with medium of phosphate buffer pH 3.0.

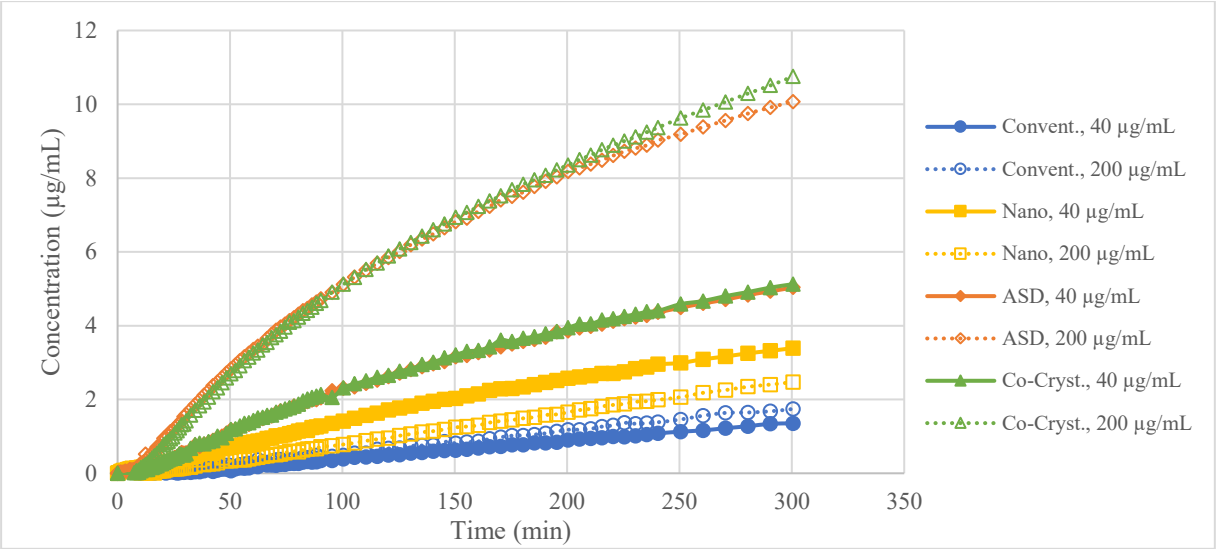

Figure 18. Different suspension formulations' acceptor chambers' concentrations (µg/mL) over time (min) with doses of 40 µg/mL and 200 µg/mL with medium of FeSSIF.

Both doses yielded a similar ranking as each other. The ranking was more dependent on the used medium. With phosphate buffer medium, ASD suspension had the highest ranking and conventional suspension the lowest. With FeSSIF medium, co-crystal suspension ranking was little bit higher than with ASD suspension. However, with FeSSIF, the co-crystal suspension had practically the same concentration level as ASD suspension and therefore the ranking between these two suspensions was quite difficult. With phosphate buffer, the difference between ASD and co-crystal suspension was notably larger and thus the ranking was more distinct. With FeSSIF, the differences between other suspensions were decreased due to lower concentration levels of ASD and co-crystal suspension, and higher concentration levels of conventional and nanosuspensions. Therefore, the used medium was seen to also effect the obtained concentration levels of suspensions as well as did the dose. With a dose of 40 µg/mL, the effect of FeSSIF medium to decrease the differences between suspensions was seen more clearly. When compared, the doses and the changes between results made using phosphate buffer and FeSSIF, decreased the differences between suspensions significantly more with a dose of 40 µg/mL. However, acceptor chamber's results showed similar ranking between suspension formulations as previously observed from *in vivo* data (Table 6). Thus, the ranking between suspension formulations was correct.

From the obtained results, it can be concluded that a dose had an effect on the observed concentration levels. However, the concentration levels did not increase five times higher as expected. Thus the larger dose of 200 µg/mL may not be within the dynamic range and therefore a lower dose is enough to obtain correct ranking and concentration results. This observation

was well correlated with the previously observed donor's side dose effect. However, from the results, it was seen that with the dose of 40 µg/mL in FeSSIF it was difficult to rank ASD and co-crystal suspensions. Therefore, with FeSSIF medium it might be necessary to use a higher dose than 40 µg/mL to achieve higher concentration levels and therefore better separation between suspensions. With phosphate buffer, the lower dose was enough to obtain selective ranking.

It can also be concluded from the results that, on top of the dose effect, the used medium had also a significant effect on the obtained results. As already seen with the different doses, the used medium also effected the obtained concentration levels and therefore the rankings. This effect was particularly seen from measurements made in FeSSIF. Conventional suspensions remained with the lowest ranking in both media, but ASD and co-crystal suspensions changed ranking in phosphate buffer and FeSSIF. Results showed also that with the FeSSIF medium, differences between each of the suspensions were smaller than with the phosphate buffer pH 3.0. FeSSIF seemed to decrease differences of concentration levels. With phosphate buffer pH 3.0, the difference between two of the lower ranking suspensions and two of the higher ranking suspensions was significantly larger than with FeSSIF. FeSSIF is known to be able to form micelles, which might affect the amount permeated through the membrane if dissolved API distributes to micelles. It also had not been studied what effect SIF would have on membrane and whether it effects its functions. Thus it can be concluded that the SIF surfactant of FeSSIF medium might affect the permeability or formation of micelles. These results indicated that different media gave significantly different results between suspensions and therefore, in the future, it is important to consider which medium is suitable for the current measurement. In drug development, it is important to monitor the behavior of the drug under different conditions and thus it might be valuable to consider if it is necessary to make measurements in both media to obtain the best and most accurate results.

8.2.3 Donor chamber's concentration-time profiles

Results with phosphate buffer pH 3.0 medium (Figure 19) showed different ranking between four different suspensions; these were different from the results in the acceptor chamber (Figure 17). The most significant difference was the ranking of nanosuspension. With the filter of 0.45 µm, nanosuspension had the highest concentration level in pH 3.0 buffer. Nanosuspension appeared to pass the 0.45 µm filter. However, other suspensions' rankings

were similar to those seen in the acceptor chamber results. With the filter 0.02 µm the ranking between suspensions were quite similar to acceptor side's results (Figure 20). However, there was a difference in behavior between the ASD and co-crystal suspensions in the latter timepoints. The concentration range of the suspensions was quite low and timepoints were at relatively long intervals, so even a slight change was highlighted and thus it could be said that with the 0.02 µm filter the ranking between suspension formulations was still correct for the latter timepoints.

With the exception of the conventional suspension, the concentration level of all other suspensions decreased significantly after the filtration of the 0.02 µm filter. The biggest difference was noticed with nanosuspension, for which the concentration level collapsed after the 0.02 µm filtration. The filter of 0.02 µm seemed to be able to filter the nanoparticles. The decrease in suspension formulations' concentrations seemed to prove that the 0.02 µm filter was able to filter suspensions well and thus show the right ranking and the amount of free dissolved particles that were present in the medium at the chosen timepoints.

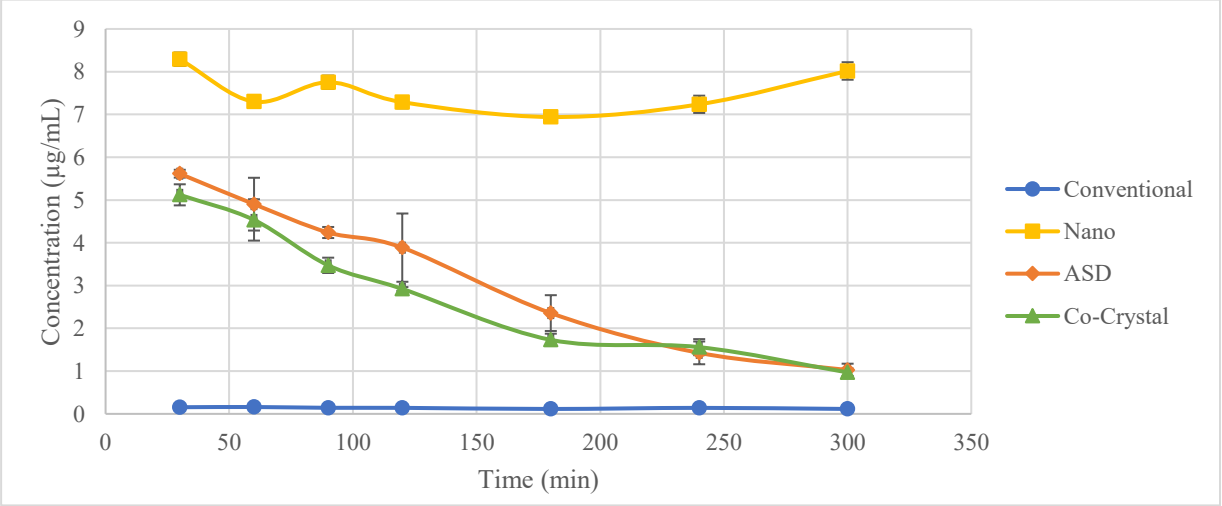

Figure 19. Different suspension formulations' donor chamber's concentrations (µg/mL) over time (min) after 0.45 µm filtration, with dose of 40 µg/mL and with medium of phosphate buffer pH 3.0.

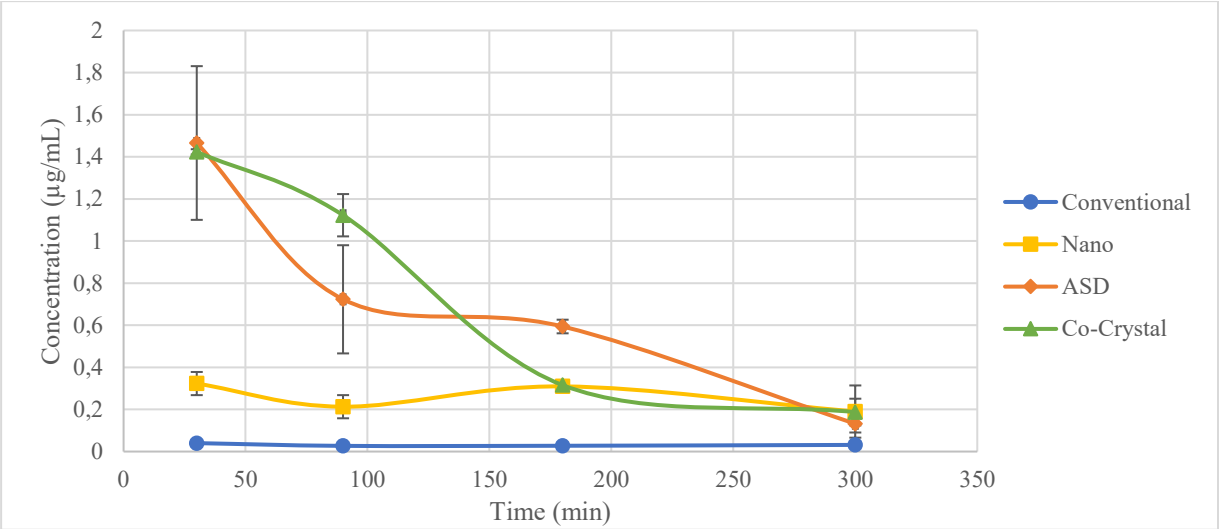

Figure 20. Different suspension formulations' donor chamber's concentrations (µg/mL) over time (min) after 0.02 µm filtration, with dose of 40 µg/mL and with medium of phosphate buffer pH 3.0.

Results with FeSSIF medium (Figure 21 and Figure 22) showed a ranking between conventional and nanosuspensions similar to the ranking shown in the acceptor chamber results (Figure 18). ASD and co-crystal suspensions also had the correct ranking. As was seen in the acceptor chamber's concentration-time profiles with a dose of 40 µg/mL in the FeSSIF medium, the ranking between ASD and co-crystal suspensions was not clear. The difference between these two suspensions was very small. However, it could be stated that the ranking between these two formulations was the same between the acceptor side and *in vivo* results.

With the exception of nanosuspenion, all other suspensions' concentration levels remained almost the same whether sample was filtered with 0.45 µm or 0.02 µm filter. Nanosuspension was the only one with a decrease in concentration levels to half after 0.02 µm filtration. This supported the previous finding that nanoparticles were able to go through the 0.45 µm filter and 0.02 µm filter was able to filter nanosuspension. However it seemed odd that other formulations concentrations were not decreased after 0.02 µm filter. It seemed that the used medium, FeSSIF could have affected the filtration.

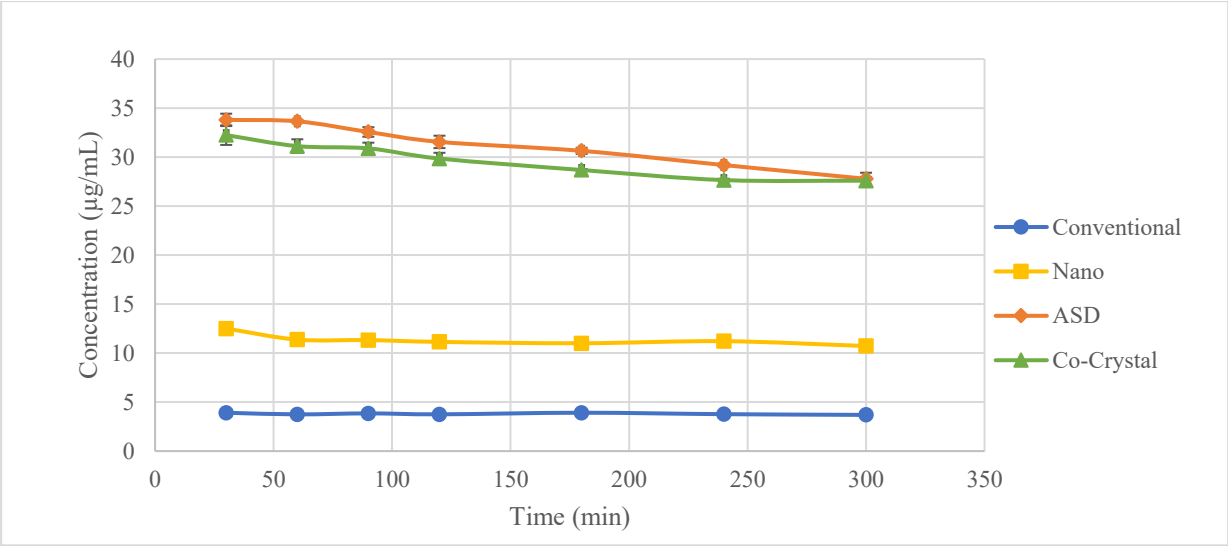

Figure 21. Different suspension formulations' donor chamber's concentrations (µg/mL) over time (min) after 0.45 µm filtration, with dose of 40 µg/mL and with medium of FeSSIF.

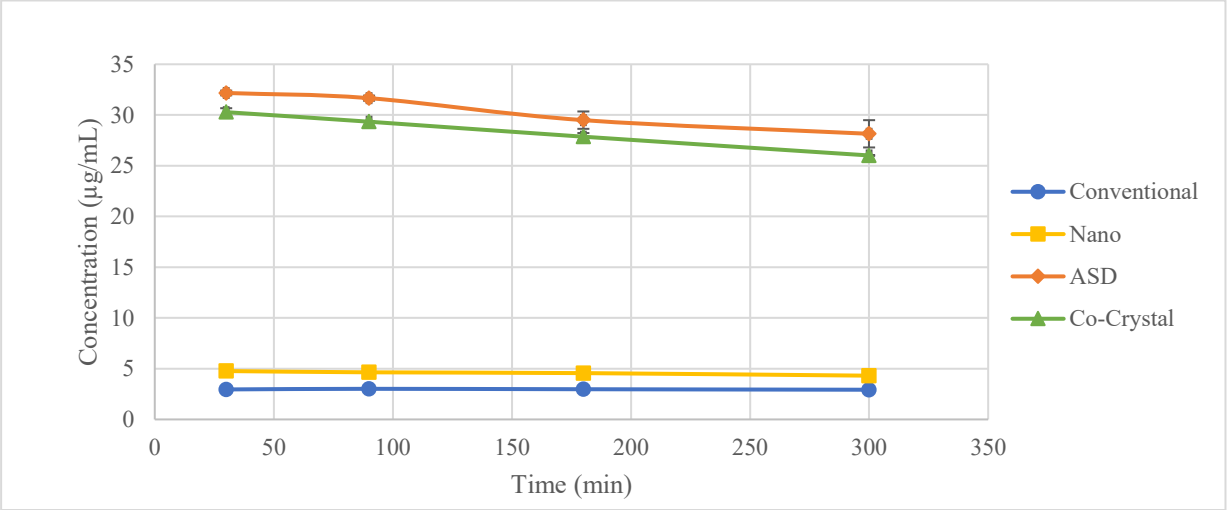

Figure 22. Different suspension formulations' donor chamber's concentrations (µg/mL) over time (min) after 0.02 µm filtration, with dose of 40 µg/mL and with medium of FeSSIF.

When summarizing the donor chambers' results in pH 3.0 or FeSSIF medium, it could be said that results differed from each other depending on the used medium. The most significant difference was the concentration levels in both media. The concentrations remained multiple times higher in FeSSIF than in pH 3.0 medium with each of the suspensions and filtration. The concentration of nanosuspension was also considerably higher in FeSSIF despite whether the sample was filtered with 0.45 µm or 0.02 µm filter. Therefore, 0.02 µm filtration might not be able to filter all micelles that FeSSIF might form, because otherwise the nanosuspension concentration should be the same in both media after 0.02 µm filtration. FeSSIF medium seems to have a notable effect on the concentrations.

The difference in FeSSIF results compared to pH 3.0 also shows the affect that different filters have on concentration. With FeSSIF medium, the concentration levels remain the same even after the 0.02 µm filtration, despite the nanosuspension. Instead, with pH 3.0 medium, the 0.02 µm filter decreased the concentration significantly. It can be stated that measurements made in FeSSIF were highly affected by the composition of FeSSIF. Suspension formulations had different vehicles and they might perform differently with different media. Therefore, these different vehicles and media, especially FeSSIF, need further research in the future.

Results obtained from donor chambers showed that sampling from the donor side gave the same ranking with formulations as seen with MicroFLUX's acceptor side and *in vivo* results. However, it was seen that the used medium had a significant effect on the results' concentrations and behaviors. It was observed that FeSSIF medium seemed to effect filtration and results. Thus it can be concluded that the donor side sampling test was comparable to MicroFLUX measurements when the test and sampling were made in phosphate buffer pH 3.0. However, when comparing the methods, it was noted that donor side sampling is more time consuming and more expensive. Donor side sampling included expensive 0.02 µm filters, and measurements included several steps including sampling, filtration, sample preparation for HPLC measurements, and HPLC measurements. These steps took time and resources to obtain the same results as were observed with MicroFLUX with just a few steps. Therefore, it can be said that donor side sampling is an option to observe the dissolution of different formulations but MicroFLUX studies were more efficient and the measurements also give valuable permeation data from the same measurement.

8.2.4 Linearity of acceptor chamber's concentration-time profiles

The measurement made with dose of 40 µg/mL (Figure 23) showed that a conventional suspension's concentration-time profile curve remained linear throughout almost the whole measurement in both media. The concentration levels in acceptor chambers were quite low, which caused the noise that was detected as a quite large deviation in the first 150 min. Due to this and the sustainable linearity of the entire measurement, the linear range was chosen to be a a wide range of 20-270 min in pH 3.0 and 42-220 min in FeSSIF to obtain suitable correlation coefficients of 0.994 and 0.996. Correlation coefficients were found to be very similar between two media with dose of 40 µg/mL.

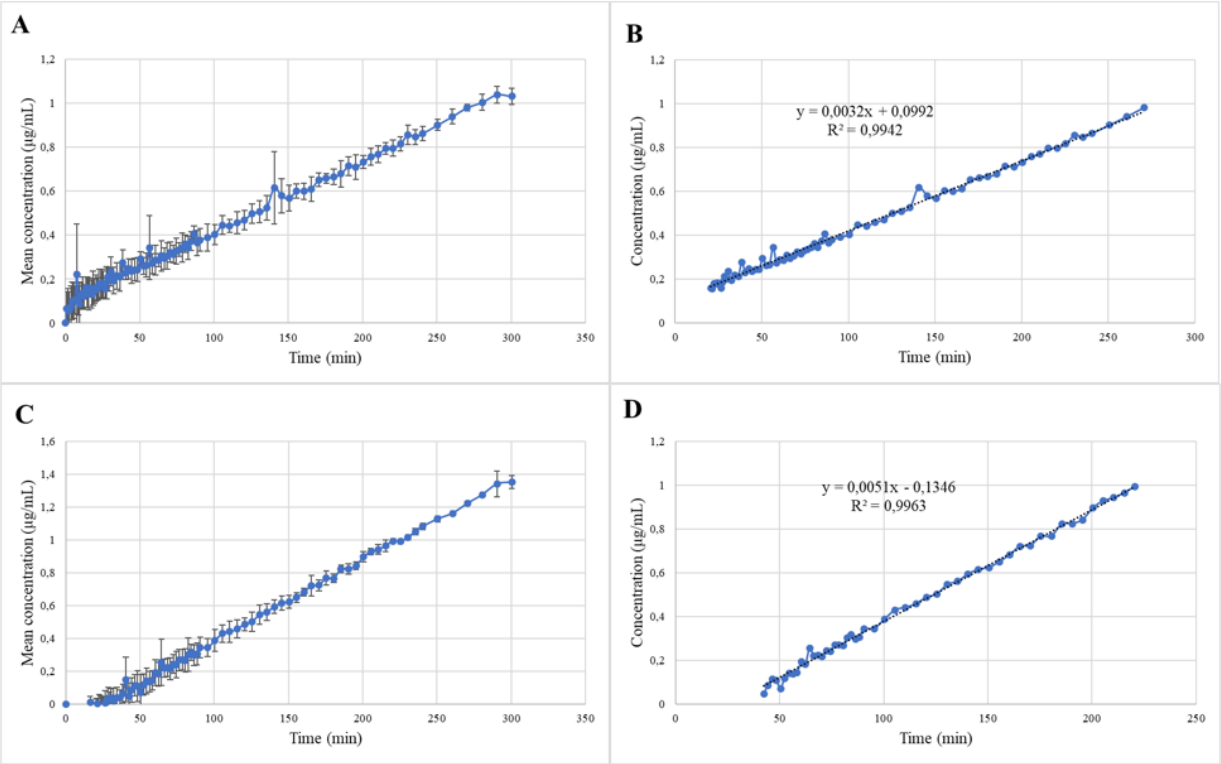

Figure 23. Conventional suspension's acceptor side concentration (µg/ml) results over time (min) and linear ranges with dose of 40 µg/mL. A = Concentration-time profile in pH 3.0, B = Linear range in selected timepoints 20-270 min in pH 3.0, C = Concentration-time profile in FeSSIF, D = Linear range in selected timepoints 42-220 min in FeSSIF.

The measurement made with dose of 200 µg/mL (Figure 24) showed that conventional suspension's concentration-time profile curve remained mostly linear during a measurement in both media, similarly as seen with a lower dose. The concentration levels were again quite low in acceptor chambers, which caused the noise and deviation throughout the measurement. Especially with measurement made in phosphate buffer, a lot of deviation was detected between replicate measurements which affected the concentration-time profile's linearity. Therefore, an acceptable correlation coefficient was not found. The best R^2 value for this measurement was found to be 0.980 in the range of 40-270 min. For measurement made in FeSSIF, the linear range was chosen to be a wide range of 40-225 min to obtain a suitable correlation coefficient of 0.994.

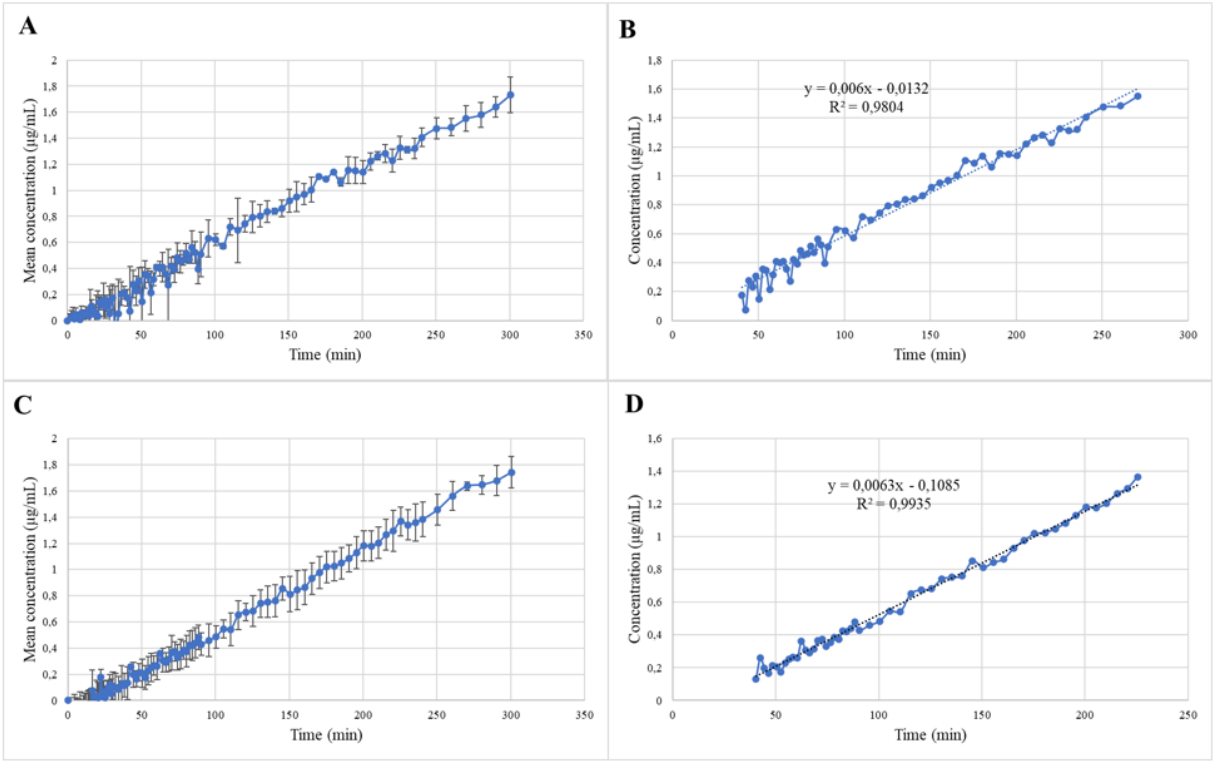

Figure 24. Conventional suspension's acceptor side concentration (µg/ml) results over time (min) and linear ranges with dose of 200 µg/mL. A = Concentration-time profile in pH 3.0, B = Linear range in selected timepoints 40-270 min in pH 3.0, C = Concentration-time profile in FeSSIF, D = Linear range in selected timepoints 40-225 min in FeSSIF.

All of the conventional suspensions' correlation coefficients were used later on the flux measurements even though one of them was not at least 0.99. However, this was assumed to be due to spectral disorder, and possibly a better wavelength range or different baseline correction from the UV spectrum could have provided less deviation in the beginning of the measurement. Concentration levels in conventional suspension results were very low and a bigger fiber optic probe head, for example 20 mm instead of 5 mm, could have been used to obtain a better result with such a low concentration level. However, it was decided to use the same parameters and equipment components throughout the measurements, to assure that the results were as comparable as possible.

The measurement made with dose of 40 µg/mL (Figure 25) showed that nanosuspension's concentration-time profile curve remained linear throughout almost the whole measurement in both media, similarly as what was seen with conventional suspension. The concentration levels in acceptor chambers were also quite low, which might have caused the deviation which was seen during the whole measurement. However, this deviation did not cause as much noise as seen with conventional suspension. Due to small disturbances in the beginning and the stable

linearity of the entire measurement, the linear range was chosen to be a wide range of 38-195 min in pH 3.0 and the obtained correlation coefficient for this range was 0.997. For the measurement made in FeSSIF, as shown in Figure 25, around the timepoint of 120 min there was a minor curving in the line. Due to this curvature, the suitable linear range was found to be from 20 min to 120 min to obtain a correlation coefficient of 0.999. Correlation coefficients were found to be very good and similar between two media with dose of 40 µg/mL.

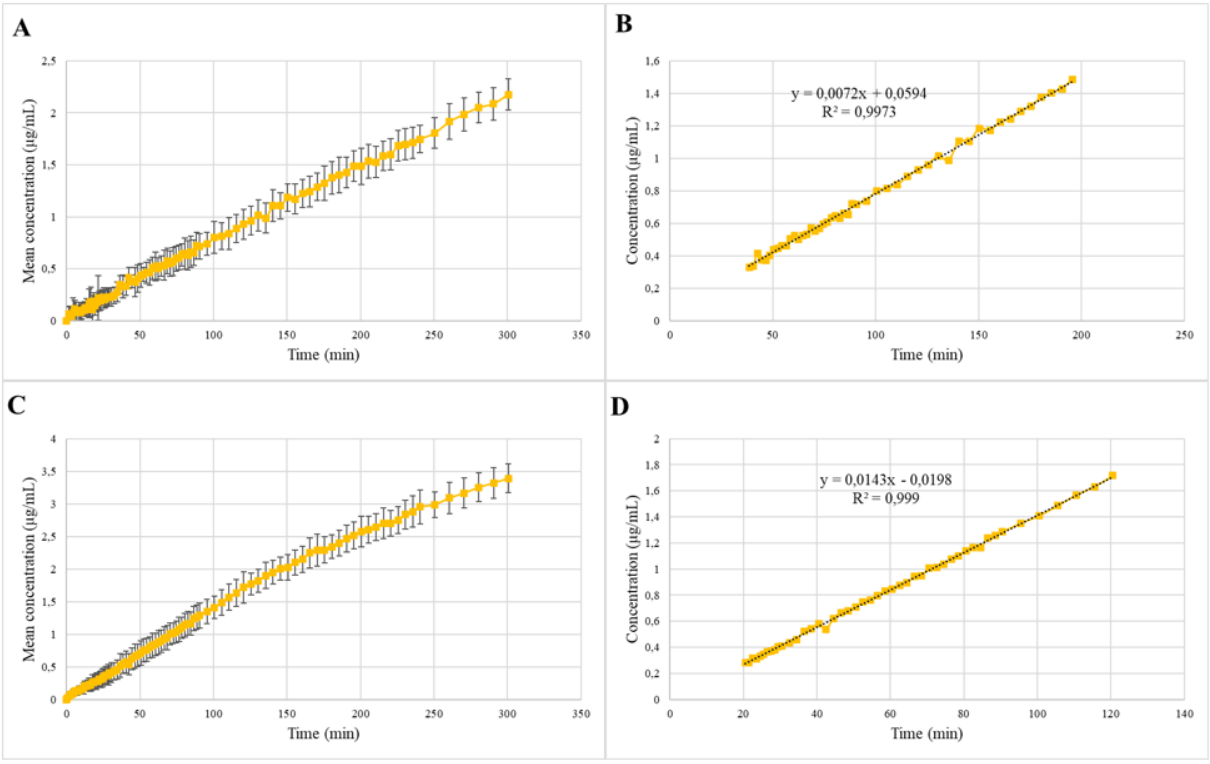

Figure 25. Nanosuspension's acceptor side concentration (µg/ml) results over time (min) and linear ranges with dose of 40 µg/mL. A = Concentration-time profile in pH 3.0, B = Linear range in selected timepoints 38-195 min in pH 3.0, C = Concentration-time profile in FeSSIF, D = Linear range in selected timepoints 20-120 min in FeSSIF.

The measurement made with a dose of 200 µg/mL (Figure 26) showed that nanosuspension's concentration-time profile line remained mostly linear during a measurement in both media, similarly as seen with lower dose. The concentration levels were again quite low in acceptor chambers which caused some disturbances in the beginning. However, when compared to the results of lower dose, with a dose of 200 µg/mL there was much less deviation. Due to disturbances in the beginning and the overall linear appearance of the concentration-time profile, the linear range was chosen to be a wide range of 40-210 min in pH 3.0 and 40-200 min in FeSSIF to obtain suitable correlation coefficients of 0.996 and 0.998. Correlation coefficients were found to be very similar between two media with dose of 200 µg/mL.

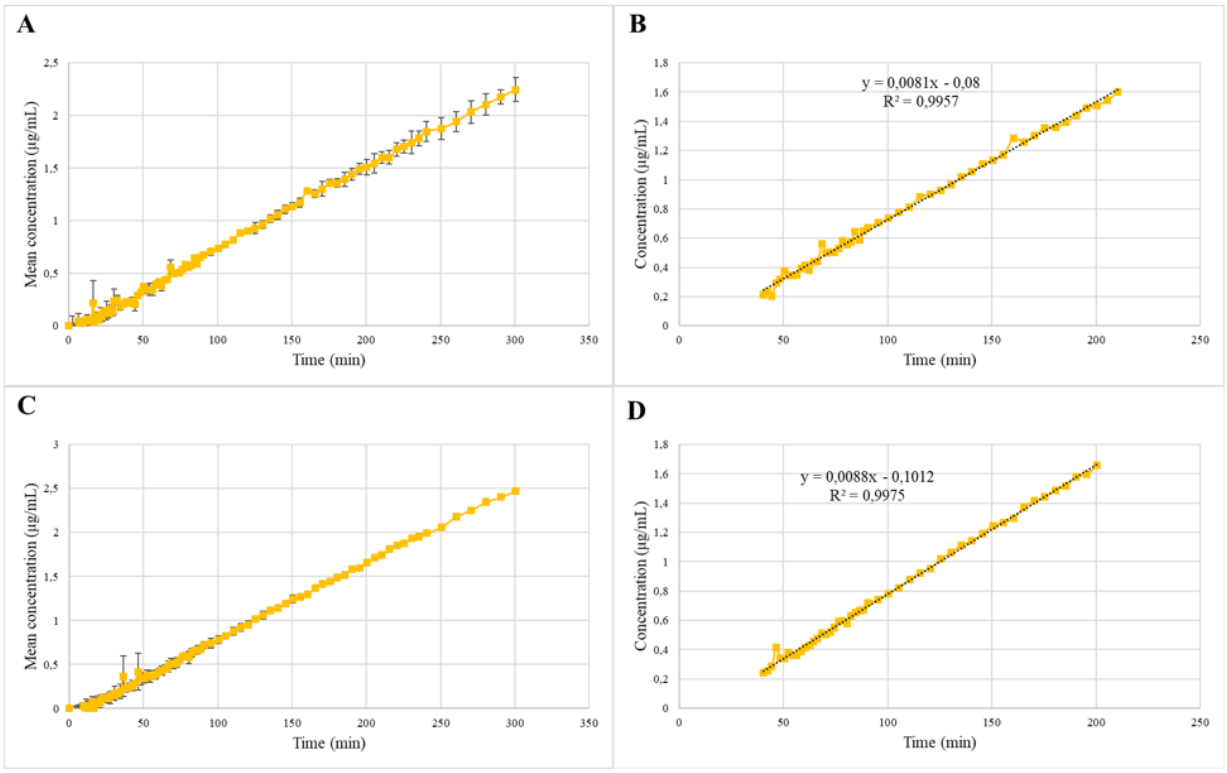

Figure 26. Nanosuspension's acceptor side concentration (µg/ml) results over time (min) and linear ranges with dose of 200 µg/mL. A = Concentration-time profile in pH 3.0, B = Linear range in selected timepoints 40-210 min in pH 3.0, C = Concentration-time profile in FeSSIF, D = Linear range in selected timepoints 40-200 min in FeSSIF.

From ASD suspension's dose of 40 µg/mL concentration-time profiles (Figure 27) in both media showed that the profiles' curves started to slowly bend after about 100 min. With phosphate buffer, the profile also showed how the deviation increased towards the end of the measurement. With FeSSIF, the deviation was quite minimal. Due to curvature after about 100 min, the linear ranges were observed before that timepoint. The best linear ranges with best correlation coefficient were found to be between 20-90 min in pH 3.0 and 20-78 min in FeSSIF to obtain suitable correlation coefficients of 0.999 and 0.997. Correlation coefficients were found to be very good and similar between two media with dose of 40 µg/mL.

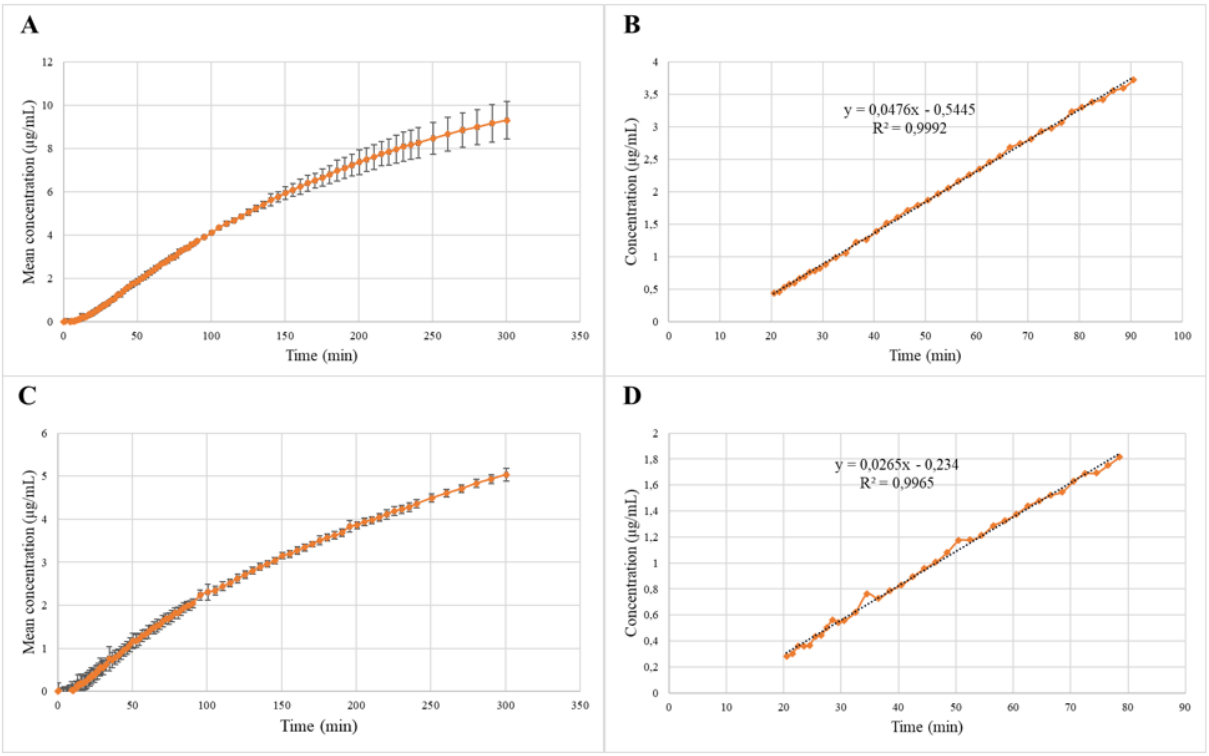

Figure 27. ASD suspension's acceptor side concentration (µg/ml) results over time (min) and linear ranges with dose of 40 µg/mL. A = Concentration-time profile in pH 3.0, B = Linear range in selected timepoints 20-90 min in pH 3.0, C = Concentration-time profile in FeSSIF, D = Linear range in selected timepoints 20-78 min in FeSSIF.

Quite similarly as seen with a dose of 40 µg/mL, ASD suspension's concentration-time profiles at a dose of 200 µg/mL (Figure 28) started to slowly bend after about 90 min in both media. The deviation remained the same with both media and increased a little bit towards the end of the measurement. Due to curvature after about 90 min, the linear ranges were observed before that timepoint. The best linear ranges with best correlation coefficient were found to be between 20-88 min in pH 3.0 and 20-78 min in FeSSIF to obtain suitable correlation coefficients of 0.999 and 0.996. Correlation coefficients were found to be good and very similar with the ones observed in a measurement made with dose of 40 µg/mL. Even the linear range between timepoints 20-78 min was the same in measurements made in FeSSIF regardless of used medium.

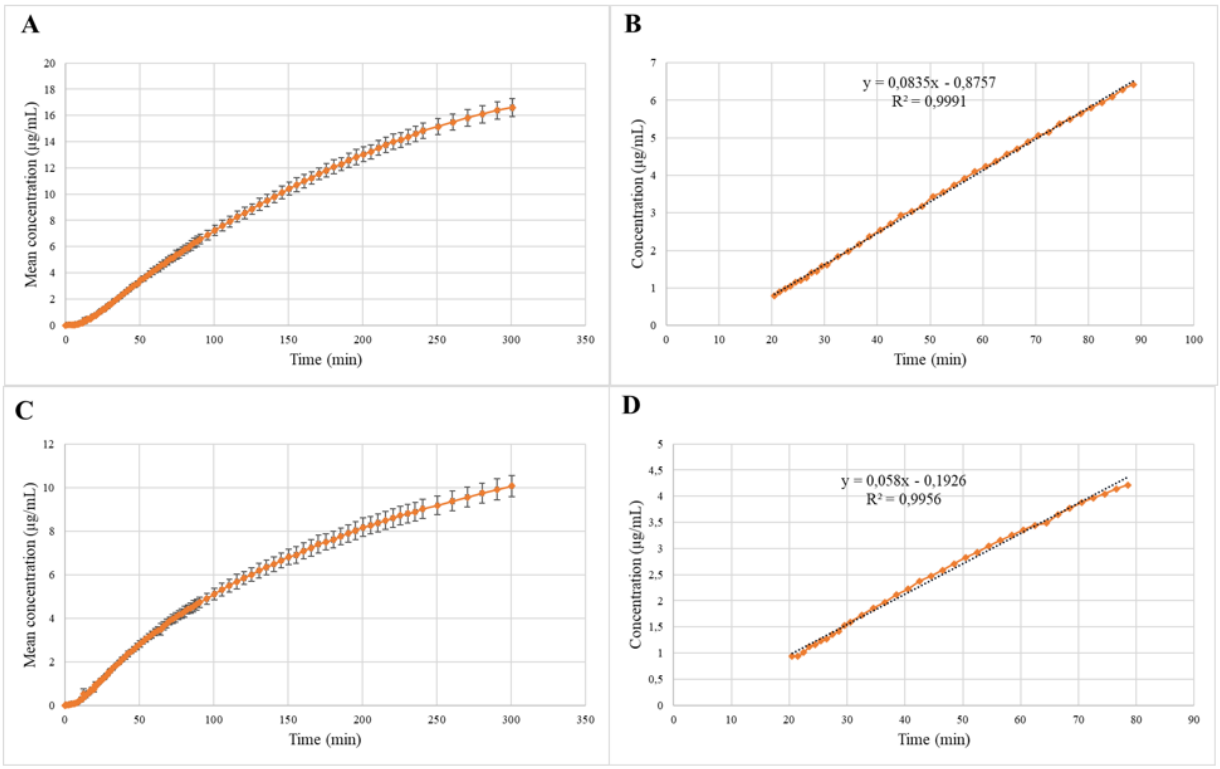

Figure 28. ASD suspension's acceptor side concentration (µg/ml) results over time (min) and linear ranges with dose of 200 µg/mL. A = Concentration-time profile in pH 3.0, B = Linear range in selected timepoints 20-88 min in pH 3.0, C = Concentration-time profile in FeSSIF, D = Linear range in selected timepoints 20-78 min in FeSSIF.

From co-crystal suspension's dose of 40 µg/mL concentration-time profiles (Figure 29), in both media it was seen that the profiles' curves started to slowly bend after about 90 min. These profiles resembled ASD suspension profiles. The deviation increased towards the end of the measurement with both media. In the profile made in FeSSIF some minor disturbances in the beginning of the curve were seen. Due to curvature after about 90 min, the linear ranges were observed before that timepoint. The best linear ranges with best correlation coefficient were found to be between 20-88 min in pH 3.0 and 20-84 min in FeSSIF to obtain suitable correlation coefficients of 1.000 and 0.995. Correlation coefficients were found to be excellent with a dose of 40 µg/mL.

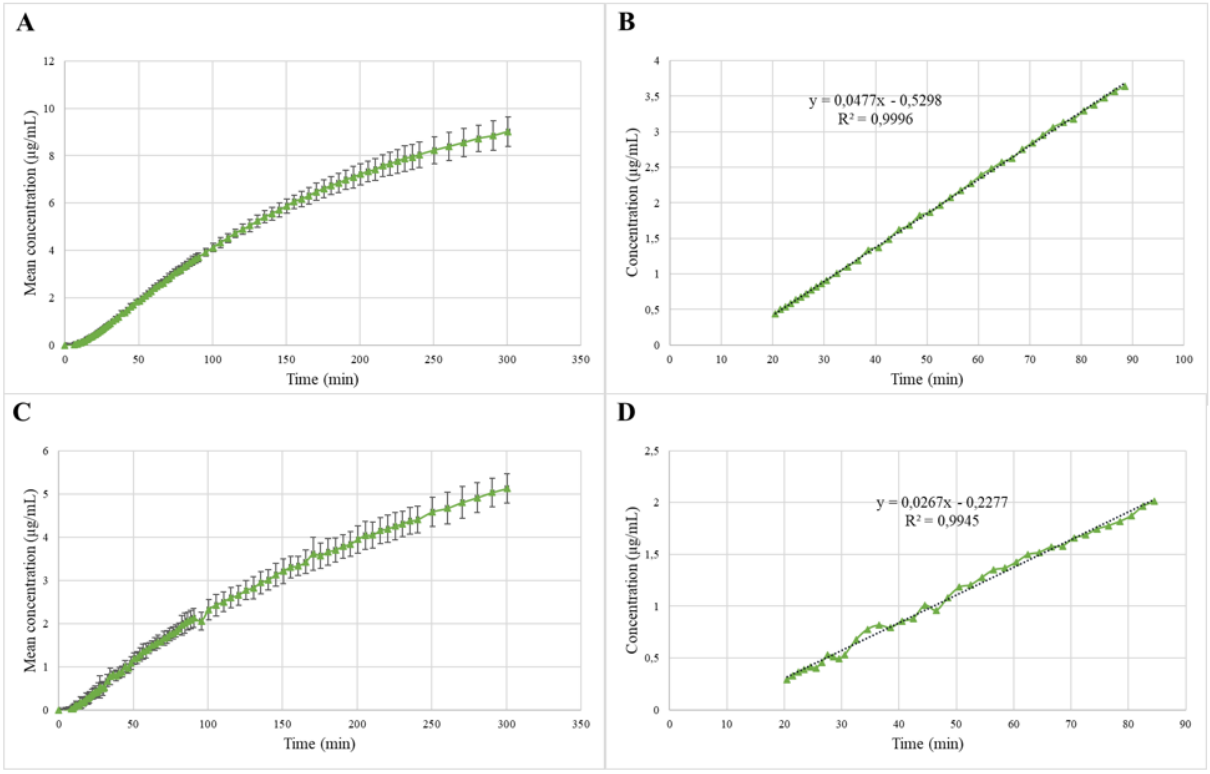

Figure 29. Co-crystal suspension's acceptor side concentration (µg/ml) results over time (min) and linear ranges with dose of 40 µg/mL. A = Concentration-time profile in pH 3.0, B = Linear range in selected timepoints 20-88 min in pH 3.0, C = Concentration-time profile in FeSSIF, D = Linear range in selected timepoints 20-84 min in FeSSIF.

Similarly as seen with a dose of 40 µg/mL, co-crystal suspension's concentration-time profiles at a dose of 200 µg/mL (Figure 30) started to slowly bend after about 90 min in both media. The deviation remained similar with both media and increased a little bit towards the end of the measurement. Any significant disturbance was not observed. Due to curvature after about 90 min, the linear ranges were observed before that timepoint. The best linear ranges with best correlation coefficient were found to be between 20-82 min in pH 3.0 and 20-76 min in FeSSIF to obtain suitable correlation coefficients of 0.999 and 0.997. Correlation coefficients were found to be good and very similar with the ones observed in measurement made with dose of 40 µg/mL.

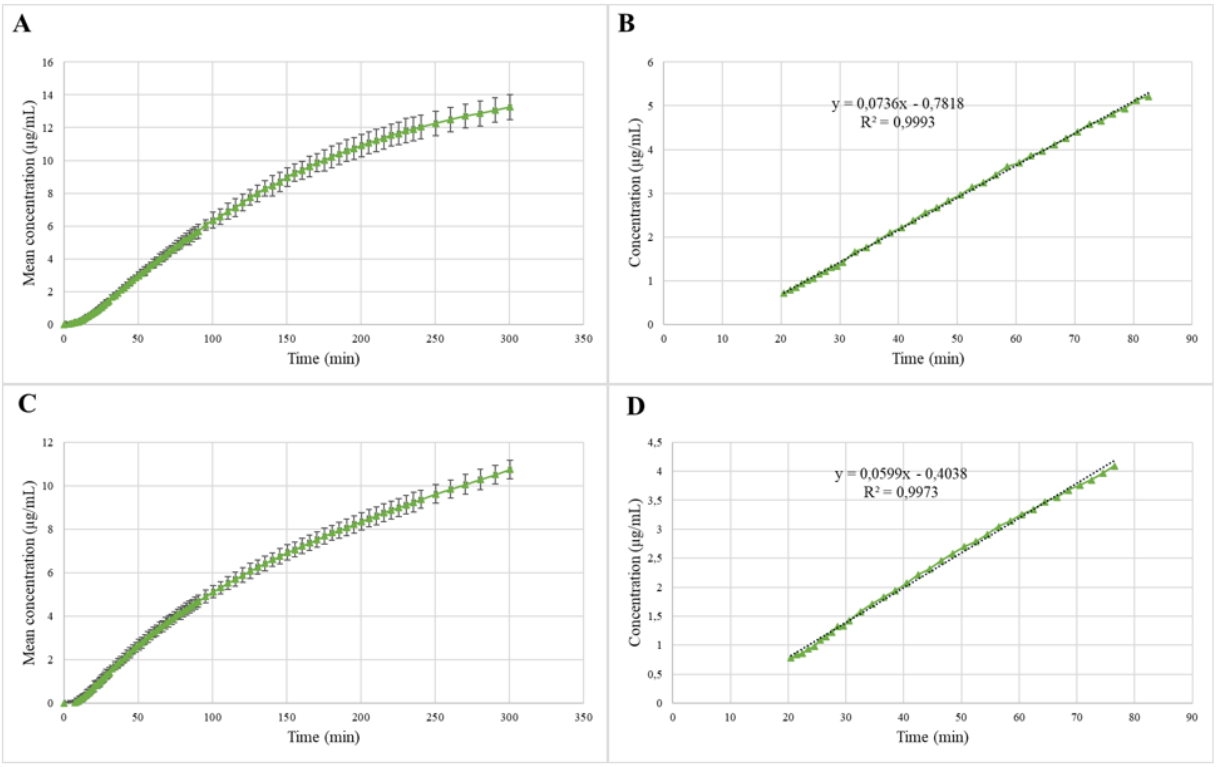

Figure 30. Co-crystal suspension's acceptor side concentration (µg/ml) results over time (min) and linear ranges with dose of 200 µg/mL. A = Concentration-time profile in pH 3.0, B = Linear range in selected timepoints 20-82 min in pH 3.0, C = Concentration-time profile in FeSSIF, D = Linear range in selected timepoints 20-76 min in FeSSIF.

8.2.5 *In vivo* relationship acceptor side, C_{max} & AUC_{0-24} vs. flux

Flux values were calculated with equation (10) and obtained values in phosphate buffer pH 3.0 are presented in Table 7 and flux values obtained in FeSSIF are presented in Table 8 with both doses and different linear ranges. From the results, it was observed that suspensions' flux values had the same ranking as seen with *in vivo* results. Co-crystal and ASD suspensions had almost the same flux values in both media. Measurements made in pH 3.0 showed that ASD suspension's flux values were a little bit higher compared to those of co-crystal suspensions. With FeSSIF, ASD, and co-crystal suspensions' ranking was opposite. However, the differences between these two flux values were quite minimal and thus it could be stated that the ranking was similar to *in vivo* data. Conventional suspension was observed to have the lowest flux values and thus lowest ranking in both media. Nanosuspension's flux values were a little bit higher than conventional's. Therefore, it could be concluded that flux values supported the previous observation that *in vitro* measurements had provided correct ranking

between formulations. From the results it was also seen that flux values from measurements made in FeSSIF had a smaller gap between the highest suspension flux value and the lowest flux value compared to measurements made in pH 3.0. The FeSSIF's effect of decreasing the differences between suspensions was also previously observed in the acceptor chamber's concentration-time profiles.

Table 7. Linear ranges timepoints and their flux values in measurements made in pH 3.0

Suspension, dose (µg/mL)	Selected timepoints (min)	Flux value (µg/(min*cm^2)) in selected timepoints	Uniform timepoints range (min)	Flux value (µg/(min*cm^2)) in uniform timepoints
Conventional susp., 200	40-270	0.12	40-82	0.14
Conventional susp., 40	20-270	0.07	38-88	0.04
Nanosusp., 200	40-210	0.16	40-82	0.17
Nanosusp., 40	38-195	0.15	38-88	0.16
ASD susp., 200	20-88	1.66	40-82	1.61
ASD susp., 40	20-90	0.94	38-88	0.93
Co-crystal susp., 200	20-82	1.45	40-82	1.43
Co-crystal susp., 40	20-88	0.94	38-88	0.92

Table 8. Linear ranges timepoints and their flux values in measurements made in FeSSIF

Suspension, dose (µg/mL)	Selected timepoints (min)	Flux value (µg/(min*cm^2)) in selected timepoints	Uniform timepoints range (min)	Flux value (µg/(min*cm^2)) in uniform timepoints
Conventional susp., 200	40-225	0.13	40-76	0.12
Conventional susp., 40	42-220	0.11	42-78	0.12
Nanosusp., 200	40-200	0.18	40-76	0.19
Nanosusp., 40	20-120	0.29	42-78	0.31
ASD susp., 200	20-78	1.13	40-76	1.06
ASD susp., 40	20-78	0.53	42-78	0.51
Co-crystal susp., 200	20-76	1.18	40-76	1.12
Co-crystal susp., 40	20-84	0.54	42-78	0.52

When observing *in vivo* data's C_{max} and $AUC_{0\text{-}24}$ values (Table 6) against flux values, it was seen that variability in correlation coefficient values existed under different conditions (Table 9). Selected timepoints' flux values, were compared to uniform timepoints' flux values. It was seen that values were quite similar and any major differences were not observed. Due to this, the best correlation coefficient between selected and uniform timepoints could be chosen on the basis of other parameters, such as dose effect and the effect of used medium. It was

decided to compare the effect of different conditions' mainly based on the value of selected timepoints.

Table 9. Correlation coefficient values between *in vivo* and *in vitro* data

	R^2 values in dose of 40 µg/mL		R^2 values in dose of 200 µg/mL	
	Selected timepoints	Uniform timepoints	Selected timepoints	Uniform timepoints
pH 3.0, C_{max}-Flux	**0.958**	0.926	**0.963**	0.956
pH 3.0, AUC_{0-24}-Flux	**0.921**	0.973	**0.814**	0.794
FeSSIF, C_{max}-Flux	**0.837**	0.815	**0.944**	0.951
FeSSIF, AUC_{0-24}-Flux	**0.985**	0.981	**0.832**	0.874

From correlation coefficient values, it was observed that values changed quite a lot depending on the conditions. With a dose of 200 µg/mL, C_{max}-flux correlations were significantly better compared to AUC_{0-24}-flux correlations in both media (Figure 31 and Figure 32). However, all of the correlation coefficient values were relatively high ($R^2 > 0.80$).

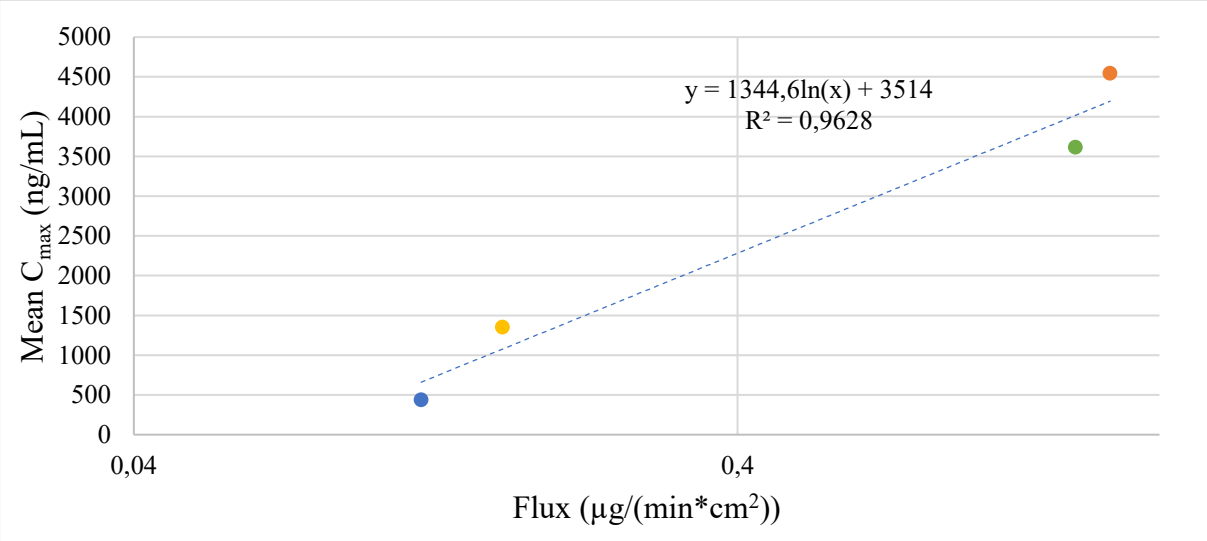

Figure 31. Linearity of C_{max} (ng/mL) and flux (µg/(min*cm^2)) values in suspension formulations' selected timepoints. Measurements made with a dose of 200 µg/mL and in medium of phosphate buffer pH 3.0. Linearity presented on a logarithmic scale. Blue = Conventional suspension, Yellow = Nanosuspension., Orange = ASD suspension, Green = Co-crystal suspension.

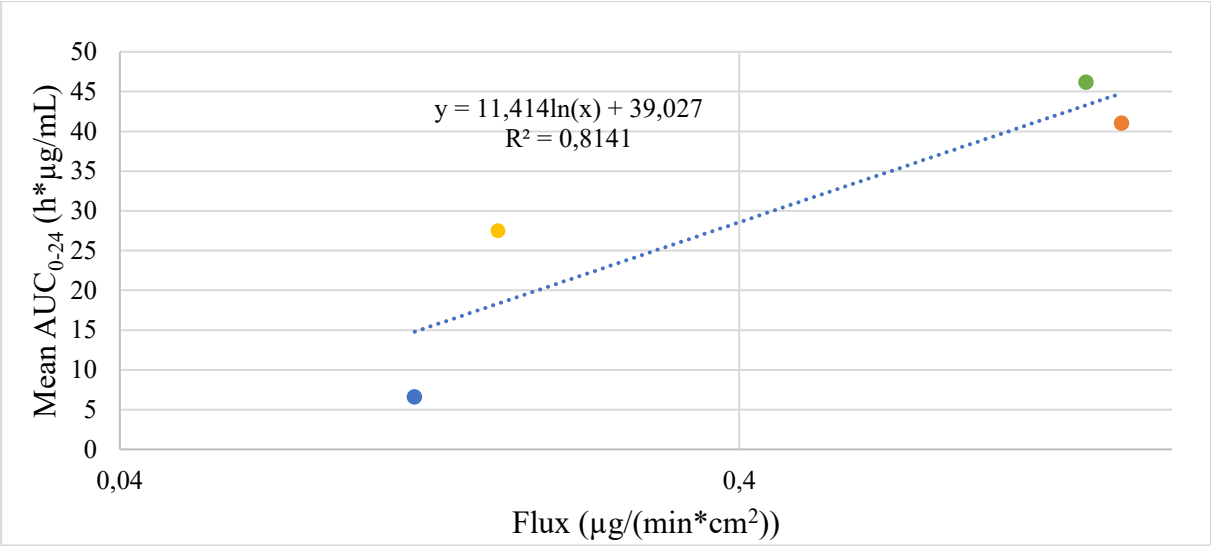

Figure 32. Linearity of $AUC_{0\text{-}24}$ (h*µg/mL) and flux (µg/(min*cm^2)) values in suspension formulations' selected timepoints. Measurement made with a dose of 200 µg/mL and in medium of phosphate buffer pH 3.0. Linearity presented on a logarithmic scale. Blue = Conventional suspension, Yellow = Nanosuspension, Orange = ASD suspension, Green = Co-crystal suspension.

With a dose of 40 µg/mL, was not observed clear trend within R^2 values. From the results, it could be seen that there was less deviation, as was seen with a higher dose between C_{max}-flux and $AUC_{0\text{-}24}$-flux correlation values. Both gave relatively good correlation.

When comparing all of the C_{max}-flux and $AUC_{0\text{-}24}$-flux correlation values, it could be concluded that C_{max}-flux correlations had a little bit less deviation between doses and used media. However, both ways to observe correlation gave good R^2 values and the differences were quite minimal. Thus it could be said that both C_{max}-flux and $AUC_{0\text{-}24}$-flux profiles were applicable to present the correlation between *in vivo* and *in vitro* data and the best profile was dependent on the effect of dose or used medium.

Results showed that, when comparing all of the correlation coefficient values, there was no significant difference between doses. It seemed that with a dose of 200 µg/mL, there was a little bit more deviation between values compared to those at lower doses. However, a higher dose gave better correlation to C_{max}-flux measurements (Figure 33 and Figure 34) in both media when compared to a lower dose's results.

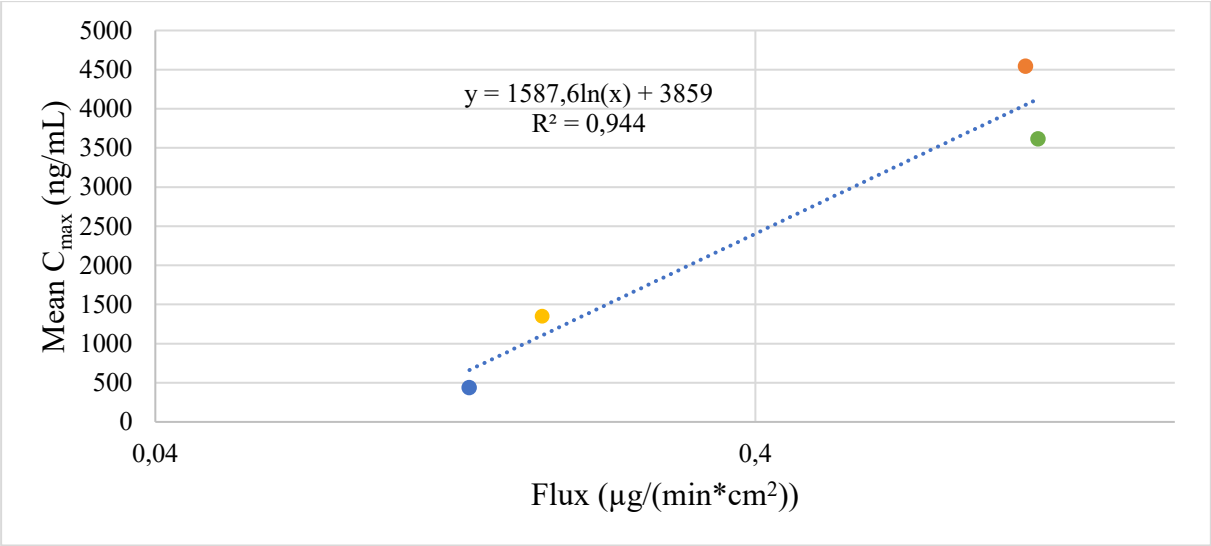

Figure 33. Linearity of C_{max} (ng/mL) and flux (µg/(min*cm^2)) values in suspension formulations' selected timepoints. Measurements made with a dose of 200 µg/mL and in medium of FeSSIF. Linearity presented on a logarithmic scale. Blue = Conventional suspension, Yellow = Nanosuspension, Orange = ASD suspension, Green = Co-crystal suspension.

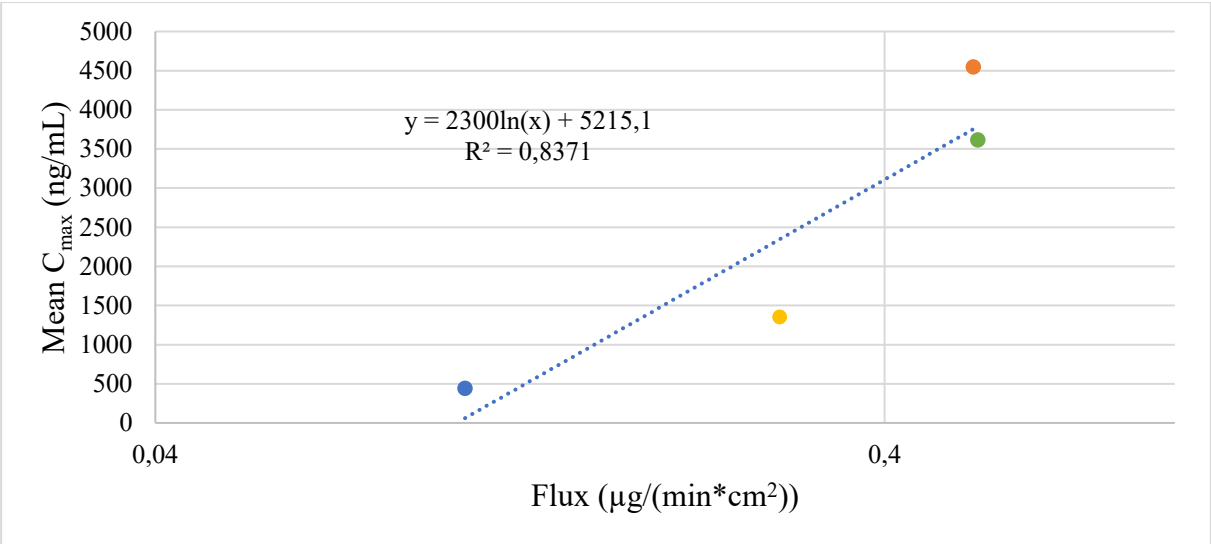

Figure 34. Linearity of C_{max} (ng/mL) and flux (µg/(min*cm^2)) values in suspension formulations' selected timepoints. Measurements made with a dose of 40 µg/mL and in medium of FeSSIF. Linearity presented on a logarithmic scale. Blue = Conventional suspension, Yellow = Nanosuspension, Orange = ASD suspension, Green = Co-crystal suspension.

However, when comparing dose effects with $AUC_{0\text{-}24}$-flux correlations, it was observed that a lower dose of 40 µg/mL gave a better correlation in both media compared to a higher dose (Figure 35 and Figure 36). It could be concluded that with a lower dose the correlation between

in vivo and *in vitro* data, should be made from AUC_{0-24}-flux correlations. Contrary to that, with a higher dose the correlation between *in vivo* and *in vitro* data should be made from C_{max}-flux correlations.

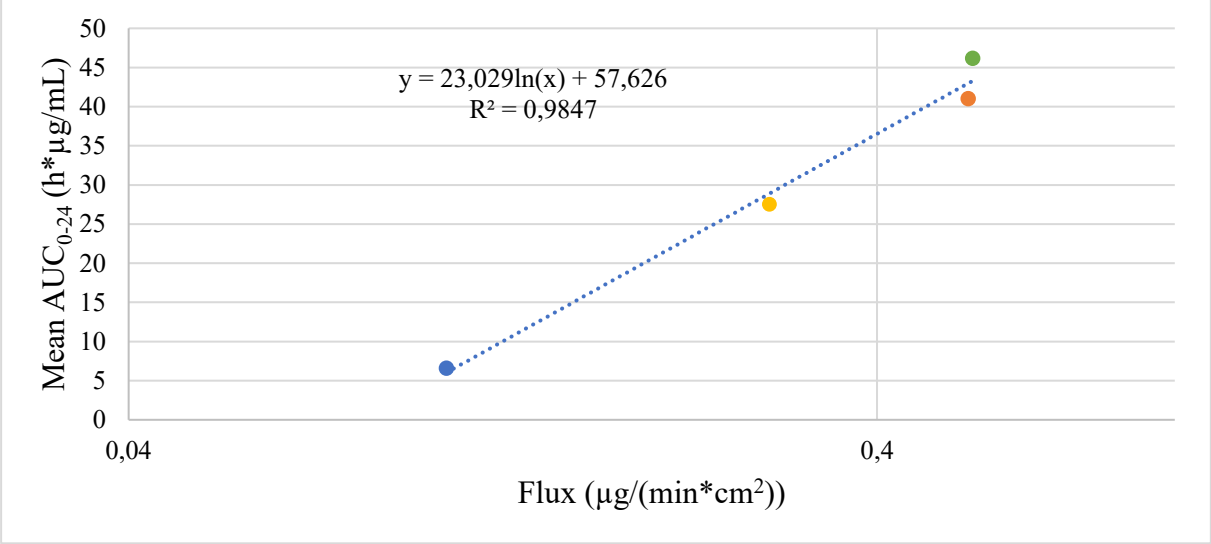

Figure 35. Linearity of AUC_{0-24} (h*µg/mL) and flux (µg/(min*cm^2)) values in suspension formulations' selected timepoints. Measurement made with a dose of 40 µg/mL and in medium of FeSSIF. Linearity presented on a logarithmic scale. Blue = Conventional suspension, Yellow = Nanosuspension, Orange = ASD suspension, Green = Co-crystal suspension.

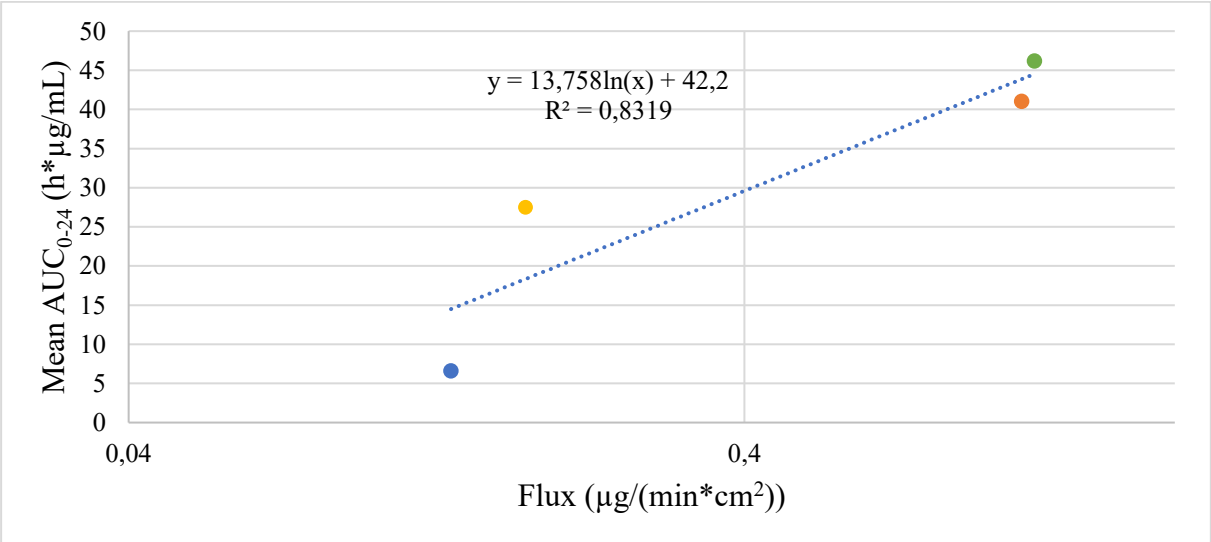

Figure 36. Linearity of AUC_{0-24} (h*µg/mL) and flux (µg/(min*cm^2)) values in suspension formulations' selected timepoints. Measurement made with a dose of 200 µg/mL and in medium of FeSSIF. Linearity presented on a logarithmic scale. Blue = Conventional suspension, Yellow = Nanosuspension, Orange = ASD suspension, Green = Co-crystal suspension.

When comparing the effect of used medium, it could be seen from the results that there was less deviation between results with pH 3.0. The difference is, however, really minimal when compared to the deviation with FeSSIF medium. Results showed that with higher dose the medium did not effect whether C_{max}-flux or AUC_{0-24}-flux correlation was better, but with lower dose the pH 3.0 gave better values in both ways of observing correlation. From the results it was also observed that C_{max}-flux correlations were better in pH 3.0 with both doses, and AUC_{0-24}-flux correlations were better in FeSSIF with both doses.

There should be more replicate measurements to help to ensure if there really is a trend with used dose or medium. Especially with measurements made with pH 3.0, there was no clear trend between C_{max}-flux and AUC_{0-24}-flux correlation coefficient values. However, results showed that when dose and medium effects were compared, atleast some trends were present, and thus it could be concluded that both dose and used medium had an effect on correlation coefficient values. Differences between correlation coefficient values with different conditions were, however, quite minimal. Phosphate buffer pH 3.0 gave good R^2 values with both C_{max}-flux and AUC_{0-24}-flux correlations when compared to FeSSIF, which had a C_{max}-flux correlation notably better than the AUC_{0-24}-flux correlation. Similarly the lower dose of 40 µg/mL gave a slightly better correlation because it seemed that lower dose results contained less deviation and was more stable, producing better correlations. However, with FeSSIF medium the higher dose was better to obtain correlation between C_{max}-flux. Therefore, it is not possible to say that only one medium or dose should be used. But after observation, it could be said that with different conditions, the correlations were relatively high and all scenarios seemed to have acceptable correlations. Therefore, it was proven that the *in vitro* data correlates to the *in vivo* data and thus the studied dissolution-permeation model was able to model rat's GI conditions.

8.2.6 *In vivo* relationship acceptor side, C_{max} & AUC_{0-24} vs. amount permeated

The amount permeated was calculated by using the equation (11) and obtained values are presented in Table 10 and Table 11. From calculated permeated amounts, the same ranking between suspension formulations as previously seen with *in vivo* results was observed. In each of the measurements, conventional suspension had the lowest permeated amount during the whole measurement, and ASD and co-crystal suspensions had the highest permeated amount. These results followed the concentration-time profiles' results and their ranking. Due to this,

the same observations could be seen with permeated amounts' results as previously observed from other acceptor side results.

Table 10. Amount permeated (µg) at different timepoints with different suspension formulations in dose of 40 µg/mL in both media

Amount permeated (µg)								
Time (min)	Convent. susp., pH 3.0	Convent. susp., FeSSIF	Nanosusp., pH 3.0	Nanosusp., FeSSIF	ASD susp., pH 3.0	ASD susp., FeSSIF	Co-crystal susp., pH 3.0	Co-crystal susp., FeSSIF
40	4.6	3.0	6.7	11.6	27.9	16.6	27.5	17.1
60	5.7	3.9	10.5	16.9	47.1	27.5	47.8	28.5
120	9.4	9.8	18.6	34.3	97.1	52.4	97.7	53.1
180	13.3	15.3	27.5	46.9	136.0	71.4	134.7	73.2
240	17.3	21.6	35.0	59.0	165.3	87.1	160.9	88.1
280	20.1	25.5	41.0	65.1	179.7	96.6	174.5	98.2
300	20.6	27.0	43.5	67.8	186.1	100.7	180.4	102.5

Table 11. Amount permeated (µg) at different timepoints with different suspension formulations in dose of 200 µg/mL in both media

Amount permeated (µg)								
Time (min)	Convent. susp., pH 3.0	Convent. susp., FeSSIF	Nanosusp., pH 3.0	Nanosusp., FeSSIF	ASD susp., pH 3.0	ASD susp., FeSSIF	Co-crystal susp., pH 3.0	Co-crystal susp., FeSSIF
40	3.5	2.7	4.3	4.9	51.0	44.5	44.3	41.3
60	8.2	5.2	8.3	8.3	84.7	67.1	73.9	65.1
120	14.9	13.5	18.0	19.1	171.3	116.9	148.5	117.7
180	22.8	20.5	27.2	29.8	241.6	152.4	204.5	156.7
240	28.1	27.7	37.0	39.8	296.6	180.5	240.9	187.4
280	31.6	33.0	42.1	46.9	322.1	195.0	257.4	205.9
300	34.7	34.9	44.9	49.4	332.1	201.5	265.1	215.0

When observing C_{max} and $AUC_{0\text{-}24}$ values (Table 6) against amount permeated with a dose of 40 µg/mL, variability in correlation coefficient values was seen between different media (Table 12). The most notable difference was observed with C_{max} vs. µg correlation made in FeSSIF. Compared to other R^2 values at a dose of 40 µg/mL, these correlation coefficient values were significantly worse than others. From Table 12, it can be observed that other correlations

were really high and deviation between different timepoints was very little. It was that R^2 values got better towards the 300 minutes' timepoint, except with C_{max} vs. µg results in pH 3.0 where the values remained quite the same throughout the measurement. However, even though most of the R^2 values increased towards the 300 minutes' timepoint, all of these correlations were relatively high throughout the measurement, except the C_{max} vs. µg correlation values made in FeSSIF. Therefore, the correlation could be searched at any timepoint. With lower dose, it could not be concluded which way was better to predict the correlation: C_{max} vs. µg correlation or AUC_{0-24} vs. µg correlation. But if considering the used medium together with dose effect, it could be said that with lower dose and pH 3.0 medium, both ways could give acceptably high correlation. But with lower dose and FeSSIF medium, AUC_{0-24} vs. µg correlation should be used.

Table 12. Correlation coefficient values for C_{max} & AUC_{0-24} vs. amount permeated (µg) in dose of 40 µg/mL

Time (min)	R^2 value in pH 3.0, C_{max} vs. µg	R^2 value in pH 3.0, AUC_{0-24} vs. µg	R^2 value in FeSSIF, C_{max} vs. µg	R^2 value in FeSSIF, AUC_{0-24} vs. µg
40	0.962	0.875	0.703	0.938
60	0.957	0.914	0.736	0.955
120	0.959	0.916	0.738	0.952
180	0.959	0.924	0.756	0.963
240	0.961	0.923	0.761	0.962
280	0.960	0.929	0.775	0.969
300	0.958	0.934	0.778	0.970

When observing C_{max} and AUC_{0-24} values (Table 6) against the amount permeated at a dose of 200 µg/mL, great variability in correlation coefficient values was also seen between different media, as well as between C_{max} and AUC_{0-24} (Table 13). From the results, it was seen that C_{max} vs. µg correlations were significantly better compared to AUC_{0-24} vs. µg results. It could be concluded that C_{max} vs. µg correlations were better than AUC_{0-24} vs. µg correlations in both media when the dose was bigger and thus C_{max} vs. µg correlations should be used with higher dose. AUC_{0-24} vs. µg correlations seemed to be a little better in FeSSIF medium, but overall the differences between media were not major. R^2 values were observed to increase towards the 300-minute timepoint with phosphate buffer but, opposite to that, R^2 values were decreasing towards the end timepoints with FeSSIF medium. However, these changes were quite minimal in both media and thus it seemed that the timepoint at which the amount permeated was observed did not really matter.

Table 13. Correlation coefficient values for C_{max} & AUC_{0-24} vs. amount permeated (µg) in dose of 200 µg/mL

Time (min)	R^2 value in pH 3.0, C_{max} vs. µg	R^2 value in pH 3.0, AUC_{0-24} vs. µg	R^2 value in FeSSIF, C_{max} vs. µg	R^2 value in FeSSIF, AUC_{0-24} vs. µg
40	0.955	0.789	0.968	0.875
60	0.940	0.746	0.961	0.857
120	0.957	0.789	0.954	0.847
180	0.959	0.785	0.953	0.862
240	0.972	0.805	0.952	0.867
280	0.975	0.808	0.949	0.871
300	0.974	0.802	0.947	0.871

Overall, it was seen that R^2 values had only minor deviation at different timepoints. It could be concluded that correlation between amount permeated and C_{max} and AUC_{0-24} values was not dependent on the observed timepoint and the correlations stayed accurate throughout the measurement when the observed *in vitro* results were permeated amounts.

When phosphate buffer was used, C_{max} vs. µg values gave averagely-better correlations than AUC_{0-24} vs. µg correlations. Doses also had effects on the results. With a lower dose of 40 µg/mL, good correlations were observed in all of the cases except C_{max} vs. µg made in FeSSIF, which was also previously seen with flux values. But with a higher dose of 200 µg/mL, C_{max} vs. µg results gave significantly better correlations. These same conclusions were observed with C_{max} and AUC_{0-24} values versus flux values. Similarly to amount permeated, it was also seen with flux that with higher dose there was a little more deviation between correlation coefficient values between C_{max} vs. flux and AUC_{0-24} vs. flux. With amount permeated and flux, it was observed that C_{max} comparisons were better with higher dose, but the differences compared to lower dose results were quite minimal. Flux and amount permeated results were surprisingly similar and thus it could be concluded that both ways to observe the correlation could therefore be used. Similarly as previously stated for flux comparisons, it could be said that amount permeated should be considered together with what medium and dose to use, to achieve the most accurate correlation.

To obtain correlation results, both flux and amount permeated correlations to *in vivo* data demand a few steps to obtain correlation results so there is not a clear answer as to which way is better to predict correlation between *in vivo* and *in vitro* results. Instead, it could be said that

both predictive ways were able to give high correlations. Overall results showed that a high correlation between amount permeated and *in vivo* results, C_{max} and AUC_{0-24} values, was found. Observed permeated amounts also gave correct ranking between formulation suspensions. Therefore it could be concluded that, again, *in vitro* data was able to model *in vivo* data correctly and thus could be used similarly as flux results.

8.3 Concentrations and dissolved fractions of suspension formulations

The average results of three replicates to concentration and the amount of dissolved fraction at a dose of 200 µg/ml for these prepared suspensions are presented in Table 14. Concentrations remained within approved limits with the exception of conventional suspension. Conventional suspension was still used in the dissolution-permeation measurements and the obtained results from these measurements were used. Results showed that the suspension formulations were prepared to the correct concentration, except conventional suspension, and thus the obtained donor and acceptor concentrations were accurate.

Table 14. Suspension formulations' concentrations (mg/mL) and dissolved fractions's concentrations (mg/mL) when prepared to dose of 200 µg/mL measurements

	Prepared suspensions for the measurements made in pH 3.0				Prepared suspensions for the measurements made in FeSSIF	
	Conventional	Nano	ASD	Co-crystal	ASD	Co-crystal
Concentration (mg/mL)	12.0	9.2	11.0	9.0	10.4	9.3
Dissolved fraction (mg/mL)	0.3	1.0	8.4	5.2	8.3	5.8

The average results of three replicates to concentration and the amount of dissolved fraction at a dose of 40 µg/ml for these suspension formulations are presented in Table 15. The concentration of each suspension formulation remained within approved limits. Same conventional- and nanosuspension was used in measurements made with both media. Results showed that the suspension formulations were prepared to the correct concentration and therefore the obtained donor and acceptor concentrations were accurate.

Table 15. Suspensions formulations' concentrations (mg/mL) and dissolved fractions's concentrations (mg/mL) when prepared to dose of 40 µg/mL measurements

	Prepared suspensions for the measurements made in pH 3.0				Prepared suspensions for the measuremetns made in FeSSIF	
	Conventional	Nano	ASD	Co-crystal	ASD	Co-crystal
Concentration (mg/mL)	10.7	9.2	10.0	9.5	10.1	9.7
Dissolved fraction (mg/mL)	0.1	1.0	7.3	4.7	7.5	5.0

8.4 Accuracy test results

The results remained within the limit values (Table 16). Thus it can be concluded that the 5 mm probes used in measurements had been functional and had provided sufficiently accurate and correct values. The accuracy results also showed that the standard measurement for MicroFLUX had been accurate and could be used for MicroFLUX analyses.

Table 16. Different doses' measured concentrations by 5 mm fiber optic probes

Dose (µg/mL)	Probe 1	Probe 2	Probe 3	Probe 4	Probe 5	Probe 6	Probe 7	Probe 8
Blank	-0.2	0.1	-0.3	-0.1	-0.3	0.1	-0.3	-0.4
5	4.8	5.3	4.5	5.1	4.6	5.2	4.5	4.8
10	9.3	10.2	9.0	9.9	10.0	10.3	9.4	9.8
20	19.6	21.1	20.0	21.2	19.8	21.0	19.8	21.0
40	38.8	41.0	38.9	42.9	39.6	42.3	38.3	40.8

8.5 Summary of the results

The intention of the study was to investigate the effect of experimental conditions on the performance of a dissolution-permeation model and whether the studied *in vitro* model could replicate previously obtained *in vivo* results. Experimental conditions were selected to be the dose and media. From the dose effect test (Figure 16) it was observed that between the dose of 50 µg/mL and 100 µg/mL there was no change in correlation levels regardless of the higher dose. Thus it was assumed that the higher dose of 200 µg/mL, which was used in measurements, was not any more on the dynamic range and a lower dose could perform as well as a dose of 200 µg/mL. Due to this, another studied dose was chosen to be 40 µg/mL. The dose effect was later on found in the results. Both doses were observed to create the same ranking between different suspension formulations (Figure 17 and Figure 18). The same ranking was also previously obtained with *in vivo* results made in rat's GI tract (Table 6). Therefore it was concluded that both doses could be used to predict the right ranking between different suspension formulations. However, when reviewing concentration results from the acceptor side it was seen that with FeSSIF medium the lower dose was challenged to make a difference between ASD and co-crystal suspension (Figure 18). Therefore, a higher dose could be more accurate with FeSSIF.

Media used in measurements had significant effect on the performance of the dissolution-permeation model. On the acceptor side results, FeSSIF decreased differences between suspension formulations by decreasing the concentrations (Figure 18). Donor side results showed that with FeSSIF (Figure 21 and Figure 22) the concentrations were significantly higher than with phosphate buffer pH 3.0 (Figure 19 and Figure 20). From these results it was concluded that FeSSIF composition and its tendency to form micelles might have an effect on the donor side results. This necessitated considering if FeSSIF had also affected the results from the acceptor side. Due to this, in the future it would be crucial to do more research on the composition and performance of FeSSIF medium. Dissolution-permeation studies could also be done in the future in both media to ensure that the effect of both media is observed with the vehicles' excipients and API under investigation. It is necessary to know in drug development if API or suspension formulations' excipients perform differently in the conditions of the stomach or small intestine. In the future, it also would be interesting to do research on the permeability of the biomimic membrane used in MicroFLUX measurements. Differences with donor and acceptor side results hinted that the permeation through this membrane might not be

as straightforward as assumed. Different micelles or excipients might affect the membrane's permeability.

As previously mentioned, chamber concentrations were reviewed from the donor side, with the dose of 40 µg/mL. Donor side results had the same ranking between suspensions and thus donor side sampling was stated to be another possible method to study dissolution. Donor side concentration also correlated well with flux values. Flux value should be low if the concentration on the donor side was low. Results showed this statement to be fulfilled. On the donor side, it was seen that conventional suspension had the lowest concentration (Figure 19-Figure 22) and also had the lowest flux value (Table 7 and Table 8). However, donor side concentrations had great differences depending on the used medium. Results showed that measurements with FeSSIF were not relatable and FeSSIF composition could be affecting the obtained results (Figure 21 and Figure 22). Thus donor side sampling could be used to predict dissolution with phosphate buffer pH 3.0 instead of MicroFLUX studies. Sampling measurements were, however, found to be a more time-consuming and expensive option than MicroFLUX studies.

When comparing obtained *in vitro* data's flux and amount permeated values to *in vivo* data's C_{max} and $AUC_{0\text{-}24}$ values (Table 6), it was seen that all of the comparisons gave good correlations (Table 9, Table 12 and Table 13). Correlation coefficient values differed depending on the used medium and dose, but overall every scenario gave acceptable correlation and thus it was concluded that the observed, small-scale, dissolution-permeation method could model rat's GI conditions.

Study included few sources for error. The obtained acceptor side concentrations were very low and, due to this, spectral disorders occurred. Especially with the conventional suspensions, it was difficult to find good linearity because acceptor side concentrations had a lot of disturbances (Figure 24). This could have been avoided with larger fiber optic probes. With MicroFLUX apparatus, smaller probes are commonly used on the donor side and larger probes on the acceptor side.[70] With these measurements it would have been helped to use 20 mm fiber optic probes on the acceptor side. Another error which occurred during this study was the incorrect concentration of conventional suspension at the dose of 200 µg/mL measurements. This conventional suspension's concentration was 12.0 mg/mL instead of the wanted concentration of 10 ± 1.0 mg/mL (Table 14). When observing donor and acceptor side results, it seemed that this difference in concentration did not affect the results when compared to results

obtained from measurements made at the dose of 40 µg/mL. However, to be sure that the wrong concentration did not affect the results, it would be important to prepare a new conventional suspension formulation with correct concentration and redo the measurements made with the wrong concentration and compare these results.

9 Conclusion

The aim of this study was to investigate what effect experimental conditions had on MicroFLUX model's performance and if the model is able to correctly replicate rat's GI conditions. Measurements made with MicroFLUX apparatus showed that used medium and dose had an effect on the performance of the dissolution-permeation model. With both media, the same ranking between four different suspension formulations was obtained. The same ranking was previously observed with *in vivo* conditions. Therefore, both media were able to repeat the correct ranking between suspension formulations. However, concentrations in the chambers differed significantly depending on the medium used. It was seen that with phosphate buffer pH 3.0, donor and acceptor chamber's concentrations were in line with each other. With FeSSIF, these concentrations were not in line with the assumptions. In acceptor chambers, FeSSIF seemed to decrease differences between suspension formulations. However, in donor chamber's results, concentrations were odd and it seemed that filtration was not working. This may have been the result of the composition of FeSSIF and its tendency to form micelles and react with formulations' excipients. It can be concluded, that in the future, measurements made with phosphate buffer pH 3.0 could provide more reliable and accurate results. Measurements with FeSSIF were also able to predict the correct ranking between suspension formulations, but the medium composition and thus the performance with other excipients needs more studies.

The dose of 200 µg/mL and 40 µg/mL were both able to form correct ranking between suspension formulations. It seemed from the results that dose itself did not have a major effect on the results, but the used medium had an effect on the performance of dose. With phosphate buffer pH 3.0, lower dose of 40 µg/mL could be used, and with FeSSIF the dose of 200 µg/mL gives more precise rankings. However, correlations between *in vivo* and *in vitro* data showed that in the future the lower dose of 40 µg/mL could be used with both media in MicroFLUX studies and therefore it is possible to save the API in these measurements.

Measurements made to compare donor side sampling and MicroFLUX measurements showed that MicroFLUX results were as accurate and correct as results obtained from donor side sampling. Donor side sampling is expensive when nanoscale filters are used and consumes many resources, including HPLC sample preparation and separate HPLC analysis. Therefore it could be concluded that a better and more efficient method to predict *in vivo* dissolution was found.

The studies were able to prove that the used small-scale dissolution-permeation model was able to model rat's GI conditions and produce correct ranking with four different suspension formulations. The MicroFLUX model and method was also proven to be as accurate as sampling from donor side chamber and therefore a more efficient choice to do dissolution studies. This functional MicroFLUX model and method means that, in the future, the amount of drug substance needed for measurements is very low or it will be possible to do more replicate measurements. It also means that, in the future, it could be possible to reduce animal testing in rats when dysfunctional formulations are observed during *in vitro* measurements.

REFERENCES

1. Pretorius, E. and Bouic, P. J. D., Permeation of four oral drugs through human intestinal mucosa, *AAPS PharmSciTech*, **2009**, *10*, 270–275.
2. Sachan, N. K.; Bhattacharya, A.; Pushkar, S. and Mishra, A., Biopharmaceutical classification system: A strategic tool for oral drug delivery technology, *Asian J. Pharm.*, **2009**, *3*, 76–81.
3. Yang, Y.; Zhao, Y.; Yu, A.; Sun, D. and Yu, L. X., Oral drug absorption: Evaluation and prediction, *Dev. Solid Oral Dos. Forms Pharm. Theory Pract. Second Ed.*, **2017**, 331–354.
4. Chavda, H. V.; Patel, C. N. and Anand, I. S., Biopharmaceutics classification system, *Syst. Rev. Pharm.*, **2010**, *1*, 62–69.
5. Dahan, A. and Miller, J. M., The solubility-permeability interplay and its implications in formulation design and development for poorly soluble drugs, *AAPS J.*, **2012**, *14*, 244–251.
6. McPherson, S.; Perrier, J.; Dunn, C.; Khadra, I.; Davidson, S.; Ainousah, B.; Wilson, C. G. and Halbert, G., Small scale design of experiment investigation of equilibrium solubility in simulated fasted and fed intestinal fluid, *Eur. J. Pharm. Biopharm.*, **2020**, *150*, 14–23.
7. Kawabata, Y.; Wada, K.; Nakatani, M.; Yamada, S. and Onoue, S., Formulation design for poorly water-soluble drugs based on biopharmaceutics classification system: Basic approaches and practical applications, *Int. J. Pharm.*, **2011**, *420*, 1–10.
8. Kostewicz, E. S.; Abrahamsson, B.; Brewster, M.; Brouwers, J.; Butler, J.; Carlert, S.; Dickinson, P. A.; Dressman, J.; Holm, R.; Klein, S.; Mann, J.; McAllister, M.; Minekus, M.; Muenster, U.; Müllertz, A.; Verwei, M.; Vertzoni, M.; Weitschies, W. and Augustijns, P., In vitro models for the prediction of in vivo performance of oral dosage forms, *Eur. J. Pharm. Sci.*, **2014**, *57*, 342–366.
9. Teleki, A.; Nylander, O. and Bergström, C. A. S., Intrinsic dissolution rate profiling of poorly water-soluble compounds in biorelevant dissolution media, *Pharmaceutics*, **2020**, *12,* 1-19.
10. National Institute of Diabetes and Digestive and Kidney Diseases, N. I. of H., Drawing of the GI tract, https://www.niddk.nih.gov/news/media-library/8952 (27.5.2022).
11. Lippincott, W. and Lippincott, W., *Lippincott Professional Guides: Anatomy & Physiology*, 2nd edition, Wolters Kluwer Health, 2002.
12. Martini, F.; Nath, J. and Bartholomew, E., *Fundamentals of Anatomy and Physiology*,

10th edition, Pearson, Edinburgh Gate, 2015.

13. Reinus, J. F. and Douglas, S., *Gastrointestinal Anatomy and Physiology: The Essentials*, John Wiley & Sons, Chichester, 2014.
14. Pyper, K.; Brouwers, J.; Augustijns, P.; Khadra, I.; Dunn, C.; Wilson, C. G. and Halbert, G. W., Multidimensional analysis of human intestinal fluid composition, *Eur. J. Pharm. Biopharm.*, **2020**, *153*, 226–240.
15. Kararli, T. T., Review article comparison, *Biopharm. Drug Dispos.*, **1995**, *16*, 351–380.
16. National Institute of Diabetes and Digestive and Kidney Diseases, N. I. of H., Illustration of the biliary system, with the liver, gallbladder, duodenum, pancreatic duct, common bile duct, pancreas, cystic duct, and hepatic ducts labeled, https://www.niddk.nih.gov/news/media-library/8889 (27.5.2022).
17. McConnell, E. L.; Basit, A. W. and Murdan, S., Measurements of rat and mouse gastrointestinal pH, fluid and lymphoid tissue, and implications for in-vivo experiments, *J. Pharm. Pharmacol.*, **2010**, *60*, 63–70.
18. Berghausen, J.; Seiler, F. H.; Gobeau, N. and Faller, B., Simulated rat intestinal fluid improves oral exposure prediction for poorly soluble compounds over a wide dose range, *ADMET DMPK*, **2016**, *4*, 35–53.
19. Kodama, Y.; Johannessen, H.; Furnes, M. W.; Zhao, C.; Johnsen, G. and Ma, R., Mechanistic Comparison between Gastric Bypass vs . Duodenal Switch with Mechanistic Comparison between Gastric Bypass vs . Duodenal Switch with Sleeve Gastrectomy in Rat Models, *Plos One,* **2013**, *8*, 2.
20. Klumpp, L.; Nagasekar, K.; McCullough, O.; Seybert, A.; Ashtikar, M. and Dressman, J., Stability of Biorelevant Media Under Various Storage Conditions, *Dissolution Technol.*, **2019**, *26*, 6–18.
21. Klein, S., The use of biorelevant dissolution media to forecast the in vivo performance of a drug, *AAPS J.*, **2010**, *12*, 397–406.
22. Fuchs, A.; Leigh, M.; Kloefer, B. and Dressman, J. B., Advances in the design of fasted state simulating intestinal fluids: FaSSIF-V3, *Eur. J. Pharm. Biopharm.*, **2015**, *94*, 229–240.
23. Fuchs, A., Entwicklung einer neuen Generation von Biorelevanten Medien zur Simulation des nüchternen humanen Dünndarms, **2015**.
24. Yilmaz Usta, D.; Demi Rtas, Ö.; ÖkÇelik, C.; Uslu, A. and Teksin, Z. Ş., Evaluation of in vitro dissolution characteristics of flurbiprofen, a BCS class IIa drug, *Fabad J. Pharm. Sci.*, **2018**, *43*, 27–34.

25. Dahlgren, D.; Venczel, M.; Ridoux, J. P.; Skjöld, C.; Müllertz, A.; Holm, R.; Augustijns, P.; Hellström, P. M. and Lennernäs, H., Fasted and fed state human duodenal fluids: Characterization, drug solubility, and comparison to simulated fluids and with human bioavailability, *Eur. J. Pharm. Biopharm.*, **2021**, *163*, 240–251.
26. Amaral Silva, D.; Al-Gousous, J.; Davies, N. M.; Bou Chacra, N.; Webster, G. K.; Lipka, E.; Amidon, G. and Löbenberg, R., Simulated, biorelevant, clinically relevant or physiologically relevant dissolution media: The hidden role of bicarbonate buffer, *Eur. J. Pharm. Biopharm.*, **2019**, *142*, 8–19.
27. ICH, ICH Q7 - Good Manufacturing Practice for Active Pharmaceutical Ingredients, *Regul. ICH*, **2001**, 1–56.
28. Yasir, M.; Asif, M.; Kumar, A. and Aggarval, A., Biopharmaceutical classification system: An account, *Int. J. PharmTech Res.*, **2010**, *2*, 1681–1690.
29. Amidon, G. L.; Lennernäs, H.; Shah, V. P. and Crison, J. R., A Theoretical Basis for a Biopharmaceutic Drug Classification: The Correlation of in Vitro Drug Product Dissolution and in Vivo Bioavailability, *Pharm. Res. An Off. J. Am. Assoc. Pharm. Sci.*, **1995**, *12*, 413–420.
30. Papich, M. G. and Martinez, M. N., Applying Biopharmaceutical Classification System (BCS) Criteria to Predict Oral Absorption of Drugs in Dogs: Challenges and Pitfalls, *AAPS J.*, **2015**, *17*, 948–964.
31. Noyes, A. A. and Whitney, W. R., The Rate of Solution of Solid Substances in Their Own Solution, *J. Am. Chem. Soc.*, **1897**, *19*, 930–934.
32. Nernst, W., Theorie der Reaktionsgeschwindigkeit in heterogenen Systemen, *Phys. Chemie*, **1904**, *47*, 52–55.
33. Horter, D. and Dressman, J., Influence of physicochemical properties on dissolution of drugs in the gastrointestinal tract, *Adv. Drug Deliv. Rev.*, **1997**, *25*, 3–14.
34. Dressman, J.; Amidon, G.; Reppas, C. and Shah, V., Dissolution testing as a prognostic tool for oral drug absorption: immeadiate release dosage forms, *Pharm. Res.*, **1998**, *15*, 11–22.
35. Sharma, S. and Prasad, B., Meta-analysis of food effect on oral absorption of efflux transporter substrate drugs: Does delayed gastric emptying influence drug transport kinetics?, *Pharmaceutics*, **2021**, *13*.
36. Loftsson, T., Drug permeation through biomembranes: Cyclodextrins and the unstirred water layer, *Pharmazie*, **2012**, *67*, 363–370.
37. Brodin, B.; Steffansen, B. and Nielsen, C. U., Passive diffusion of drug substances: the concepts of flux and permeability, *Mol. Biopharm.*, **2002**, *18,* 135-152.

38. Dahlgren, D. and Lennernäs, H., Intestinal permeability and drug absorption: predictive experimental, computational and in vivo approaches, *Pharmaceutics*, **2019**, *11*, 1-18.
39. Bevernage, J.; Brouwers, J.; Brewster, M. E. and Augustijns, P., Evaluation of gastrointestinal drug supersaturation and precipitation: Strategies and issues, *Int. J. Pharm.*, **2013**, *453*, 25–35.
40. Brouwers, J.; Brewster, M. E. and Augustijns, P., Supersaturating drug delivery systems: The answer to solubility-limited oral bioavailability?, *J. Pharm. Sci.*, **2009**, *98*, 2549–2572.
41. Kuentz, M., Drug supersaturation during formulation digestion, including real-time analytical approaches, *Adv. Drug Deliv. Rev.*, **2019**, *142*, 50–61.
42. Currie, G. M., Pharmacology, part 2: Introduction to pharmacokinetics, *J. Nucl. Med. Technol.*, **2018**, *46*, 221–230.
43. Urso, R.; Blardi, P. and Giorgi, G., A short introduction to pharmacokinetics, *Eur. Rev. Med. Pharmacol. Sci.*, **2002**, *6*, 33–44.
44. Lipinski, C. A.; Lombardo, F.; Dominy, B. W. and Feeney, P. J., Experimental and computational approaches to estimate solubility and permeability in drug discovery and development settings, *Adv. Drug Deliv. Rev.*, **2012**, *64*, 4–17.
45. Lin, L. and Wong, H., Predicting oral drug absorption: Mini review on physiologically-based pharmacokinetic models, *Pharmaceutics*, **2017**, *9*, 1-14.
46. Sareen, S.; Joseph, L. and Mathew, G., Improvement in solubility of poor water-soluble drugs by solid dispersion, *Int. J. Pharm. Investig.*, **2012**, *2*, 12.
47. Savjani, K. T.; Gajjar, A. K. and Savjani, J. K., Drug Solubility: Importance and Enhancement Techniques, *ISRN Pharm.*, **2012**, *2012*, 1–10.
48. Kim, D. H.; Kim, Y. W.; Tin, Y. Y.; Soe, M. T. P.; Ko, B. H.; Park, S. J. and Lee, J. W., Recent technologies for amorphization of poorly water-soluble drugs, *Pharmaceutics*, **2021**, *13*, 1-21.
49. Dizaj, S. M.; Vazifehasl, Z.; Salatin, S.; Adibkia, K. and Javadzadeh, Y., Nanosizing of drugs : Effect on dissolution rate Nanosizing of drugs : Effect on dissolution rate, **2015**, *10*, 95-108.
50. Elder, D. P.; Kuentz, M. and Holm, R., Pharmaceutical excipients - Quality, regulatory and biopharmaceutical considerations, *Eur. J. Pharm. Sci.*, **2016**, *87*, 88–99.
51. Vranic, E., Drug-excipients interactions, *Born J Basic Med Sci,***2004**, *2*, 56–58.
52. Cui, X.; Mao, S.; Liu, M.; Yuan, H. and Du, Y., Mechanism of surfactant micelle formation, *Langmuir*, **2008**, *24*, 10771–10775.
53. Chevalier, Y. and Zemb, T., The structure of micelles and microemulsions, *Reports*

Prog. Phys., **1990**, *53*, 279–371.

54. Perinelli, D. R.; Cespi, M.; Lorusso, N.; Palmieri, G. F.; Bonacucina, G. and Blasi, P., Surfactant Self-Assembling and Critical Micelle Concentration: One Approach Fits All?, *Langmuir*, **2020**, *36*, 5745–5753.
55. Mah, P. T.; Peltonen, L.; Novakovic, D.; Rades, T.; Strachan, C. J. and Laaksonen, T., The effect of surfactants on the dissolution behavior of amorphous formulations, *Eur. J. Pharm. Biopharm.*, **2016**, *103*, 13–22.
56. Wu, S.; Liang, F.; Hu, D.; Li, H.; Yang, W. and Zhu, Q., Determining the Critical Micelle Concentration of Surfactants by a Simple and Fast Titration Method, *Anal. Chem.*, **2020**, *92*, 4259–4265.
57. Lu, Y.; Zhang, E.; Yang, J. and Cao, Z., Strategies to improve micelle stability for drug delivery, *Nano Res.*, **2018**, *11*, 4985–4998.
58. Kapare, H. S. and Metkar, S. R., Micellar drug delivery system : a review, *Pharmaceutical resonance,* **2020**, *2*, 21-26.
59. Seeta Rama Raju, G.; Benton, L.; Pavitra, E. and Yu, J. S., Multifunctional nanoparticles: Recent progress in cancer therapeutics, *Chem. Commun.*, **2015**, *51*, 13248–13259.
60. Ahmad, Z.; Shah, A.; Siddiq, M. and Kraatz, H. B., Polymeric micelles as drug delivery vehicles, *RSC Adv.*, **2014**, *4*, 17028–17038.
61. Kabedev, A.; Hossain, S.; Hubert, M.; Larsson, P. and Bergström, C. A. S., Molecular Dynamics Simulations Reveal Membrane Interactions for Poorly Water-Soluble Drugs: Impact of Bile Solubilization and Drug Aggregation, *J. Pharm. Sci.*, **2021**, *110*, 176–185.
62. Kuentz, M., Analytical technologies for real-time drug dissolution and precipitation testing on a small scale, *J. Pharm. Pharmacol.*, **2015**, *67*, 143–159.
63. Wolrd Health Organization, International Meeting of World Pharmacopoeias, *WHO Drug Inf.*, **2013**, *2*, 119–128.
64. Gowthamarajan, K. and Singh, S. K., Dissolution testing for poorly soluble drugs: A continuing perspective, *Dissolution Technol.*, **2010**, *17*, 24–32.
65. Borbás, E.; Kádár, S.; Tsinman, K.; Tsinman, O.; Csicsák, D.; Takács-Novák, K.; Völgyi, G.; Sinkó, B. and Pataki, H., Prediction of Bioequivalence and Food Effect Using Flux- and Solubility-Based Methods, *Mol. Pharm.*, **2019**, *16*, 4121–4130.
66. Eriksen, J. B.; Messerschmid, R.; Andersen, M. L.; Wada, K.; Bauer-Brandl, A. and Brandl, M., Dissolution/permeation with PermeaLoop™: Experience and IVIVC exemplified by dipyridamole enabling formulations, *Eur. J. Pharm. Sci.*, **2020**, *154*,

105532.

67. Sironi, D.; Rosenberg, J.; Bauer-Brandl, A. and Brandl, M., PermeaLoop^{TM} a novel in vitro tool for small-scale drug-dissolution/permeation studies, *J. Pharm. Biomed. Anal.*, **2018**, *156*, 247–251.
68. Borbás, E.; Tözsér, P.; Tsinman, K.; Tsinman, O.; Takács-Novák, K.; Völgyi, G.; Sinkó, B. and Nagy, Z. K., Effect of Formulation Additives on Drug Transport through Size-Exclusion Membranes, *Mol. Pharm.*, **2018**, *15*, 3308–3317.
69. Borbás, E.; Nagy, Z. K.; Nagy, B.; Balogh, A.; Farkas, B.; Tsinman, O.; Tsinman, K. and Sinkó, B., The effect of formulation additives on in vitro dissolution-absorption profile and in vivo bioavailability of telmisartan from brand and generic formulations, *Eur. J. Pharm. Sci.*, **2018**, *114*, 310–317.
70. Tsinman, K.; Tsinman, O.; Lingamaneni, R.; Zhu, S.; Riebesehl, B.; Grandeury, A.; Juhnke, M. and Van Eerdenbrugh, B., Ranking Itraconazole Formulations Based on the Flux through Artificial Lipophilic Membrane, *Pharm. Res.*, **2018**, *35*, 1-13.